Structure-based drug discovery against a novel antimalarial drug target, *S*-adenosylmethionine decarboxylase/ornithine decarboxylase

By
Jonathan J. Reynolds

Submitted in partial fulfilment of the requirements for the degree *Magister Scientiae*
In the Faculty of Natural and Agricultural Sciences

Department of Biochemistry
University of Pretoria
Pretoria
October 2012

SUBMISSION DECLARATION

I declare that the dissertation, which I hereby submit for the degree MSc. Biochemistry at the University of Pretoria, is my own work and has not previously been submitted by me or a degree at this or any other tertiary institution.

Signature:…….

Date:…….

PLAGIARISM DECLARATION

Structure-based drug discovery against a novel antimalarial drug target, *S*-adenosylmethionine decarboxylase/ornithine decarboxylase.

University of Pretoria
Department of Biochemistry

Full name: Jonathan James Reynolds

Student number: 26044383

Declaration

1. I understand what plagiarism entails and I am aware of the University's policy in this regard.
2. I declare that this dissertation is my own, original work. Where someone else's work was used (whether from a printed source, the internet, or any other source) due acknowledgment was given and reference was made according to departmental requirements.
3. I did not make use of another student's previous work and submit it as my own.
4. I did not allow and will not allow anyone to copy my work with intention of presenting it as his or her own work.

Signature:_____ Date:_____

Acknowledgements

- Prof. Lyn-Marie Birkholtz, my supervisor, for her encouragement and leadership.

- Prof. A.I. Louw, my co-supervisor, for his insight and alternative ideas.

- South African Malaria Initiative for providing the funding for this research.

- The NRF for the block bursary and University of Pretoria Postgraduate bursary to enable me to pursue postgraduate studies.

- Esmaré Human for her help with codon harmonisation and training.

- My family and friends for their support and encouragement.

Summary

Malaria is one of the most life-threatening diseases affecting mankind, with over 3 billion people being at risk of infection, with most of these people living in Africa, South America and Asia. As the malaria parasite is rapidly becoming resistant to many of the possible treatments on the market, it is of upmost importance to identify new possible drug targets and describe drugs against these that are inexpensive, easy to manufacture and have a long shelf-life in order to combat malaria.

One such target is the polyamine pathway. The polyamines putrescine, spermidine, and spermine are crucial for cell differentiation and proliferation. Interference with polyamine biosynthesis by inhibition of the rate-limiting enzymes ornithine decarboxylase (ODC) and *S*-adenosylmethionine decarboxylase (AdoMetDC) has been discussed as a potential chemotherapy of cancer and parasitic infections. Usually, both enzymes are individually transcribed and highly regulated as monofunctional proteins. However, ODC and AdoMetDC from *P. falciparum* (*Pf*ODC and *Pf*AdoMetDC, respectively) are found as a unique bifunctional protein (*Pf*AdoMetDC/ODC) in the malaria parasite, making it an enticing target for new, selective antimalarial chemotherapies. In order to apply structure-based drug discovery strategies to design inhibitors for *Pf*AdoMetDC/ODC, the atomic resolution structures of these proteins are needed. Each individual domain has had its structure proposed through homology modelling; however atomic resolution structures of these domains are not yet available. The homology model of *Pf*AdoMetDC/ODC has not yet been elucidated due to the interactions between the domains of the bifunctional protein not being fully understood. High levels of recombinant expression of the bifunctional protein have been either unsuccessful or resulted in the formation of insoluble proteins being produced. The purpose of this project is to optimise the recombinant expression of *Pf*AdoMetDC/ODC, and the *Pf*ODC domain, to produce high yields of pure, soluble protein for subsequent atomic resolution structure determination. Ultimately, this will enable the utilisation of *Pf*AdoMetDC/ODC in structure-based drug discovery strategies.

Overexpression of *P. falciparum* proteins in *E. coli* is notoriously difficult, mainly due to the codon bias between the two species. Comparative studies were performed on four constructs of the *Pf*AdoMetDC/ODC gene, containing either the wild-type, fully codon harmonised, or partially codon harmonised gene sequences to analyse the effect codon harmonisation had on protein expression and activity of both domains of *Pf*AdoMetDC/ODC as well as on the monofunctional *Pf*ODC domain. Codon harmonisation did not improve the expression levels or the purity of recombinantly expressed *Pf*AdoMetDC/ODC or the monofunctional *Pf*ODC domain. Truncated versions of both proteins, and contamination by the *E. coli* chaperone proteins DnaK and GroEL, were present in the protein samples even after purification by affinity chromatography. However, codon harmonisation improved the activity levels of the *Pf*AdoMetDC domain, while decreasing the activity of the *Pf*ODC

domain of *Pf*AdoMetDC/ODC. Harmonisation of the monofunctional *Pf*ODC domain resulted in a decrease in the activity of the protein.

In order to identify possible inhibitors of the *Pf*ODC domain of the bifunctional protein, a structure-based drug discovery study was initiated based on a homology model for *Pf*ODC. Four hundred compounds with known antimalarial activity were virtually screened against the *Pf*ODC homology model and the top two scoring compounds were selected for enzyme inhibition assays based on their predictive binding affinity against the enzyme, and two medium scoring compounds were selected as controls. Enzyme inhibition studies were performed on the bifunctional *Pf*AdoMetDC/ODC to determine the effect the compounds had on both domains of the protein. Of the compounds assayed one of the compounds significantly reduced the activity levels of both domains of *Pf*AdoMetDC/ODC. Additionally, one compound significantly reduced the activity level of the *Pf*AdoMetDC domain of *Pf*AdoMetDC/ODC.

This work therefore contributes towards characterisation of the unique *Pf*AdoMetDC/ODC in malaria parasites as a novel drug target.

Contents

List of Figures

List of Tables

Abbreviations and Nomenclature

ABC	Ammonium bicarbonate
ACN	Acetonitrile
ACT	Artemisinin combination therapy
ADME	Absorption, distribution, metabolism, excretion
AdoMet	*S*-adenosylmethionine
AdoMetDC	*S*-adenosylmethionine decarboxylase
AHT	Anhydrotetracycline
amp	Ampicilin
BSA	Bovine serum albumin
CAPS	(Cyclohexylamino)-1-propanesulphonic acid
dcAdoMet	Decarboxylated adenosylmethionine
DDT	Dichloro-diphenyl-trichloroethane
DFMO	α-Difluoromethylornithine
DHFR	Dihydrofolate reductase
DHODase	Dihydroorotate dehydrogenase
DHPS	Dihydropteroate synthase
DTT	Dithiothreitol
FA	Formic acid
FV	Food vacuole
GSK	GlaxoSmithKline
HABA	Hydroxyazobenzene-2-carboxylic acid
HTS	High-throughput screening
IAA	Iodoacetamide
IRS	Indoor residual spraying
ITNs	Insecticide treated nets
LB	Luria-Bertani
LC-MS/MS	Liquid chromatography mass spectrometry
log*P*	Partition coefficient
MMV	Medicines for Malaria Venture
MTA	5'-methylthioadenosine
OD_{600}	Optical density at 600 nm
ODC	Ornithine decarboxylase
OWMM	Open water marsh management
PC	Phosphatidylcholine
PD	Pharmacodynamics
*Pf*AdoMetDC	*P. falciparum S*-adenosylmethionine decarboxylase
*Pf*AdoMetDC/ODC	*P. falciparum S*-adenosylmethionine decarboxylase/ornithine decarboxylase
*Pf*DHFR	*P. falciparum* dihydrofolate reductase
*Pf*DHFR/TS	*P. falciparum* dihydrofolate reductase-thymidylate synthase
*Pf*GCHI	*P. falciparum* GTP cyclohydrolase I
*Pf*Hsp70-1	*P. falciparum* heat shock protein 70-1

*Pf*ODC	*P. falciparum* ornithine decarboxylase
*Pf*Spds	*P. falciparum* spermidine synthase
*Pf*TS	*P. falciparum* thymidylate synthase
PK	Pharmacokinetic
PLP	Pyridoxal-5'-phosphate
-PMF	Potential of Mean Force
PPM	Parasite plasma membrane
PV	Parasitophorous vacuole
PVDF	Polyvinyldifluoride
RBC	Red blood cell
RMSD	Root-mean-square deviation
SAMI	South African Malaria Initiative
SD	Shine-Dalgarno
SDS-PAGE	Sodium dodecyl sulphate-polyacrylamide gel electrophoresis
SP	Sulphadoxine/pyrimethamine
SpdS	Spermidine synthase
SpmS	Spermine synthase
VS	Virtual screening
WHO	World Health Organisation

Chapter 1: Introduction

1.1 Malaria

1.1.1 Introduction and prevalence

Malaria is a mosquito-borne disease caused by eukaryotic parasites of the genus *Plasmodium*. Malaria is caused in humans by four major species of plasmodia that are transferred by the bite of a blood-feeding female *Anopheles* mosquito. *Plasmodium vivax, P. ovale* and *P. malariae* cause the less virulent form of malaria, with *P. falciparum* causing the most serious form of the disease [1]. It has been recently discovered that the simian form of malaria (*P. knowlesi*) can be zoonotically transferred to humans, indicating the need for the tight control of the spread of the parasite to humans [2].

Malaria is widespread in Africa, South America and Asia, affects 225 million people, causes death to approximately 800 000 people per year and poses a risk to over 3 billion people annually. The majority of malaria cases occur in sub-Saharan Africa, causing death mainly in young children [3].

Malaria is present in the three northern provinces of South Africa that border Mozambique and Swaziland. Seasonal transmission occurs between October and April. Only 4% of the population is at high risk of malaria and 6% at low risk, while 90% live in malaria-free areas. Almost all cases are caused by *P. falciparum*. The number of reported malaria cases decreased from an annual average of 36 360 between 2000 and 2005 to 6072 cases. During the same period, the number of reported deaths fell from 127 to 45. The principle vector control implemented in South Africa is indoor residual spraying (IRS), protecting about 4 million people per year [3].

The World Health Organization (WHO) has declared malaria control a global development priority but this is not an easy task for many reasons, such as the development of drug resistance in malaria as well as the gap in the development of new and affordable antimalarials [4]. A number of organisations, such as the Medicines for Malaria Venture (MMV, http://www.mmv.org), are involved in the development of novel antimalarials. The identification of novel drug targets is dependent on the study of the disease pathology, parasite invasion and immune response to invasion, parasite transmission, and parasite growth and development.

1.2 *P. falciparum* life cycle

When an infected female *Anopheles* mosquito feeds on a human, sporozoites are released from the mosquito's salivary gland and enter the human's bloodstream. The sporozoites are cleared from the bloodstream within 30 minutes as they quickly invade hepatocytes. During

the next 14 days, the liver-stage parasites differentiate and undergo asexual multiplication resulting in thousands of merozoites which burst from the hepatocyte (Figure 1.1) [5].

Individual merozoites invade erythrocytes, where the parasite spreads itself into a thin biconcave disc that is thicker around the perimeter and thinner in the middle, giving it the appearance of a ring in Giemsa-stained blood smears [6]. The parasite is found in a membrane-lined cavity in the erythrocyte known as the parasitophorous vacuole (PV). The parasite metabolises haemoglobin through its cytostome and takes up other nutrients transported in from the plasma. As the ring stage enlarges it exports molecules into the erythrocyte [7]. These molecules modify the erythrocyte membrane which then adheres to the lining of blood vessels [8]. The ring eventually grows into the more rounded trophozoite stage [5].

The trophozoite is the most active feeding, growth and erythrocyte modifying period of the parasite's intra-erythrocytic life cycle. *P. falciparum* erythrocyte membrane protein 1 is synthesised and exported from the parasite to the erythrocyte's membrane. This protein causes the infected erythrocytes to adhere to the endothelium of blood vessels in order to reduce parasite removal from the blood stream by the defence of the body via the spleen. Infected erythrocytes that adhere to the brain-blood vessel walls can cause cerebral malaria [9]. Foetal growth can be affected when infected erythrocytes adhere to blood vessels in the placenta [10]. The parasite continues to feed on haemoglobin, and the products of haemoglobin digestion crystallise into haemozoin within the food vacuole (FV) [5].

The parasite then undergoes a series of nuclear divisions to from a multinucleated schizont. Up to 32 nuclei are generated and these move into merozoite buds around the schizont's periphery. The merozoites eventually pinch off from the residual body of the cytoplasm. The erythrocyte membrane and PV membrane are lysed in a protease-dependent process [11]. The released merozoites invade additional, uninfected erythrocytes [12]. The length of the erythrocytic stage is typically 48 hours for *P. falciparum.* The clinical manifestations of malaria, namely fever and chills, are associated with the synchronous rupture of infected erythrocytes [13].

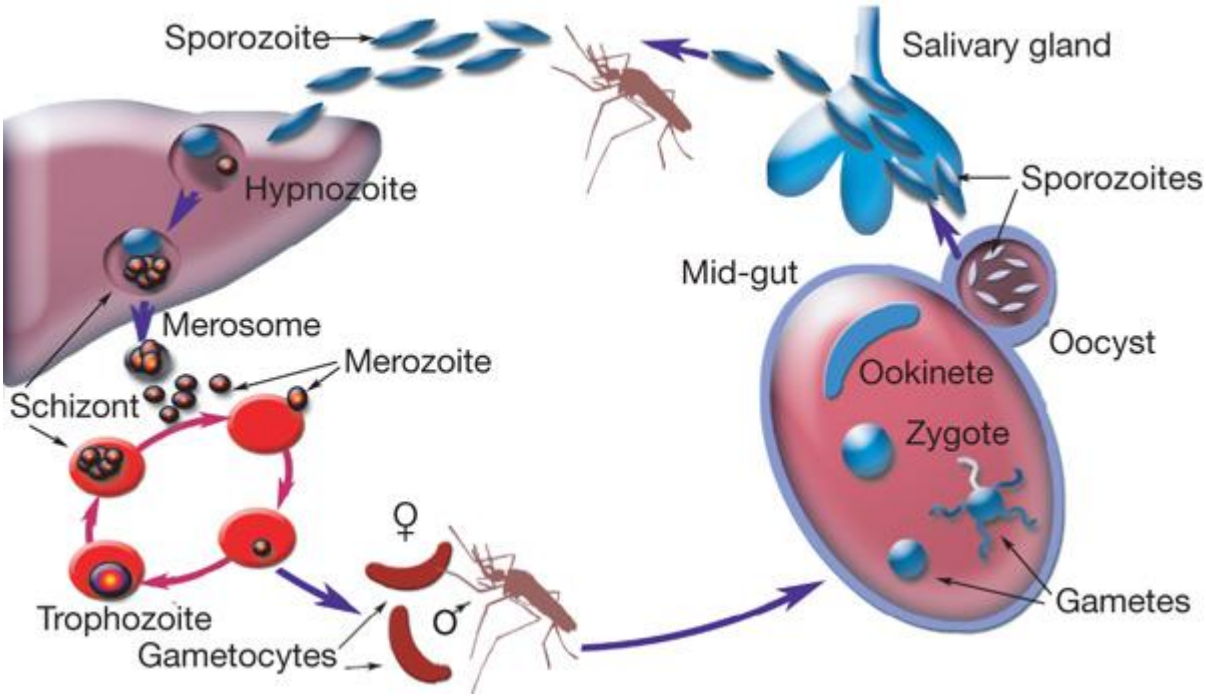

Figure 1.1: The life cycle of the malaria parasite in the human body. *P. falciparum* parasites are transmitted by the bite of an infected mosquito in which hundreds of sporozoites are released into the human host's bloodstream. The parasites eventually migrate to the liver and form parasitophorous vacuoles in hepatocytes. At this stage they initiate development that results in the production of thousands of merozoites. The parasites then induce detachment of the infected hepatocyte, allowing it to migrate to the liver sinusoid where budding of parasite-filled vesicles called merosomes occurs. The new merozoites quickly invade erythrocytes where they replicate, sometimes synchronously, in a cycle that may correspond to the cycle of fever and chills in malaria. In response to a cue that is not well understood, some parasites differentiate into male and female gametocytes, which are the forms taken up by the mosquito. Once they enter the mosquito via a blood meal they rapidly undergo transition into activated male and female gametes. The motile and short-lived diploid parasite form, the ookinete, migrates out of the blood meal, across the peritrophic matrix to the mid-gut wall where an oocyst is formed. After a meiotic reduction in chromosome number sporozoites are formed within the oocyst. Eventually the oocyst ruptures and the sporozoites migrate to the salivary gland where they await transfer to the human host [14].

A small proportion of the merozoites develop into male and female gametocytes in a process known as gametocytogenesis [15]. These gametocytes are taken up by the female *Anopheles* mosquito during a blood meal. Once in the midgut of the mosquito, the gametocytes develop into male and female gametes. The male gametes undergo a rapid nuclear division to produce eight flagellated microgametes which fertilize the female macrogamete. The resulting ookinete traverses the mosquito gut wall and encysts on the exterior of the gut wall as an oocyst. The oocyst soon ruptures, releasing hundreds of sporozoites into the mosquito body cavity, where they eventually migrate to the mosquito salivary gland to infect another human host [12].

1.3 Control and treatment of malaria

1.3.1 Controlling the mosquito vector

A mosquito control program focuses on mosquito control as a tool for the prevention of vector-borne disease and/or for the reduction of nuisance-biting mosquito populations. This definition is based on the understanding that the presence of disease pathogen-transmitting mosquitoes can serve as a serious health threat, and many mosquito species can cause moderate to severe annoyance and stress to inhabitants that are afflicted [16]. Vector control includes any activity such as killing of mosquito larvae and adults with chemical and biological insecticides, environmental management (such as drainage of standing water that may be used as mosquito breeding grounds), the use of insecticide treated nets (ITNs), indoor residual spraying (IRS), mosquito control legislation, and mosquito control education that results in reduced mosquito populations. Differences in mosquito control methods in different countries may be attributed to the control of different vectors, environments, social settings and economic conditions [16].

Before the discovery of dichloro-diphenyl-trichloroethane (DDT), the main approach to controlling the mosquito vector was directed towards the larval stage. This required a detailed knowledge of the mosquito and its environment, a high level of community participation and a continuity of effort for decades to ensure slow but sustainable progress. This method of vector control resulted in the eradication of *An. gambiae* from Brazil and Egypt. Antilarval methods include open water marsh management (OWMM), biocontrol, oil drip, and larviciding. OWMM involves the use of shallow ditches to connect marshes to a pond or canal. This drains the mosquito habitat and lets in fish that will feed on the mosquito larvae [17]. Biocontrol is the use of natural enemies to manage mosquito populations. This includes the direct introduction of parasites, pathogens and predators that target various life stages of the mosquito [18]. An oil drip can was a common and non-toxic antimosquito method that involved placing a thin layer of oil on top of the water used by mosquitoes for breeding. This prevents the mosquito larvae from penetrating the oil film with their breathing tubes, so they drown and die, and by preventing adult mosquitoes from laying eggs in the water [19]. Larviciding includes the use of chemical (contact poisons, growth regulators, etc) and biological agents (fungi, nematodes, copepods and fish) to decrease the mosquito larvae populations [20].

Control measures that are directed towards adult mosquitoes are more broadly applicable geographically than the location and ecology specific measures directed towards larvae. IRS and ITNs are two control measures against adult mosquitoes [21]. IRS remains the most widely used malaria vector control method. IRS involves the spraying of insecticides on the indoor surfaces of houses once or twice a year. The selection of insecticide has to take into account the vector's resistance to insecticides and the duration of the residual effect of the insecticide with the length of the transmission season. The main effect of IRS is the killing of

mosquitoes that enter houses and rest on sprayed surfaces. This method is not useful for the control of vectors that tend to rest outdoors, but it may be effective on outdoor biting mosquitoes which enter houses for resting after feeding [22].

The development of pyrethroids with long residual action and a very low mammalian toxicity made it possible to treat mosquito nets. Since mosquitoes are attracted by the odour of the person sleeping inside the net, they are blocked from reaching the sleeper by the net and the insecticidal effect of the treated nets adds a chemical barrier. ITNs also prevent mosquito feeding, hence reducing the reproductive potential of the mosquito population. Community-wide use of ITNs reduces the vector population and shortens the mean mosquito lifespan. As with IRS, this will reduce the malaria parasite sporozoites rate because very few mosquitoes will survive long enough for the sporogonic cycle to be completed [23].

IRS is more suitable than ITNs for the rapid protection of a population; however IRS needs to be continued for many years and requires the community's acceptance of spraying. ITNs are generally more accepted by communities and are more suitable for progressive introduction and incorporation into sustainable population habits [21].

Several challenges to mosquito control exist in urban areas. Major biological challenges to mosquito control include insecticide resistance [24] and vector behaviour [25]. Mosquitoes can also adapt to new environmental pressures, increasing the need for novel mosquito control approaches [26]. Increases in the human population, increased pressure on resources, and breakdown in municipal management result in detrimental effects on the mosquito control program's efficiency [27]. Insufficient funding, weak health infrastructures, limited skilled human capacity, and poor quality private sector services are additional challenges of managing mosquito control programs [28].

A novel approach to controlling the mosquito vector is the development of transgenic mosquitoes that are resistant to diseases. This approach relies on transgenic mosquitoes that have the ability to survive and out-compete the wild-type population of mosquitoes. The transgenic mosquitoes carry specific genes that make them resistant to plasmodium or inhibit the vector-specific stages of the parasite's life cycle. As these "disease-resistant" genes are passed on to following generations of mosquitoes the disease will consequently fade away after some time. Since there will be interactions between transgenic and wild-type mosquito populations once the transgenic mosquitoes have been released, it must be ensured that the disease-resistant genes are more dominant than the wild-type genes to ensure that the disease-resistant phenotype isn't diluted, and eventually lost in later generations [29].

Entomopathogenic fungi have been tested as a novel approach to kill anopheline mosquitoes. Fungal entomopathogens have been screened for their ability to kill adult mosquitoes. Fungal spores were suspended in an oil formulation and applied by spraying to

the walls of containers. Upon contact with mosquitoes in the container, the fungal spores begin development and invade the mosquito. The fungus multiplies and kills the mosquito within two weeks. This is approximately the same amount of time that the malaria parasite takes to develop into sporozoites [30]. The fungus *Beauveria bassiana* was chosen for further studies as it is already in use as an agricultural biopesticide. The fungi are non-pathogenic to humans, approved for insect pest control, and can be easily applied to surfaces as a spray. However, even though fungal spores are relatively stable when kept in suspension, their lifetime rapidly decreases when applied to a surface [31]. Thus surfaces would require retreatment at a frequency higher than typical IRS with pyrethroids [32].

1.3.2 Vaccines

The control of malaria through the use of drugs and insecticides may not be able to be sustained for too long as they rely on too few compounds. The emergence of drug-resistant parasites is becoming a major problem, with resistance to the promising drug artemisinin being reported [33]. Therefore, the development and employment of new malaria vaccines is essential in the eradication of malaria [34]. Currently, the first ever Phase III clinical trials are being conducted on a vaccine against malaria. Unfortunately, it has already been established that its efficacy will not be 100% [35] but the important fact is that it would contribute to a decrease in the number of new malaria cases. The development of malaria vaccines are generally divided into three groups based on stages of the parasite life cycle targeted by the vaccine. They are pre-erythrocytic vaccines, asexual blood-stage vaccines and transmission blocking vaccines. Figure 1.2 shows the stages of the life cycle targeted by the three groups of vaccines [36].

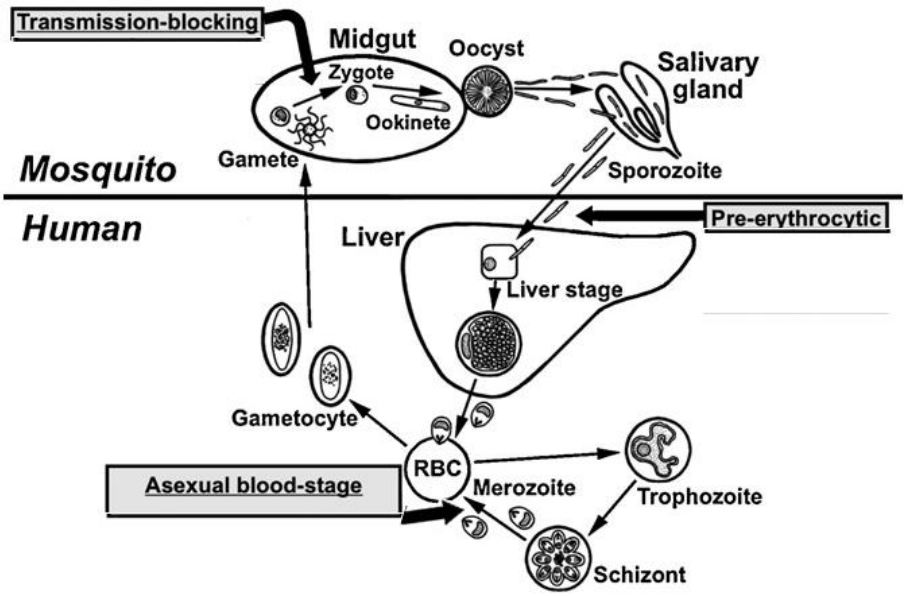

Figure 1.2: Malaria vaccines in clinical trials mapped on the parasite life cycle. Malaria vaccines are categorized into three groups based on the target stages of the parasite life cycle. They are pre-erythrocytic, asexual blood-stage, and transmission blocking vaccines. RBC: red blood cell (Adapted from [36].)

Pre-erythrocytic vaccines have been designed to prevent entry of sporozoites into hepatocytes and the development of liver stage parasites [36]. Asexual blood-stage vaccines are designed to reduce merozoites invasion, multiplication and growth in order to protect against the clinical symptoms and particularly severe disease. It is widely understood that this vaccine induces antibodies that may have roles in prevention of merozoite invasion, clearance of infected erythrocytes, prevention of adhesion and sequestration of parasitised erythrocytes in the vasculature. It is also possible that an effective blood-stage vaccine may also contribute to malaria eradication by reducing the efficiency of the transmission of parasites from human host to mosquito by interrupting the blood-stage life cycle in the human body [37].

Transmission-blocking vaccines are aimed at interrupting the parasite life cycle in the mosquito blood meal. These vaccines elicit antibodies against antigens that are expressed by the sexual stages of the parasite and stop their subsequent development in the mosquito midgut [38]. These transmission-blocking vaccines, if used in combination with pre-erythrocytic or asexual blood-stage vaccines, might play a key role in finally breaking the transmission of parasites, leading to eradication of the disease.

It is an accepted view that an effective malaria vaccine need to target several stages of parasite and several components of the different stages of parasite and it must induce protective immune responses equivalent to, or better than, those provided by naturally acquired immunity or immunization with attenuated whole parasite [39].

1.3.3 Current antimalarials

The antimalarial market is one of the largest with over half a billion treatments needed per year, but the majority of patients have almost no ability to pay for their treatment. The pharmaceutical industry has been unwilling to invest into a market where they would not recoup their investment. This has left many stages of antimalarial drug discovery to academic institutions and philanthropic endeavours. Funding from the Global Fund, the President's Malaria Initiative, the Bill and Melinda Gates Foundation, and others have made it possible to develop new tools to control malaria [4]. Companies such as GlaxoSmithKline (GSK), Pfizer, and Novartis have released large compound libraries to allow for screening of compounds for antimalarial activity.

Listed in Figure 1.3 are the structures of the drugs commonly used in the treatment of malaria – quinine, chloroquine, sulphadoxine, pyrimethamine, mefloquine, and artemisinin. The hypothesised targets of these blood schizontocides acting on intra-erythrocytic (asexual and partly sexual stage) *P. falciparum* parasites, and the mechanism by which the parasite becomes resistant to the drugs, will be briefly discussed below.

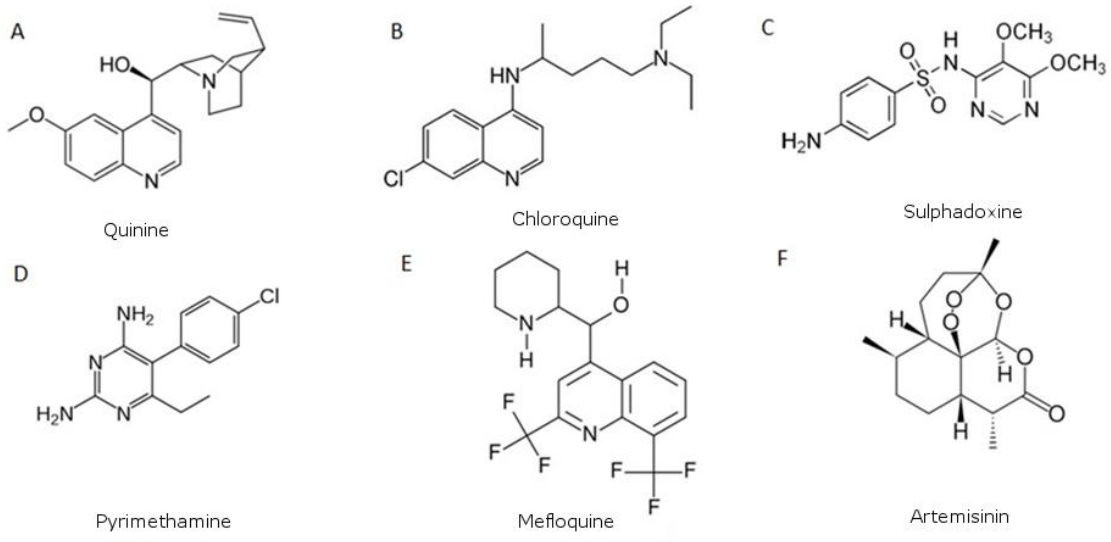

Figure 1.3: The structures of commonly used drugs in the treatment of malaria.

1.3.3.1.1 Quinoline-containing drugs

Quinine (Figure 1.3A) comes from the *Cinchona* tree native to South America. Quinine remains an important treatment for malaria, despite sporadic observations of quinine resistance [40]. The quinoline-containing drugs fall under two main classes: the type-1 drugs (4-aminoquinolines: chloroquine and the Mannich-base amodiaquine, pyronaridine) which are weak bases, diprotonated and hydrophilic at a neutral pH; and the type-2 drugs (the aryl-amino alcohols quinine, quinidine, mefloquine, halofantrine) which are weaker bases and lipid soluble at a neutral pH [41].

Following World War II, chloroquine and DDT emerged as the two principle medications in WHO's global eradication malaria campaign. Subsequently, chloroquine resistant *P. falciparum* parasites probably arose in four separate locations, starting with the Thai-Cambodia border around 1957; in Venezuela and parts of Colombia around 1960; in Papua New Guinea in the mid-1970s and in Africa, starting in 1978 in Kenya and Tanzania, and spreading by 1983 to Sudan, Uganda, Zambia and Malawi [40].

The development of mefloquine (Figure 1.3E) was a collaborative achievement of the US Army Medical Research and Development Command, WHO/TDR and Hoffman-La Roche, Inc. Mefloquine's efficacy in preventing falciparum malaria when taken regularly was shown in 1974 and its potential as a successful treatment agent was shown soon after. Mefloquine is linked to adverse events such as sleep disorders, psychiatric changes, and gastro-intestinal intolerability. Pre-clinical studies suggest that the single (+)-*erythro*-enantiomer may have an improved safety profile. Mefloquine resistance is known following widespread use, and is currently used in combination with artesunate [42].

Despite decades of use, the mechanism of action and resistance to the quinoline drugs is not fully understood. Various mechanisms have been proposed for the action of chloroquine and its related compounds to be either extra- or intravacuolar. Proposed mechanisms, such

as the inhibition of protein synthesis [43], inhibition of FV lipase [44] and aspartic proteinase [45], and inhibition of DNA and RNA synthesis [46], are regarded as being unlikely as they would require higher drug concentrations than those achieved *in vivo.*

The weak base properties of chloroquine (pKa_1 = 8.1; pKa_2 = 10.2) explains its selective accumulation in the FV. At neutral pH, chloroquine would be uncharged and thus able to freely diffuse through membranes. However, in the acidic pH of the FV chloroquine would become double protonated and thus membrane-impermeable and would be trapped inside the FV. Chloroquine then prevents the polymerisation of haem to haemozoin crystals by forming adducts with the haem monomers. Thus, the formation of haemozoin crystals is prevented and molecular oxygen can oxidise the haem monomers and create superoxide, which can then cause peroxidative damage to lipids and proteins [41]. The resistance to chloroquine has been linked to a mutation that replaces the codon for Lys76 of the parasite's chloroquine resistance transporter gene to a codon for Thr [47].

1.3.3.1.2 Artemisinin-type compounds

Artemisinin (Figure 1.3F) was isolated by Chinese scientists in 1972 from *Artemisia annua* (sweet wormwood), better known to Chinese herbalists for more than 2000 years as Qinghao. In the early 1970s, initial testing by Chinese scientists of Qinghao extracts in mice infected with malaria showed it to be as effective as chloroquine and quinine in clearing the parasite. Mao Tse Tung's scientists then began with tests in humans and in 1979 published their findings in the Chinese Medical Journal [40]. Artemisinin and other artemether-group drugs are currently the main line of defence against drug resistant malaria in many parts of South-East Asia [40].

All of the members of this drug class display activity throughout the phases of the asexual intra-erythrocytic schizogenic cycle and on young gametocytes. The mechanism of action is not completely understood, but the most accepted hypothesis is the reductive cleavage of intact endoperoxide of artemisinin by the ferroheme, ferrous-protoporphyrin IX (Fe(II)PPIX), which produces C-centred radicals [48]. The C-centred radicals cause many specific effects on the parasite, such as dismantling the haemozoin pool, inhibition of FV cysteinyl proteases, and inhibition of *Pf*ATP6 outside of the FV [49].

Artemisinin is a very potent and effective antimalarial drug, especially when used in combination with other malaria medications. However, the WHO has recently reported cases of malaria resistant to artemisinin [50]. Cases of artemisinin resistance have been reported on the Thai-Cambodia border, historically a site of emerging antimalarial resistance [33]. Monotherapy is no longer used because of the concern for resistance. The first drug combination that became available was artemether-lumefantrine and has had a profound effect on malaria control. Artemether-lumefantrine is the only artemisinin combination therapy (ACT) approved for use in Europe and is highly effective in immune as well as non-immune patients [51]. It has been shown to quickly clear the parasitaemia and

gametocytaemia resulting in rapid clinical improvement and block transmission of the malaria parasite. Dihydroartemisinin-piperaquine has recently been shown to be more effective and better to tolerate than artesunate-amodiaquine [52].

1.3.3.2 Nucleic acid inhibitors

Inhibition of the enzymes of the folate pathway results in decreased thymine and purine synthesis, resulting in reduced DNA, serine and methionine formation. The activities of these inhibitors are exerted at all growing stages of the asexual erythrocytic cycle and on young gametocytes [41].

1.3.3.2.1 Folate antagonists

One of the largest classes of antimalarials is the folate antagonist class; however there has been a rapid emergence of resistance against these compounds under drug pressure. A pyrimidine derivative, proguanil, was developed during World War II. Proguanil's success in treating humans led to further study of its chemical class and to the development of pyrimethamine (Figure 1.3D). Resistance to the two monotherapies appeared quickly (within one year in the case of proguanil). Sulphones and sulphonamides were then combined with proguanil or pyrimethamine in hopes of increasing efficacy and forestalling or preventing resistance. By 1953, *P. falciparum* resistance had already been noted in Tanzania. When sulphadoxine/pyrimethamine (Figure 1.3D) (SP) was introduced in Thailand in 1967, however, resistance appeared that same year and spread quickly throughout South-East Asia. Resistance to SP in Africa remained low until the late 1990s but since then it has spread quickly [40].

Inhibition of the enzymes in the folate pathway results in decreased pyrimidine synthesis (thus, reduced DNA levels), serine and methionine formation. The folate antagonists exhibit antimalarial activity at all growing stages of the asexual erythrocytic cycle and on young gametocytes. The antifolates are separated into two classes. Type-1 antifolates (sulphonamides and sulfones) mimic *p*-aminobenzoic acid and prevent the formation of dihydropteroate from hydroxymethyldihydropterin, a reaction catalysed by the enzyme dihydropteroate synthase (DHPS), by competing for the active site of DHPS. Type-2 antifolates (pyrimethamine, biguanides and quinazolines) inhibit dihydrofolate reductase (DHFR). This prevents the NADPH-dependent reduction of dihydrofolate to tetrahydrofolate, which is a necessary cofactor for the biosynthesis of purine nucleotides, certain amino acids and thymidylate [41]. Resistance to antifolates is conferred by mutations of the genes coding for DHPS and DHFR, resulting in substitutions in the amino acid side chain of the expressed protein, which prevents inhibition by the antifolates. These mutations generally occur in hotspots in the gene under drug pressure [48].

1.3.3.2.2 Atovaquone

Atovaquone (2-[trans-4-(4-chlorophenyl)cyclohexyl]-3-hydroxy-1,4-naphthoquinone) is a hydroxynaphthoquinone that is used for the treatment and prevention of malaria. Since resistance against atovaquone is rapidly developed when used as a monotherapy, it is used in a fixed combination with proguanil. Atovaquone is known to act primarily on mitochondrial functions but its mode of action and synergy with proguanil is not yet clearly understood. Atovaquone is believed to act on the mitochondrial electron transport chain, and through its synergy with proguanil it interferes with the mitochondrial membrane potential.

A proposed site for atovaquone's activity is dihydroorotate dehydrogenase (DHODase), an enzyme that is critical in electron transport. DHODase catalyses the reaction of dihydroorotate to orotate, which is then used in pyrimidine *de novo* synthesis. Inhibition of DHODase blocks pyrimidine synthesis, and it is through this action that the synergistic effects of atovaquone and proguanil (which is metabolised to the active form, cycloguanil, which inhibits pyrimidine synthesis) are believed to take place.

When used as a monotherapy, one out of every 3 patients displayed failure in treatment due to the parasite developing resistance against atovaquone. Resistance is believed to arise due to mutations in the cytochrome b gene, resulting in amino acid changes in one of the ubiquinone (coenzyme Q) binding sites. Atovaquone has a slow uptake and high lipophilicity, which exposes the parasite to sub-optimal doses of the drug over an extended time, leading to resistance [53].

1.3.4 Novel targets

The ability of the malaria parasite to develop resistance has made it essential that any drug development program continues to do surveillance for drug resistance on present drugs as well as drugs in development [54]. Studies of drug pharmacokinetics (PK) and pharmacodynamics (PD), which determine the effective therapeutic dose and window in addition to minimum exposure to prevent selection of antimalarial resistance, are being used to design combination drugs. It is hoped that combination therapy will protect the new drugs and slow the development of resistance [55].

The identification of novel drug targets in the malaria parasite could reduce the prevalence of malaria without inducing rapid resistance. A common method of determining novel drug targets is by comparing metabolic pathways between the host and the parasite. The presence or absence of enzymes in a metabolic pathway can be investigated for chemotherapeutic intervention strategies [56]. Some of the novel targets being investigated are discussed below.

1.3.4.1 Parasite membrane biosynthesis and transporters

Intra-erythrocytic parasites possess different membranes such as the FV membrane, the parasite plasma membrane (PPM) and the parasitophorous vacuolar membrane. Therefore, the amount of lipids in infected erythrocytes is significantly higher than that of uninfected erythrocytes. Growing and dividing malaria parasites require large amounts of phospholipids, which are synthesised from fatty acids obtained from the plasma. The major phospholipid in parasite membranes is phosphatidylcholine (PC), with most of the PC synthesised *de novo* from choline. Choline mobility increases significantly in infected erythrocytes, due to parasite-driven synthesis of a new carrier. Molecules have been designed to target the parasite's supply of PC. Quaternary ammonium and bis-ammonium salts with one long lipophilic alkyl chain have shown *in vitro* parasite inhibition at the nanomolar range [57]. Other compounds that inhibit *de novo* PC biosynthesis in the parasite have been developed [58], with G25 being identified as the lead compound. G25 potently inhibited *in vitro* growth of *P. falciparum* and *P. vivax* at a nanomolar range and was 1000-fold less toxic to mammalian cell lines. A very low dose of G25 can cure monkeys infected with *P. falciparum* and *P. cynomolgi* [59].

The properties of parasite-induced transport systems are significantly different from those in normal cells. The parasite also contains transporter proteins that are specific to the parasite. These transport systems could potentially be exploited as targets for antimalarial chemotherapy [56]. Designing cytotoxic drugs that are able to enter the parasite through these transporters will allow the drugs to be delivered to their target more efficiently [60]. Examples of targets under study are the vacuolar-type proton pump found on the PPM [61], and the *P. falciparum* hexose transporter [62].

1.3.4.2 Parasite proteases

Plasmodial proteases pay an important role in parasite survival by hydrolysing host erythrocyte proteins. Approximately 80% of the host erythrocyte's haemoglobin is broken down to individual amino acids, some of which is used by the parasite for protein synthesis. The malaria parasite has two main classes of proteases: those involved in the invasion and rupturing of erythrocytes, and those involved in haemoglobin degradation [63]. The merozoite surface protein's involvement in erythrocyte invasion has been relatively well studied. Cysteine proteases are believed to play a role in the release of merozoites from infected erythrocytes [64], with the use of cysteine protease inhibitors *in vitro* blocking the rupture of the erythrocyte membrane. Cysteine protease inhibitors can be used as a template for the development of new inhibitors that are specific for plasmodial proteases [65].

1.3.4.3 Targeting the apicoplast

The *P. falciparum* parasite contains a plastid-like organelle called the apicoplast, which is expected to be derived from the engulfment of photosynthetic red algae in ancient times, based on similarities between the apicoplast and photosynthetic red algae. The *P. falciparum* apicoplast genome is smaller than its plastid ancestor, containing no photosynthetic genes and most of the proteins of this organelle are encoded for by the nuclear genome and are transported to the apicoplast. The apicoplast contains unique metabolic pathways such as fatty acid, isoprenoid and haem synthesis, which are not found in the human host [66]. These parasite-specific metabolic pathways provide an ideal source of drug targets.

1.3.4.4 Polyamine biosynthesis

The polyamine pathway has received interest as a target in proliferative diseases such as cancer and parasitic infections [67]. The polyamine pathway as a drug target for *P. falciparum* will be discussed in detail in the following sections.

1.4 Polyamine pathway

1.4.1 Polyamines

Polyamines are structured, aliphatic amines. The common polyamines are the di-amine putrescine (Figure 1.4A); the tri-amine spermidine (Figure 1.4B); and tetra-amine spermine (Figure 1.4C). Polyamines are found in all organisms except the methano- and halobacteriales [68].

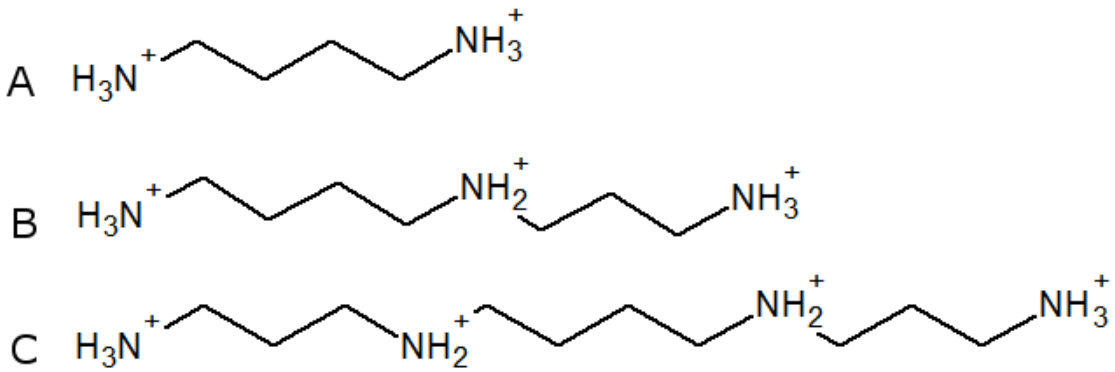

Figure 1.4: Structure of the three most common polyamines. A: putrescine; B: spermidine; C: spermine. Charges at physiological pH are indicated.

The versatile functions of polyamines are, generally, proposed to be due to their ability to have reversible ionic interactions with negatively charged macromolecules, such as nucleic acids and membrane proteins [69]. Polyamines are able to stabilise the nucleic acids of DNA via electrostatic interactions. These interactions can promote DNA bending, and indirectly influence DNA transcription by altering the availability of genes to gene regulatory elements

[70]. Additionally, histone acetyltransferase can be stimulated by polyamines to modify chromatin structure [71].

Polyamines have been implicated in many growth processes, such as cell proliferation and differentiation [72], due to the increased abundance of polyamines and the activities of polyamine biosynthetic enzymes during these processes [73]. The depletion of polyamines results in growth arrest, while their accumulation may result in apoptosis [74]. The accumulation of excess intracellular putrescine has been shown to trigger apoptosis, which is hypothesised to be due to an imbalance of positive and negative charges within the cell [75]. Therefore, polyamine levels are controlled by tight regulation of their synthesis, degradation, uptake and secretion [76].

Putrescine is formed by ornithine decarboxylase (ODC, EC 4.1.1.17) from ornithine. This is the first and rate-limiting step of the polyamine biosynthetic pathway [73]. An overexpression of ODC is associated with rapidly proliferating cells [77]. Spermidine is formed by putrescine by spermidine synthase (SPDS, EC 2.5.1.16). Spermine synthase (SpmS, EC 2.5.1.22) forms spermine from spermidine. Additionally, *S*-adenosylmethionine (AdoMet) has to be activated to donate aminopropyl moieties to putrescine for the synthesis of spermidine and spermine; this reaction being catalysed by the enzyme AdoMet decarboxylase (AdoMetDC, EC 4.1.1.50) [69].

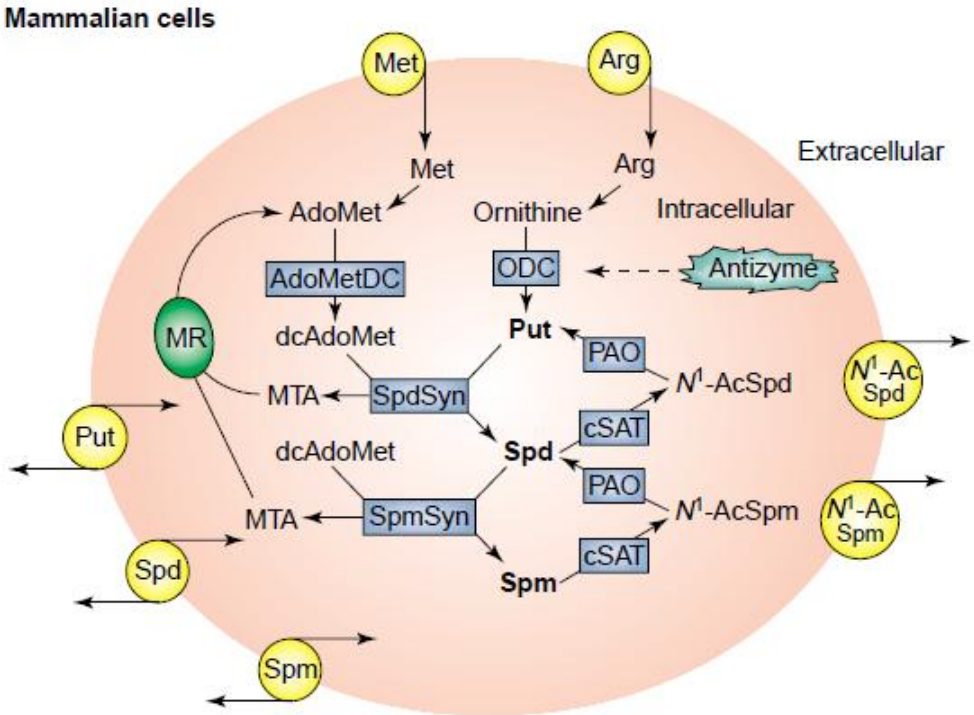

Figure 1.5: Regulation of polyamine levels in mammalian cells. Regulation of polyamine levels in mammalian cells. Precursors of polyamines, such as Met and Arg, are supplied by amino acid synthetic pathways, the urea cycle or by transport into the cell. Antizyme promotes the degradation of ODC. Polyamines can be back converted by the 'interconversion pathway' involving cSAT and PAO, regulated via different transport systems or excreted. MTA, the by-product of polyamine biosynthesis, is recycled to Met and hence AdoMet via a multi-enzyme pathway (MR). AdoMet: *S*-adenosylmethionine; AdoMetDC: *S*-adenosylmethionine decarboxylase; cSAT: cytosolic N1-acetyltransferase specific for spermidine and spermine; dcAdoMet: decarboxylated *S*-adenosylmethionine; MR: Met recycling pathway; MTA: methylthioadenosine; N1-AcSpd: N1-acetyl spermidine; N1-AcSpm: N1-acetyl spermine; ODC: ornithine decarboxylase; PAO: polyamine oxidase; Put: putrescine; Spd: spermidine; SpdSyn: spermidine synthase; Spm: spermine; SpmSyn: spermine synthase [78].

Due to their importance in cell growth, development and proliferation, polyamines have conventionally been considered attractive targets for developing antitumour drugs. A major difficulty in exploiting many of the putative targets is that the intracellular concentrations of polyamines in mammalian cells are regulated by feedback mechanisms and involve multiple routes of synthesis and interconversion (Figure 1.5). The feedback mechanisms enable cells to adapt to considerable changes of extra- and intracellular polyamine concentrations [79]. Nevertheless, there remains some optimism that such compounds, in combination with structural analogues of polyamines, might be beneficial, affecting uptake, synthesis and polyamine functioning simultaneously [78].

1.4.2 Polyamine metabolism in *P. falciparum*

Erythrocytes are devoid of polyamine biosynthetic machinery and only contain traces of putrescine, spermidine and spermine. However, in *P. falciparum* infected erythrocytes, the levels of polyamines and enzymes regulating the synthesis of polyamines, such as ODC and

AdoMetDC, are known to increase [80]. The polyamines are major metabolites of the parasite, and have been shown to make up 14% of the *P. falciparum* metabolome [81]. Erythrocytes infected by *P. falciparum* contain high levels of putrescine and spermidine, but only low levels of spermine [82]. This is due to spermine being synthesised by *Pf*SpdS, which is somewhat promiscuous in that it can use putrescine as well as spermidine as a substrate in the parasite [83].

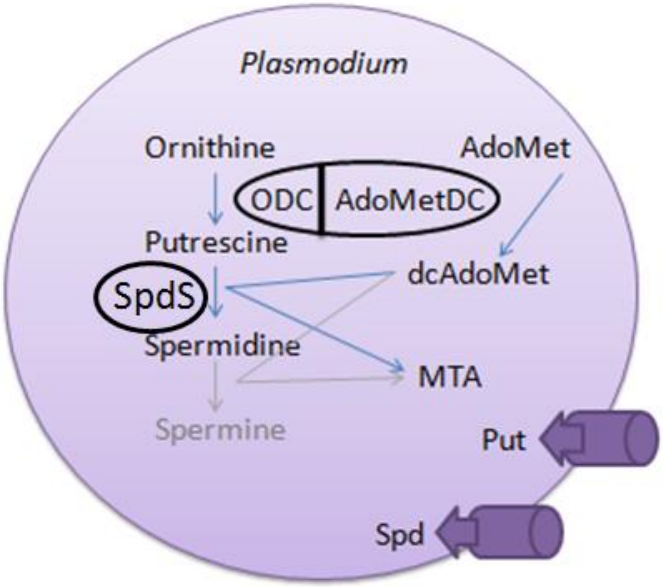

Figure 1.6: Polyamine metabolism in *Plasmodium falciparum*. The biosynthetic steps which provide Put and dcAdoMet for SpdS are represented by the bifunctional protein *Pf*AdoMetDC/ODC. The presence of spermine synthesis is questionable as no SpmS activity has been identified in *P. falciparum*, although the parasite contains appreciable amounts of this polyamine. Transport systems for Put and Spd are present in *P. falciparum*. Spm transport has not been shown but seems likely considering the probable absence of Spm synthesis. ODC: ornithine decarboxylase. SpdS: spermidine synthase. AdoMetDC: *S*-adenosyl methionine decarboxylase. AdoMet: *S*-adenosyl methionine. dcAdoMet: decarboxylated *S*-adenosyl methionine. MTA: 5'-methylthioadenosine. Put: putrescine. Spd: spermidine (Adapted from [76])

The *P. falciparum* parasite's polyamine pathway (Figure 1.6) is distinctly different from that of the human host. In *P. falciparum* parasites, a single open reading frame that encodes for a bifunctional protein that has both ODC and AdoMetDC activities [84]. Monofunctional mammalian AdoMetDC and ODC have a half-life of approximately 15 minutes, while *Pf*AdoMetDC/ODC has a half-life of more than two hours [78]. Mammalian ODC is barely inhibited by putrescine, while *Pf*ODC activity is regulated by feedback inhibition by putrescine. *Pf*AdoMetDC activity is not stimulated by putrescine unlike the mammalian protein [85]. The retro-conversion pathway present in the mammalian pathway is not present in *P. falciparum* [78]. No SpmS activity has been identified in *P. falciparum,* however, *Pf*SpdS has been shown to be capable of synthesising low levels of spermine [83]. These differences can be exploited to interfere with the parasite's polyamine biosynthetic pathway in such a way that it will minimise severe consequences on the host [78].

1.4.3 *Pf*AdoMetDC/ODC

The most distinctive feature of the polyamine pathway in *P. falciparum* is the single open reading frame that encodes a N-terminal AdoMetDC domain connected to the C-terminal ODC domain via an intervening linker region of 274 residues (Figure 1.7) [85]. The *Pf*AdoMetDC domain exists as a protomer that is post-translationally cleaved into a ~55 kDa α-subunit and a ~9 kDa β-subunit. The ~165 kDa heterodimeric polypeptide is required to dimerise with another heterodimeric polypeptide due to an obligatory association through the *Pf*ODC domain, to form the active ~330 kDa bifunctional complex [84].

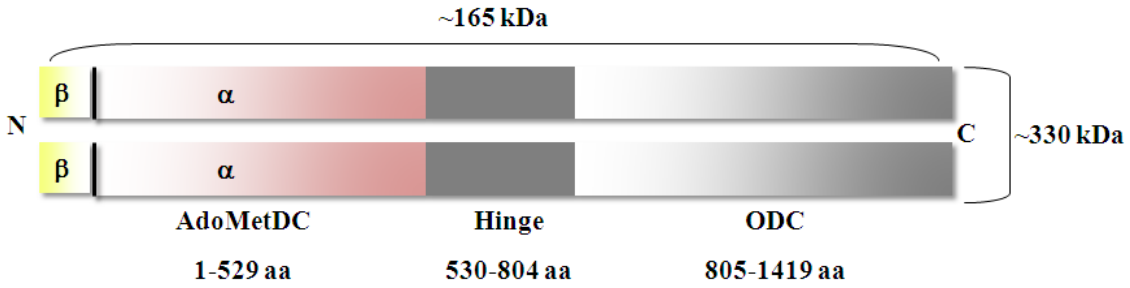

Figure 1.7: Schematic diagram of the bifunctional *P. falciparum* AdoMetDC/ODC protein. The N-terminal *Pf*AdoMetDC domain consists of α- and β-subunits. This domain is connected to the C-terminal *Pf*ODC via a hinge region. The sizes of the heterodimeric and heterotetrameric complexes are shown [76].

The hinge region plays a role in quaternary structure formation and conformational stability of the *Pf*ODC domain [86]. The hinge stabilises the heterotetrameric *Pf*AdoMetDC/ODC complex by interactions between the two domains [87].

Protein-protein interactions, as well as long-range protein communications, have been proposed to modulate the activities of the *Pf*ODC and *Pf*AdoMetDC domains within the bifunctional protein [87]. The activity of the *Pf*ODC domain is stimulated by the presence of the *Pf*AdoMetDC domain [87], and the activity of the AdoMetDC domain is reduced by the presence of the *Pf*ODC domain [86]. However, each active site is able to function independently of the other [86]. This effect of dual stimulation and inhibition allows *Pf*AdoMetDC/ODC to produce equimolar levels of putrescine and decarboxylated AdoMet [76]. *Pf*AdoMetDC in the bifunctional *Pf*AdoMetDC/ODC has a 6-fold lower K_m and slightly lower enzyme efficiency when compared to the monofunctional *Pf*AdoMetDC. The affinities of both enzymes for their substrates is improved in the bifunctional *Pf*AdoMetDC/ODC arrangement, and their catalytic rates are synchronized [86]. Long-range effects of the two enzymes in the bifunctional complex cause subtle changes in the active site [88].

The bifunctional organisation therefore guarantees coordinated transcription and translation of the rate-limiting enzymes of the polyamine synthetic pathways during the life cycle of *P. falciparum.* This unusual organisation of *Pf*AdoMetDC/ODC offers new possibilities for intervening with polyamine biosynthesis in these parasites, particularly because the regulatory mechanisms for the bifunctional *Pf*AdoMetDC/ODC differ from those in mammals [78].

1.4.3.1 AdoMetDC domain of the bifunctional *Pf*AdoMetDC/ODC

The *Pf*AdoMetDC domain of the bifunctional *Pf*AdoMetDC/ODC is comprised of two subunits that result from an internal proteolytic cleavage of the active site. The proteolytic cleavage creates a larger C-terminal α-subunit and a smaller N-terminal β-subunit. Most decarboxylase enzymes require pyridoxal-5'-phosphate (PLP) as a cofactor; however, AdoMetDC is in a class of enzymes that use pyruvoyl as a cofactor instead. At the cleavage site, a serine residue is utilised to generate pyruvoyl during an autocatalytic, non-hydrolytic cleavage reaction. Pyruvoyl acts as an electron sink during the decarboxylation of AdoMet by allowing the carboxyl moiety to act as a leaving group [89, 90]. Pyruvoyl is essential for enzyme activity [86].

The *Pf*AdoMetDC domain of the bifunctional *Pf*AdoMetDC/ODC was modelled using the human and potato X-ray crystal structures as templates (Figure 1.8) [91]. Three parasite-specific inserts and the core active site region was identified using a structure-based alignment approach. The domain was modelled without the two largest inserts, to give a root mean square deviation (RMSD) of 1.85 Å from the human template. Contact with the rest of the bifunctional complex is predicted to occur on one face of the *Pf*AdoMetDC domain. In the active site there are four substitutions compared to the human template. One of these substitutions may be responsible for the lack of inhibition by Tris, compared to the mammalian AdoMetDC. The model also provides an explanation for the lack of putrescine stimulation in PfAdoMetDC compared to mammalian AdoMetDC. A network of residues that connects the putrescine binding site with the active site in human AdoMetDC is conserved in the malarial and plant cognates. Internal basic residues are found to assume the role of putrescine, based on the model and site-directed mutagenesis: Arg11 is absolutely required for normal activity, while disrupting Lys15 and Lys215 each causes 50% inhibition of AdoMetDC activity. These novel features of malarial AdoMetDC suggest possibilities for the discovery of parasite-specific inhibitors [92].

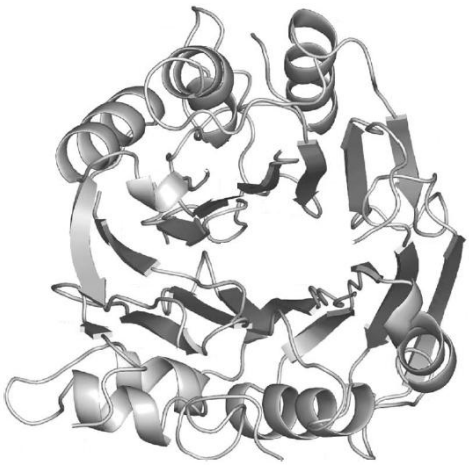

Figure 1.8: The homology model of *Pf*AdoMetDC. Cartoon diagram of PfAdoMetDC model (modified from [92]).

1.4.3.2 ODC domain of the bifunctional *Pf*AdoMetDC/ODC

Eukaryotic ODC associates as a homodimer in a head-to-tail manner to form an active doughnut-shaped enzyme. The active sites are formed at the interface between the two monomers, making it an obligate dimer. The active site residues of *Pf*ODC are conserved and also share the consensus sequences of other ODCs; however there are parasite-specific inserts present in the protein. The functions of these inserts are not yet known [93]. The hinge region plays an important role in the activity of monofunctional *Pf*ODC, as it is involved with substrate binding and increases the specific activity of the enzyme [85].

The ODC domain was modelled using the crystal structures of the human and *T. brucei* ODCs as a template. The model (Figure 1.9A) revealed that the *Pf*ODC monomer consists of a N-terminal α/β TIM barrel and a C-terminal modified Greek-key β-barrel [93], which is similar to all other eukaryotic ODC structures that have been characterised [94], [95].

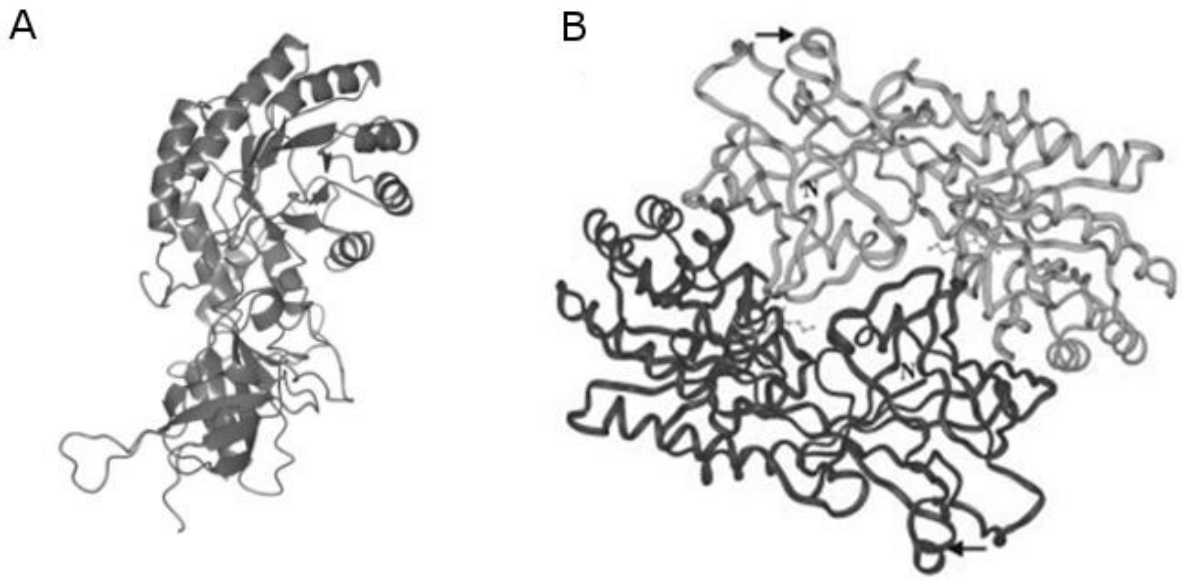

Figure 1.9: The homology model of *Pf*ODC. A: The homology model of monomeric *Pf*ODC [76]. B: The homology model of dimeric *Pf*ODC [93].

The homology model of dimeric PfODC (Figure 1.9B) revealed several interactions between the two domains. The dimer interface of PfODC is characterised by an aromatic amino acid zipper. The aromatic amino acids are involved in hydrophobic contacts by forming antiparallel stacked interactions, via their aromatic rings, across the dimer interface. A salt bridge is also predicted between the two monomers.

1.4.4 Spermidine synthase

*Pf*SpdS produces spermidine from decarboxylated *S*-adenosylmethionine (dcAdoMet) and putrescine via an aminopropyl transferase reaction. 5'-methylthioadenosine(MTA) is produced as a stoichiometric by-product and acts as a feedback inhibitor on *Pf*SpdS. *Pf*SpdS also produces low levels of spermine [83]. *Pf*SpdS has a monomeric molecular mass of ~37

kDa, and associates as a homodimer (Figure 1.10). The crystal structure of *Pf*SpdS has been elucidated and shows that the N-terminal of *Pf*SpdS consists of a six-stranded β-sheet, and the C-terminal contains a seven-stranded β-sheet followed by nine α-helices [96].

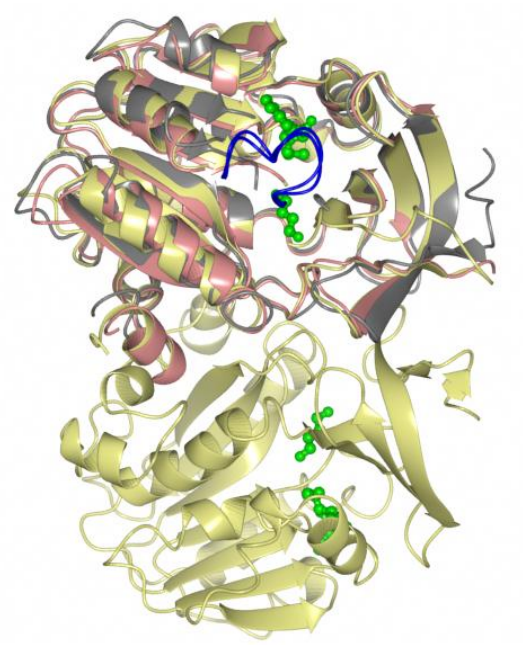

Figure 1.10: The structure of homodimeric SpdS from *P. falciparum* superimposed with the human protein. The crystal structure of homodimeric human SpdS (2O06, yellow) [97] superimposed with the crystal structures of *T. cruzi* (3BWC, grey) (Bosch, *et al*. unpublished results) and *P. falciparum* (2I7C, pink) [98]. MTA and putrescine within the active site are shown in green. The gate-keeping loops of human and *P. falciparum* SpdS are shown in blue.

The binding of dcAdoMet is stabilised by an active site gate-keeping loop that controls access of the substrates into the active site pocket [99]. The flexible loop opens to allow the exit of MTA and spermidine. *Pf*SpdS in complex with the specific inhibitor 4MCHA revealed important binding sites that could be used to design more potent inhibitors [78].

1.4.5 The *P. falciparum* polyamine biosynthetic enzymes as a drug target

Polyamine metabolism has been investigated as a target for antiproliferative therapy, especially in the interference of the polyamine pathways in tumour cells as an anticancer therapy and prevention. However, the use of enzyme inhibitors to disrupt the synthesis of polyamines has not yet been as successful for cancer treatment as anticipated. The use of these compounds as chemopreventive agents and in the combination with other drugs has provided some benefit in multiple cancer trials. One of the promising compounds from these studies has been α-difluoromethylornithine (DFMO) (Figure 1.11). DFMO was designed as an enzyme-activated irreversible inhibitor of ODC [69].

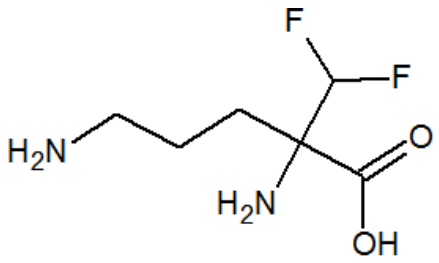

Figure 1.11: The structure of α-difluoromethylornithine.

Since there are rapid proliferation rates of protozoan parasites during infections, there is an associated high demand of polyamines for cell proliferation, and thus the blockade of polyamine biosynthesis was proposed to be a potential drug target against parasite infections. DFMO was successfully exploited against trypanosomes (*Trypanosoma brucei gambiense*) and is the only clinically relevant drug against West African human sleeping sickness [100].

Encouraged by the success in the treatment of African sleeping sickness, DFMO and other structure-related ODC inhibitors were used as lead compounds to test the validity of the polyamine synthesis pathway in malaria parasites as a point for chemotherapeutic intervention [69]. In *P. falciparum* parasites, addition of DFMO resulted in >99% decrease in putrescine levels, and >80% decrease in spermidine levels, with changes in spermine levels ranging from relatively unchanged to only a two-fold increase [101]. Depleting the malaria parasite of polyamines is therefore extremely deleterious to its growth and seems to be an attractive target for developing antimalarial agents [80].

According to the WHO's Tropical Diseases Research Targets Database, *Pf*AdoMetDC/ODC is considered to be a highly druggable protein, with an index of 0.8 out of 1, and is listed as one of the top 20 novel antimalarial targets (http://tdrtargets.org). Inhibition of either *Pf*ODC or *Pf*AdoMetDC activities alone causes a cytostatic rather than a cytotoxic effect, with arrest seen in the trophozoite stage of the parasite schizogony in erythrocytes *in vitro* [102].

Other ODC inhibitors such as 3-aminooxy-1-aminopropane, and its derivatives CGP52622A and CGP54169A, and the AdoMetDC inhibitors CGP40215A and CGP48664A, inhibit the activities of *Pf*ODC and *Pf*AdoMetDC in the bifunctional protein and result in reduced intracellular polyamine concentrations [82]. *Pf*AdoMetDC is irreversibly inhibited by 5'-([(Z)-4-amino-2-butenyl]methylamino)-5'-deoxyadenosine (also referred to as MDL73811 or AbeAdo), and is roughly a 1000-fold more effective than DFMO treatment [103]. The bis(benzyl)-polyamine analogue, MDL27695, inhibits the *in vitro* growth of chloroquine-sensitive and -resistant *P. falciparum* strains rapidly, and in combination with DFMO, cures *P. berghei*-infected mice [104]. The *Pf*SpdS inhibitor, dicyclohexylamine, completely arrests growth of chloroquine-sensitive and resistant strains of *P. falciparum in vitro* [105]. These results all chemically validate these proteins as potential novel antimalarial drug targets. However, novel, chemically distinct and therapeutically useful inhibitors of these proteins

are required, and a typical drug discovery program that may result in such descriptors are discussed below.

1.5 Drug discovery pathway

Developing a new drug from an original idea to the launch of a finished product is a complex process which can take 12–15 years and costs in excess of US$1 billion. The idea for a target can come from a variety of sources including academic and clinical research and from the commercial sector. It may take many years to build up a body of supporting evidence before selecting a target for a costly drug discovery programme (Figure 1.12).

Drug discovery is especially challenging for antimalarials for several reasons: 1) antimalarial drugs need to be well tolerated and safe for humans with limited side effects, since follow-up healthcare is underdeveloped in countries where malaria is prevalent; 2) antimalarials need to be orally bioavailable and have a three-day maximum therapy for cure with once or twice a day dosing, in order to make administration of the drug in a non-hospital setting easier and to reduce risk of development of resistance to the drug; 3) drugs need to be used in combination in order to reduce the risk of resistance; and 4) antimalarial drugs need to be cheap to produce since the majority of antimalarials are used in developing countries [106]

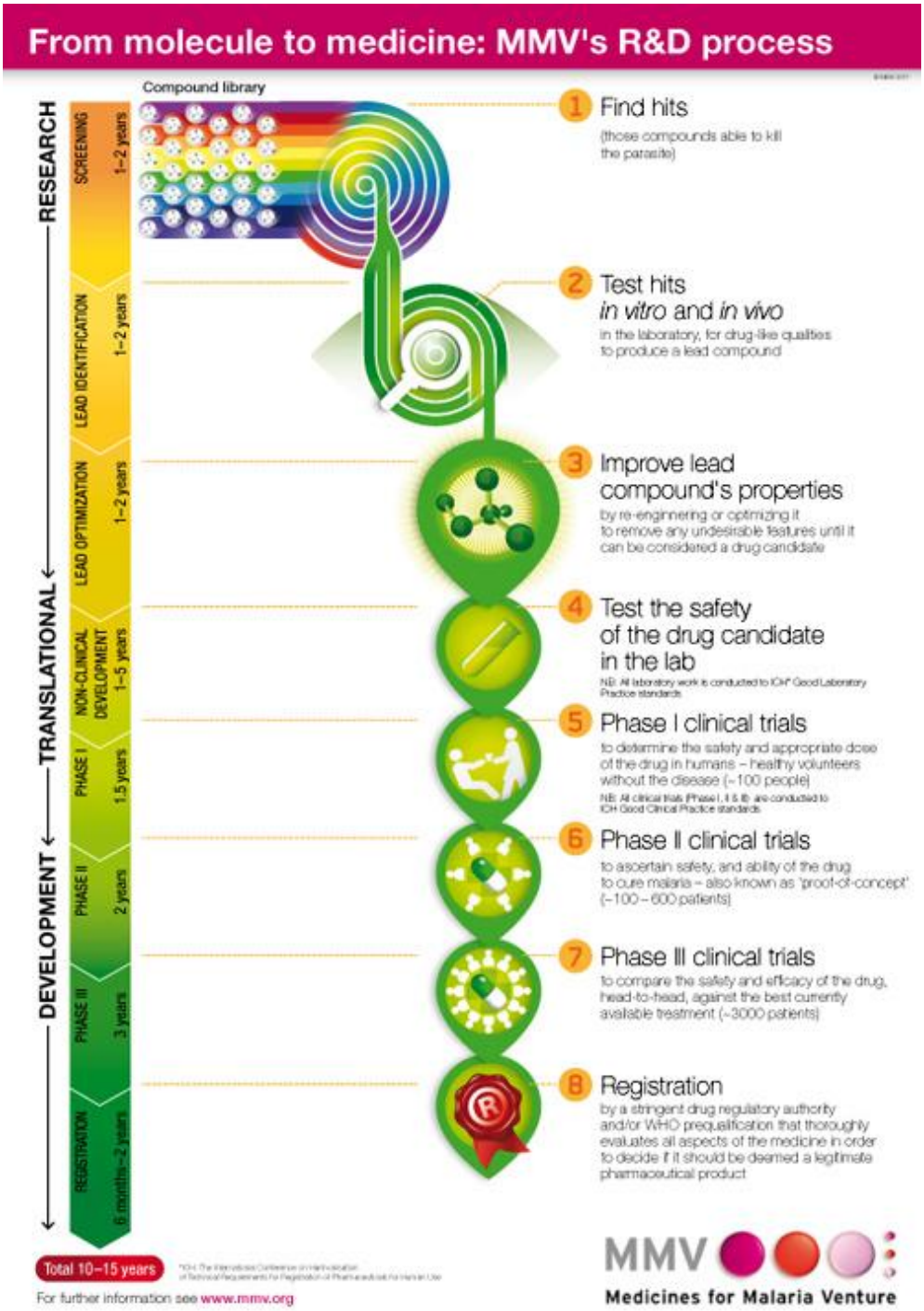

Figure 1.12: The antimalarial drug discovery pathway. The process for discovering a marketable antimalarial involves many years and phases before it can reach the market. Steps for drug discovery involve identifying molecules that kill the parasite by testing it *in vitro* and *in vivo*. Lead compounds are improved to remove undesirable features and improve drug-like qualities. The safety of the drug candidate is then tested on animal models and, if successful, goes through clinical trials to test safety and efficacy in humans. Once a drug has passed all these stages it can be registered for market use. The research, translational and development stages of drug research typically takes 10 to 15 years to complete (www.mmv.org).

The drug discovery process involves the following steps: target identification, target validation, assay development, hit-to-lead phase and lead optimisation (Figure 1.13).

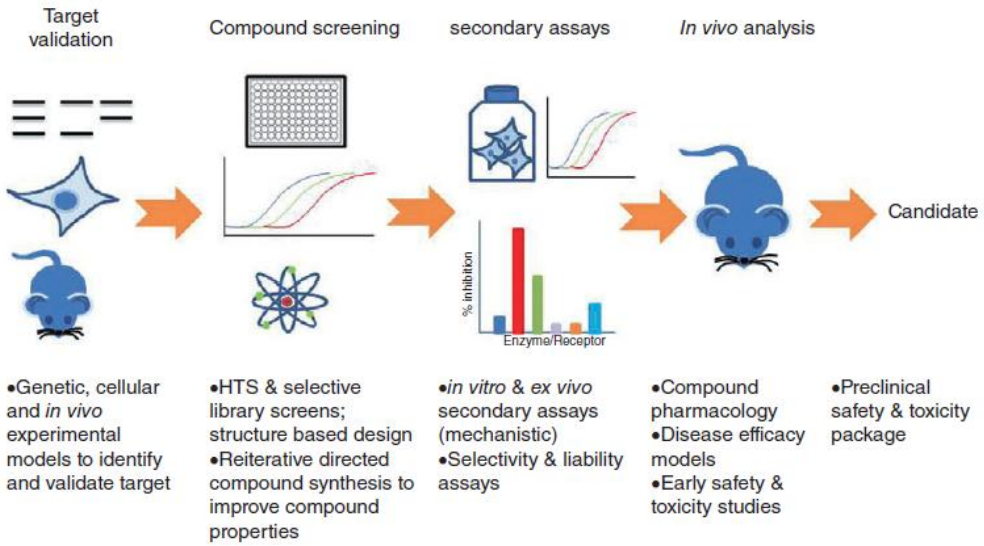

Figure 1.13: The drug discovery process. The drug discovery process typically involves target validation, compound screening, secondary assays, and *in vivo* analysis. Compounds that pass these stages are then carried through to clinical trials [107].

Once a target has been chosen, the pharmaceutical industry and, more recently, some academic centres have streamlined a number of early processes to identify molecules which possess suitable characteristics to make acceptable drugs.

The two main reasons for drugs failing in the clinic are that they do not show efficacy in humans, or that they are not safe. Target identification and validation are important steps in developing new drugs. A good drug target is one that is efficacious, safe, meets clinical and commercial needs, and must be accessible to the drug target. A putative drug molecule must elicit a biological response *in vitro* and *in vivo* [108].

1.5.1 Target identification and validation

The identification and validation of novel therapeutic targets is a highly complex and resource-intensive process, and requires an integrated use of tools, approaches and information. Genomic and proteomic tools in the post-genome era will speed up the process, lower costs and lead to high-throughput processes [109]. Comparison of the target in drug-sensitive and drug-resistant parasites, as well as knockout of the parasite gene encoding the target are important for correlating target inhibition and antiparasite activity. However, direct validation cannot always be achieved as the parasite's gene cannot be deleted, or the gene deletions do not correlate with the drug induced phenotype. The inability to conclusively identify the target or the mechanism of action does not necessarily terminate the development of a promising drug candidate as several of the antiparasitics currently in drug trials, as well as those currently used as therapy, do not have well-defined targets or mechanisms of action [110].

Target identification attempts to identify new targets, usually proteins or DNA and RNA, whose modulation might inhibit or reverse disease progression. Changes in gene and

protein expression with human disease have been studied in the hope of finding new targets. Microarrays can be used to assess gene and protein expression (via nucleic or protein microarrays) to identify novel targets, and can be used to validate the found targets at the tissue or cell-scale (via tissue or cell microarrays) [111].

Rather than finding drugs for targets, forward chemical genomics finds targets for known drugs. This allows for the study of the biochemistry underlying the phenotype changes induced by chemicals based on the molecular targets and pathways the chemicals target. One method for the identification of targets is using an affinity matrix made of the immobilised hit compound. However, the synthesis of an efficient affinity matrix without loss of the compound's activity is challenging, due to the difficulties of adequate linker attachment. Cell lysate is run through the affinity matrix, and only targets that have affinity for the hit compound remain in the matrix [112]. High-throughput NMR-based screening is also used for the fast identification of drug-target interactions [113].

1.5.2 Compound screening

Once a target has been validated as a possible drug target, compound screening assays are developed for hit identification and the lead discovery phase of the drug discovery process. A "hit" molecule is defined as a compound that has the desired activity in a compound screen, and whose activity has been confirmed upon retesting. A variety of screening methods are available to identify hit molecules. The most common method is high throughput screening (HTS), which involves the screening of a library of compounds against the drug target or a cell-based assay [114]. This type of assay assumes no prior knowledge of the nature of the chemotype likely to have activity at the target protein. However, focused-based screening involves selecting compounds that are likely to have activity on the drug target, based on the structure of the target protein [115]. Focused-based screening requires either the homology model or the experimentally derived 3D structure. Fragment screening involves the generation of small molecular weight compound libraries that are screened at high concentrations, and is often accompanied by the generation of protein-fragment 3D co-structures to enable compound progression [116].

1.5.2.1 Virtual screening

The identification of novel molecular targets and the characterisation of their 3D structures have been increasing dramatically. Due to the high costs involved with and the low hit rate of HTS, it is often desirable to decrease the size of the compound library to be tested but at the same time to increase the probability of finding possible lead compounds. One way of achieving this is virtual screening (VS) of the compound library against a 3D structure or model of the tested molecular target [117]. While the majority of drug candidates currently being developed have been found using HTS methods, high-throughput docking and pharmacophore-based searching algorithms are becoming a major source of lead molecules

in drug discovery [107]. A pharmacophore is the ensemble of steric and electronic features that is necessary to ensure the optimal supramolecular interactions with a specific biological target structure and to trigger (or to block) its biological response [118]. Refinement and optimisation of docking methods have led to improvements in hit identification [107].

VS also allows investigators to determine whether a compound may have an inhibitory effect on the target of interest before purchasing the compound, thus potentially decreasing the costs of screening efforts by removing compounds that are unlikely to have an effect on the target molecule [107].

The pharmacological relevance, reproducibility, cost, and quality are important factors in the choice of assay for the screening of compounds [107]. Compound libraries are typically assembled to obey chemical parameters such as the Lipinski "Rule of Five" and generally have molecular weights of less than 400 and have an octanol-water partition coefficient log*P* (a measure of lipophilicity, which affects absorption into the body) of less than 4. Lipinski's rule states that, in general, an orally active drug has no more than one violation of the following criteria: not more than five hydrogen bond donors (nitrogen or oxygen atoms with one or more hydrogen atoms); not more than ten hydrogen bond acceptors (nitrogen or oxygen atoms); a molecular mass less than 500 Daltons; and a log*P* not greater than 5. Fitting compounds against the Lipinski's rule is done to prevent the screening of compounds that won't be pharmacologically relevant even if they show activity in the assay [119].

Once a number of hits have been identified by VS or HTS, compounds that are the best to work with are defined. Computational chemistry algorithms have been developed to group hits based on structural similarity in order to ensure that a broad range of chemical classes are present in the set of compounds to be tested further. These algorithms also determine potency and factors such as ligand efficiency (an indication of how well a compound binds for its size).

1.5.3 Hit-to-lead phase

The aim of the hit-to-lead stage of the drug discovery process is to refine each hit series to produce more potent and selective compounds that have properties that will allow them to be studied in *in vivo* models. Solubility and permeability assessments determine the bioavailability of a compound including its ability to reach its intended target. Antimalarial drugs need to have access to the patient's circulation, and absorption through the digestive system is preferred to injection. Antimalarials also have to cross the erythrocyte membrane, the PPM and parasitophorous vacuole membrane to reach its target. A compound that is neither soluble nor permeable is unlikely to become a drug no matter how potent it is in the primary screening assay. Microsomal stability is a measure of the ability of *in vivo* enzymes to modify and remove a compound. This can be assessed using hepatocytes and would give more extensive results, however they are not routinely used as they need to be prepared freshly on a regular basis. Inhibition of CYP450 is an important predictor of whether a

compound might have an influence on the metabolism of other drugs it may be co-administered with. Compounds that have the necessary PK properties (target potency, selectivity, physiochemical, and ADME (absorption, distribution, metabolism, excretion) are then assessed for PK in rats or mice. A half-life above 60 minutes when the compound is administered intravenously and a fraction in excess of 20% absorbed when dosed orally are preferred for druggable compounds [107].

1.5.4 Lead optimisation

Lead optimisation is the final stage of the drug discovery process and involves improving deficiencies in the lead structure while maintaining favourable qualities. Molecules need to be tested for genotoxicity, general behaviour in *in vivo* models, high-dose pharmacology, dose linearity, and drug-induced metabolism and metabolic profiling. Chemical stability and salt selection issues also need to be considered [107].

The drug discovery process, from hit generation to preclinical candidate selection, takes many years. The quality of hit-to-lead starting point and the expertise of the research team are important factors of a successful outcome of the drug discovery process. Within industry a project with a library of 200 000 to millions of compounds might be initially screened, resulting in one or two candidate molecules after hit-to-lead and lead optimisation. Only 10% of small molecule projects in industry might make the transition to candidate. Failure can occur at many stages, including (i) inability to configure a reliable assay; (ii) no hits identified from HTS; (iii) compounds are toxic *in vitro* or *in vivo*; (iv) compounds have undesirable side effects that cannot be prevented without affecting the mode of action of the target; (v) inability to obtain a good PK profile in line with the typical dosing regimen required by humans due to an unsuitable half-life of the drug; and (vi) inability to cross the blood brain barrier for compounds that have targets within the central nervous system [107].

1.5.4.1. MMV's "Malaria Box"

The Medicines for Malaria Venture (MMV) was established in 1999 in response to a lack of incentives for malaria drug research and development. The MMV aims to discover, develop and deliver safe, effective and affordable treatments for malaria through public-private partnerships. These partnerships allow for the discovery and development for new drugs that neither the public nor the private sector could do on their own [120].

In an attempt to improve the rate of neglected disease drug discovery, the MMV and SCYNEXIS, Inc. (www.scynexis.com) assembled a collection of 400 carefully selected commercial compounds with antimalarial activity and provide it to researchers at no cost. The 400 compounds were selected by extensive screening of over 4 million compounds from the chemical libraries of St. Jude Children's Hospital [121], Novartis and GlaxoSmithKline [122]. Antimalarial activity of the drugs was confirmed *in vitro* against the

blood stage of the 3D7 strain (chloroquine sensitive but sulphadoxine resistant) of *P. falciparum*. The compounds have also been tested for cytotoxicity on human embryonic kidney cell lines (HEK-293), and are within levels considered acceptable for an in initial drug discovery programme (i.e. they are typically 10-fold less potent against the human cell line than the *P. falciparum* target). The Malaria Box includes 200 drug-like compounds and 200 probe-like compounds.

The drug-like compounds have been selected to be as diverse as possible while being compliant of the Lipinski "rule-of-5" physiochemical properties. However, their oral absorption has not been confirmed through *in vitro* or *in vivo* pharmacokinetic studies. Known toxicophores have been removed from the set. These compounds are therefore considered to be those most useful as starting points for drug discovery activities such as lead optimisation.

The probe-like compounds are intended to represent the broadest cross-section of chemical structural diversity. They might find most use as tools for probing mechanisms of action against a particular target. Some of these compounds are not compliant with the "rule-of-5" physiochemical properties, and may be considered less useful for drug discovery activities where the intention is to identify orally active compounds.

1.6 Previous attempts at recombinant expression of *Pf*AdoMetDC/ODC

The beginning stages of a drug discovery program require large amounts of recombinantly expressed protein for drug screening assays. As previously mentioned, VS is more accurate if the experimentally derived 3D structure of a protein is used instead of a homology model, however, large amounts of pure recombinantly expressed protein is required for crystallisation trials. *P. falciparum* is well known for having proteins that are refractory to recombinant expression, and a variety of factors are thought to account for this: the genes contain on average one intron each, requiring the use of cDNA for cloning; the genome has a codon bias that is far removed from that of *E. coli*; the genes have long stretches of adenosines and thymidines [123]; glycosylation patterns that are unique to the parasite are utilised [124]; and the *P. falciparum* proteins are generally larger than homologues in other species due to parasite specific inserts, which often possess long, disordered loops resulting in the *P. falciparum* proteins having a high pI [125], [126]. This is currently a problem with the recombinant expression of *Pf*AdoMetDC/ODC, as this protein has not yet been expressed at the levels and purity required for crystallisation trials.

In a previous study [84], cDNA isolated from *P. falciparum* that encoded *Pf*AdoMetDC/ODC, was subcloned into an expression vector and transformed into an EWH331 *E. coli* cell line (deficient of both AdoMetDC and ODC) [127]. The resulting recombinant protein had both AdoMetDC and ODC activities but the protein was expressed at only very low levels and could not be purified to homogeneity, due to the presence of contaminating *E. coli* chaperone proteins as well as truncated versions of the protein [84]. Tandem affinity

purification using an N-terminal His-tag and C-terminal *Strep*-tag, size exclusion chromatography and an protease inhibitor cocktail to prevent enzymatic degradation were used to try to optimise the concentration and improve the purity of recombinantly expressed *Pf*AdoMetDC/ODC. The use of ATP for the removal of ATP-dependent heat shock proteins was also used. However, none of these methods improved the concentration of *Pf*AdoMetDC/ODC and truncated versions of *Pf*AdoMetDC/ODC were still present, as well as an *E. coli* heat shock protein [128].

Additionally, attempts at expressing the monofunctional forms of the protein (i.e. the *Pf*AdoMetDC and *Pf*ODC domains individually cloned and expressed) revealed that both the domains express only at low levels in their wild type forms ([87], [85]). Interestingly, a codon harmonised version of the *Pf*AdoMetDC domain improved the expression levels as well as protein stability of monofunctional PfAdoMetDC. The reduction of Hsp70 co-purification in the PfAdoMetDC sample also gives an indication that less pressure was placed on *E. coli* during protein translation and folding [129]. Two constructs of the *Pf*ODC domain, one with and one without the hinge region have been expressed at very poor levels. Expression with the hinge was shown to decrease the total expression 2.5-fold, however the presence of the hinge region increased the activity of the construct [85].

1.6.1 Codon harmonisation

The frequencies with which different codons are used differ between organisms, proteins expressed at high or low levels within the same organism, and potentially even within the same operon [130]. Codon bias has been speculated to have arisen in order to reduce the diversity of iso-acceptor tRNAs as this would lower the metabolic load and may be beneficial to organisms that spend part of their lifetime under rapid growth conditions [131]. One the major disadvantages of the recombinant expression of proteins are that the codon bias differences between organisms has a profound impact on the soluble expression of recombinant proteins.

One method to overcome the negative effect of codon bias on heterologous gene expression is to increase the pool of rare tRNAs in the expression host. The use of strains that contain genes for rare tRNAs, such as the Rosetta strain, can be used to overcome codon bias. Even though over-expression of tRNAs appears to be a beneficial solution to the codon bias problem between organisms it does have drawbacks as it may affect amino acylation and tRNA modifications and thus the composition of the over-expressed protein may not be consistent. A problem with the tRNA over-expression strategy is that producing a fully functional tRNA requires other cellular components (e.g. amino acids) that might be in limiting supply when the tRNA alone is over-produced [130].

The more codons that a gene contains that are rarely used in the expression host, the less likely it is that the protein will be recombinantly expressed at reasonable soluble levels in the expression host. One strategy to improve expression is to replace the rare codons in the

gene with codons that are more frequently used in the expression host, in a process termed codon optimisation. Due to the degeneracy of the genetic code this will result in the same protein being expressed, but from a gene that has a codon usage that closely reflects that of the host [130]. Techniques for codon optimisation range from sequential site directed mutagenesis [132] to resynthesis of the entire gene [133].

Comparative analysis of *E. coli* gene sequences and their respective protein structures shows that amino acid sequences encoded by more frequently used codons are associated with highly ordered structural elements such as α-helices and β-sheets. Sequences containing clusters of less frequently used codons tend to be associated with the protein domain boundaries, such as link or end segments, which separate such elements. This analysis also showed that the link or end segments tend to be populated with amino acids that have bulky hydrophobic side chains or side chains that can hydrogen bond to the peptide backbone. When such residues appear in link or end segments, they tend to be encoded by infrequently-used codons [134]. Therefore, the positioning of clusters of relatively high and low abundance codons on mRNA transcripts may be a purposeful rather than a random occurrence. The idea that link or end segments, which separate elements of higher order protein structure, are encoded by clusters of low-usage frequency codons led to the hypothesis that slow or pausing of translational progression through such regions of mRNA would allow the preceding nascent structural element to fold, at least partially, within the environment of the ribosomal tunnel prior to initiation of synthesis of the next structural element. These areas are referred to as pause sites. Such a temporal control mechanism would minimize the interaction between partially folded nascent polypeptides in the cytosol, an event which can lead to degradation, or aggregation and precipitation [135].

Based on the concept that protein synthesis and folding in *E. coli* is co-translational and that nucleotide sequence-dependent modulation of translation kinetics might influence nascent polypeptide folding strategies have been developed to ‘‘recode’’ target gene sequences for recombinant expression in *E. coli* by substituting the native codons with synonymous ones having the same or similar usage frequencies in the expression host. This approach is termed ‘‘codon harmonisation’’ (Figure 1.14). Synonymous codons from *E. coli* are selected that match as closely as possible the codon usage frequency used in the native gene, unless empirical structure calculations show that the codons are associated with putative link/end segments and therefore should be translated slowly. Such regions are recoded by selecting the closest matching synonymous *E. coli* codon having a usage frequency equal to or less than that of its respective iso-acceptor codon’s usage frequency in the native gene’s host. Disharmony between codon usage patterns for *P. falciparum* malaria parasite target genes and *E. coli* has proven particularly challenging for recombinant expression in *E. coli* owing to the 80% A+T bias in the structural genes from *P. falciparum* [136]. Additionally, any false Shine-Dalgarno (SD) sites are removed that may result in the truncation of the proteins within the expression host.

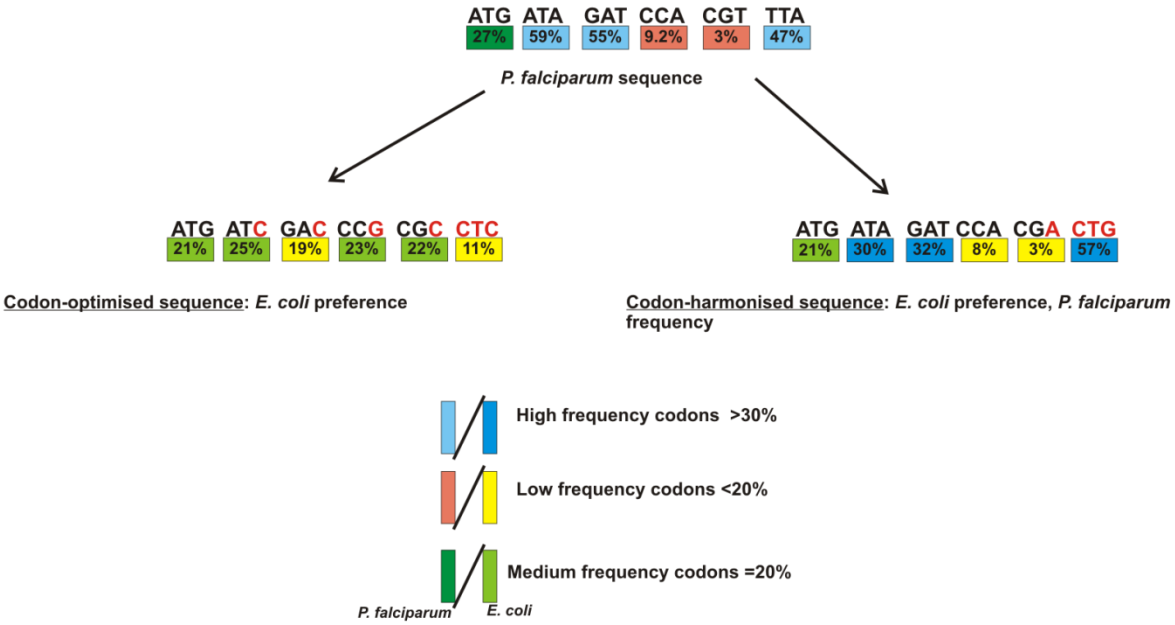

Figure 1.14: Diagrammatic representation of the difference between codon optimisation and codon harmonisation. Codon optimisation of a gene sequence involves replacing the codons for the *P. falciparum* gene sequence with those that are preferably used by the recombinant protein expression host, *E. coli*. Codon harmonisation replaces the codons for the *P. falciparum* gene sequence with codons that are used by *E. coli* at the same preference as those used by *P. falciparum;* this ensures that pause sites are conserved in the synthetic gene. Red letters indicates nucleotides that are changed. Codon usage frequencies are indicated by coloured blocks [137].

As codon harmonisation was highly successful in allowing expression of *Pf*AdoMetDC [129], the effect of codon harmonisation on the recombinant expression of *Pf*AdoMetDC/ODC and the *Pf*ODC domain was investigated in this study. The successful production of high levels of pure, soluble proteins will allow the use thereof in drug discovery strategies as explained earlier.

1.7 Aims

- To develop methods for the improved expression of the *P. falciparum* AdoMetDC/ODC, optimal for the purification of suitable quantities for crystallization of the bifunctional enzyme, as well as of the monofunctional *Pf*ODC component.
- To virtually screen a compound library against the homology model of *Pf*ODC in order to determine possible lead compounds. The levels of inhibition of *Pf*ODC activity by the lead compounds will then be determined by an enzyme inhibition assay.

1.8 Objectives

- Create a codon harmonised construct of the *adometdc/odc* gene, as well as constructs that contain a full length codon harmonised wild-type and codon harmonised portions of the gene.
- Recombinantly express and purify the chimeric *Pf*AdoMetDC/ODC and compare to wild-type *Pf*AdoMetDC/ODC.
- Determine effect harmonization has on the enzyme activity of both domains of *Pf*AdoMetDC/ODC.
- Create a codon harmonised construct of *odc.*
- Recombinantly express and purify harmonised *Pf*ODC and compare to wild-type *Pf*ODC.
- Determine effect harmonization has on the enzyme activity of *Pf*ODC.
- Virtually screen a compound library against the homology model of *Pf*ODC.
- Perform enzyme inhibition assays using the top scoring compounds from virtual screening on both domains of wild-type *Pf*AdoMetDC/ODC

1.9 Outputs

1. Human, E., Reynolds, J.J., Williams, M., de Ridder, J., Wells, G.A., Louw, A.I. and Birkholtz, L.M. "A codon-harmonised approach for the improvement of heterologous expression of *S*-Adenosylmethionine decarboxylase/Ornithine decarboxylase." Poster presentation. 6th Symposium on Polyamines in Parasites, Phalaborwa, South Africa in August 2010
2. Reynolds, J.J., Human, E., Williams, M., de Ridder, J., Wells, G.A., Louw, A.I. and Birkholtz, L.M. "A codon-harmonised approach for the improvement of heterologous expression of *S*-Adenosylmethionine decarboxylase/Ornithine decarboxylase." Poster presentation. 23rd congress of the South African Society of Biochemistry and Molecular Biology Congress, Drakensberg, South Africa in January 2012

Chapter 2: Materials and Methods

Part 2.1: Optimisation of the recombinant expression of *Pf*AdoMetDC/ODC and the ODC domain

2.1.1 Codon harmonisation

Codon harmonisation of the *P. falciparum adometdc/odc* gene was performed with the use of a codon harmonisation algorithm that is available as a PHP-script driven interface on the South African Malaria Initiative's (SAMI) website (www.sami.org.za/equalize/index.php) (J. de Ridder, G. Wells). The algorithm compares the codon preference of the entered gene and replaces it with codons used at a similar frequency to that of the target genome's codon preference. This approach conserves the ribosomal pause site profile of the wild-type gene in the recombinant expression system. The algorithm can then search the codon harmonised sequence for Shine-Dalgarno (SD) sites that have been inserted during the harmonisation process. The false start sites are removed by replacing the codons in the site to codons with the next closest codon-usage frequency. The harmonised gene was then manually inspected and excessively repeated poly-A stretches were modified as these may cause ribosomal slippage.

The codon harmonised *adometdc* (1 – 1475 bp) and *odc* (1476 - 4260 bp) domains were synthesised by GENEART (Regensburg, Germany), and were received in a pGA6 vector. Creation of the full length *adometdc/odc* constructs containing portions of wild-type and harmonised *adometdc* and *odc* was achieved by using restriction enzymes on the genes and ligating the sticky ends of the wild-type and harmonised genes together (E. Human). Using site-directed mutagenesis, the Shine-Dalgarno site in the harmonised *odc* gene was removed (J. Niemand). The hybrid bifunctional genes were then subcloned into the pASK-IBA3 vector, which attaches a *Strep*-tag on the C-terminus of the genes (Figure 2.1).

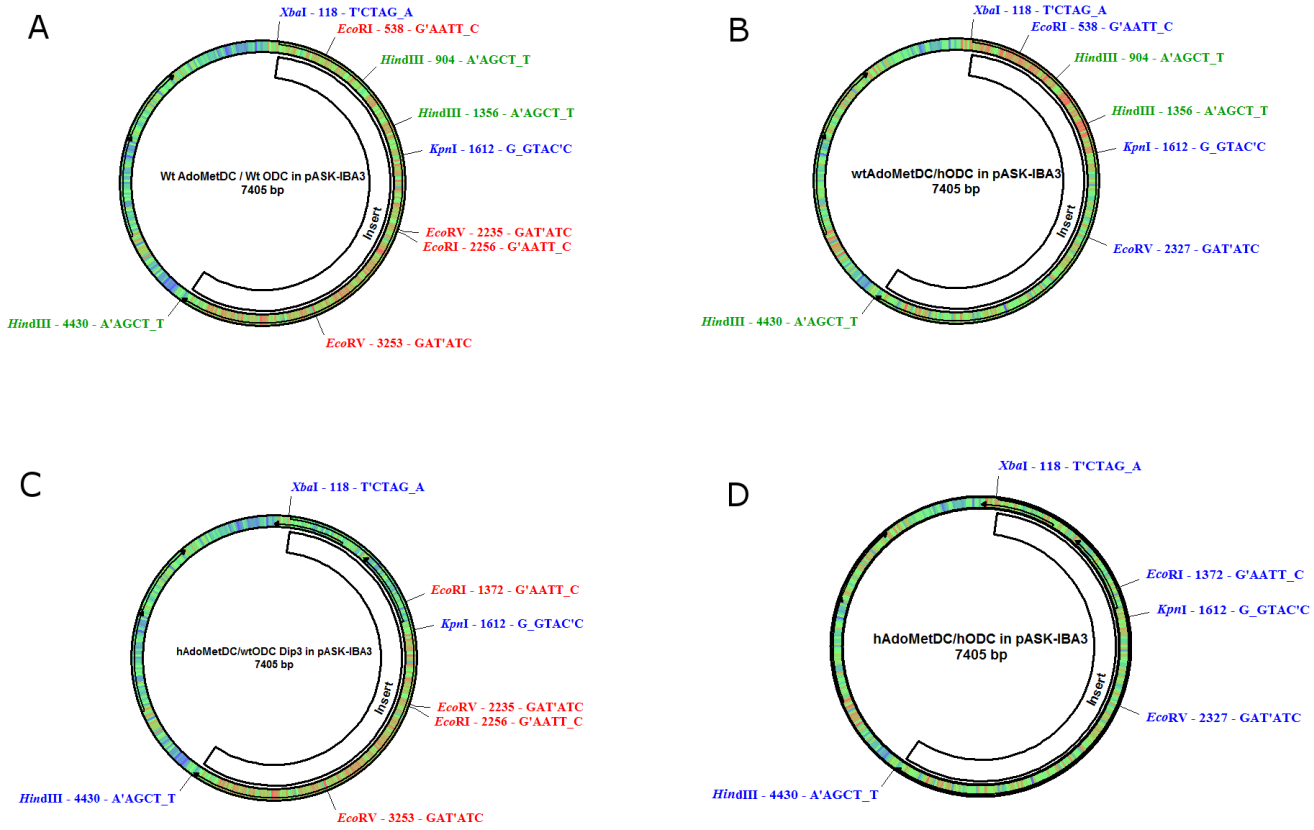

Figure 2.1: The four *Pf*AdoMetDC/ODC constructs subcloned into the pASK-IBA3 vector. A: wA/wO, B: wA/hO, C: hA/wO, and D: hA/hO in pASK-IBA3. Restriction sites and the sequences at which each restriction enzyme cut are indicated.

The wild-type and harmonised *Pf*ODC domains (referred to as wODC and hODC respectively) containing a portion of the hinge region (from amino acid 660 to 803 of the full-length bifunctional protein) were subcloned into the pASK-IBA7 vector, which attaches a *Strep*-tag on the N-terminus of the gene (Figure 2.2).

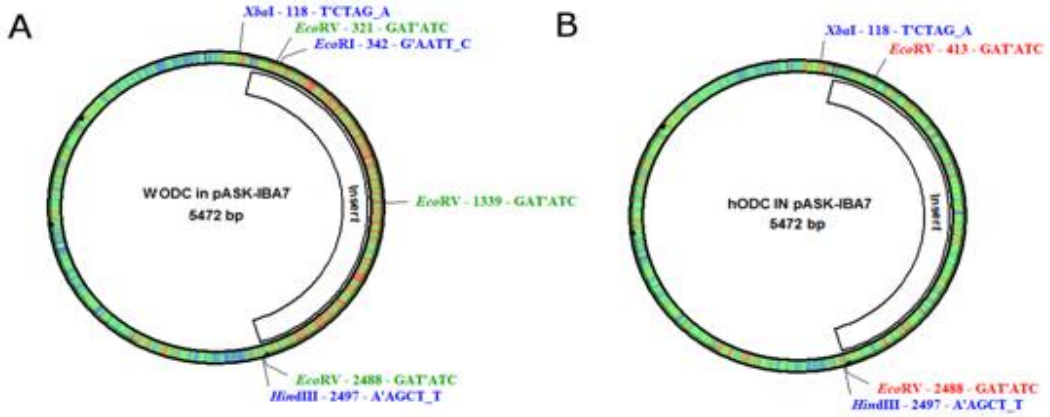

Figure 2.2: Vector diagrams for the two *Pf*ODC constructs subcloned into the pASK-IBA7 plasmid. A: wODC, and B; hODC in pASK-IBA7. Restriction sites and the sequences at which each restriction enzyme cut are indicated.

2.1.2 Heat shock transformation

BL21(DE3) Star cells (Invitrogen, USA. Genotype: F– ompT hsdSB(rB–, mB–) gal dcm rne131 (DE3)) were grown overnight in 5 mL Luria-Bertani (LB)-medium (0.063 M tryptone, 0.17 M NaCl, 5 g/L yeast extract) at 37°C with shaking at 150 rpm. The culture was diluted 1:10 in 50 mL LB and grown at 37°C until an optical density at 600 nm (OD_{600}) of 0.4 was reached. The culture was then transferred into 50 mL centrifuge tubes and incubated on ice for 10 minutes. The cells were collected by centrifugation at 2000xg and 4°C for 20 minutes. The supernatant was discarded and the pellet was resuspended in 25 mL ice cold 0.1 M $CaCl_2$. Cells were collected by centrifugation as above, supernatant discarded and the pellets resuspended in 2.5 mL ice cold 0.1 M $CaCl_2$, with 0.009% glycerol (v/v). The cells were incubated on ice for 1 hour, after which they were aliquoted into 200 µL fractions into ice-cold Eppendorf tubes and stored at -70°C.

The prepared heat shock competent BL21(DE3) Star cells (200 µL) were thawed on ice to which 10 ng plasmid DNA were added individually, and incubated on ice for 30 minutes. The cell suspensions were heat-shocked for 90 seconds at 42°C and immediately transferred to ice for 2 minutes. To each transformation reaction, 900 µL of pre-warmed LB-glucose (20 mM glucose in LB-medium) was added and the cells were incubated at 37°C for 1 hour with agitation. To check for successful transformation, 100 µL of the transformation mixture was plated on LB-amp plates (2% w/v agar in LB-medium with 100 µg/ml ampicilin). If the transformation reactions were highly efficient this would result in the growth of individual colonies on the LB-amp plate. To ensure that individual colonies are observed in the case of low transformation efficiency, the remaining cells were concentrated by a short centrifugation step. The pelleted cells were resuspended in 100 µL LB-glucose (as above) and plated on the agar plates.

2.1.3 Recombinant protein expression and isolation of *Pf*AdoMetDC/ODC proteins

The previously transformed BL21 (DE3) Star cells containing the pASK-IBA3 vectors with the wild type *Pf*AdoMetDC/ODC gene (wA/wO), partially harmonised *Pf*AdoMetDC/ODC gene (hA/wO and wA/hO), and fully harmonised *Pf*AdoMetDC/ODC (hA/hO), and pASK-IBA7 with wODC and hODC, were grown overnight in 5 mL LB-amp (LB-medium with 50 µg/mL ampicillin) at 37°C with agitation at 250 rpm.

2.1.3.1 Protein expression induction and expression

The overnight cultures were diluted 1:100 in 500 mL LB-amp and grown at 37°C with agitation until an OD_{600} of 0.5 was reached. Protein expression of the constructs was induced with the addition of 200 ng/mL anhydrotetracycline (AHT) for the controlled expression from the *tet* promoter. The *tet* repressor is constitutively expressed and keeps the *tet* promoter in the repressed state until the repression is relieved by the addition of AHT. Recombinant expression was then allowed to take place overnight at 22°C with shaking

at 200 rpm for the bifunctional *Pf*AdoMetDC/ODC constructs [84], and at 30°C for 4 hours for the *Pf*ODC constructs [85].

2.1.3.2 Isolation of recombinant proteins

The cells were harvested by centrifugation at 3500xg for 15 minutes at 4°C. The supernatant was discarded and the pellet was resuspended in 2 mL ice-cold wash buffer (150 mM NaCl, 1 mM EDTA, 100 mM Tris, pH 8). Approximately 0.1 mg/mL lysozyme was added to each sample to degrade the cell membranes. The cells were disrupted by sonication with an attached flat tip by pulsing the suspension for 10 cycles of 20 seconds each with 1 minute rest periods in between at an output control of 4. The suspensions were transferred to ice-cold 10 mL ultracentrifuge tubes and ultracentrifuged at 4°C for 1 hour at 100 000xg. The supernatants were transferred into ice-cold sterile 15 mL tubes.

The recombinant proteins were purified from the total soluble protein extracts with *Strep*-tactin affinity chromatography, as the pASK-IBA3 vector adds a *Strep*-tag at the C-terminal of the gene inserted in the vector, and pASK-IBA7 adds a *Strep*-tag at the N-terminal of the gene inserted in the vector. The *Strep*-tag fused to the recombinant proteins has a high affinity for *Strep*tavidin. Each protein extract was loaded onto a column containing 1 mL *Strep*-tactin beads at 4°C and was allowed to run through the column three times. The *Strep*-tactin beads were washed three times with 10 mL wash buffer. The protein was eluted from the column by the addition of 3 mL elution buffer (150 mM NaCl, 1 mM EDTA, 2.5 mM D-desthiobiotin, and 100 mM Tris, pH 8). The D-desthiobiotin in the elution buffer reversibly competes with binding to the *Strep*tavidin and thus releases the *Strep*-tag fused proteins. The *Strep*-tactin beads were regenerated for future use with regeneration buffer (150 mM NaCl, 1 mM EDTA, 1 mM 4-hydroxy azobenzene-2-carboxylic acid [HABA], 100 mM Tris, pH 8). HABA displaces the D-desthiobiotin from the affinity beads so they can be used in further protein isolation experiments. The purified protein samples were kept at 4°C until further use.

2.1.3.3 Protein concentration determination

The concentrations of the isolated proteins were determined by means of the Bradford assay. Binding of the dye to the basic and aromatic residues in the protein leads to an absorbency shift from 465 to 595 nm, which can be detected by a spectrophotometer. Bovine serum albumin (BSA) was used as the standard protein to set up a standard curve from which the unknown protein's concentration could be determined. A 1 mg/mL stock BSA solution was used to prepare a standard two-fold dilution series consisting of 200, 100, 50, 25, 12.5, and 6.25 µg/mL. A 96-well ELISA plate was used to which 150 µL of Bradford dye was added per 50 µl of each standard dilution and the purified protein fractions in duplicate. The absorbance at 595 nm was read in a spectrophotometer and the trend line

resulting from the standard curve of absorbency at 595 nm vs. standard dilution was deemed reliable if the R^2 value was above 95%.

2.1.3.4 SDS-PAGE analysis

The isolated proteins were separated with SDS-polyacrylamide gel electrophoresis (SDS-PAGE). The gel was composed of a 4% stacking gel (4% w/v acrylamide, 0.13 M Tris-HCl, pH 6.8, 0.1% w/v SDS) and a 7.5% separating gel (7.5% w/v acrylamide, 0.375 M Tris-HCl, pH 8.8, 0.1% w/v SDS). The samples were diluted 4:1 in sample buffer (0.06 M Tris-HCl, pH 6.8, 0.1% v/v glycerol, 2% w/v SDS, 0.05% v/v β-mercaptoethanol, 0.025% v/v bromophenol blue) and boiled for 5 minutes. Electrophoresis was carried out with SDS electrophoresis running buffer (0.25 M Tris-HCl, pH 8.3, 0.1% w/v SDS, 192 mM glycine) in an electrophoresis system. A 10-200 kDa protein ladder was loaded as a molecular marker, along with each protein sample. Electrophoresis was run at 60 V until the front had reached the separating gel, after which the voltage was increased to 100 V.

The protein bands were visualised with Coomassie staining, which is based on the colloidal properties of Coomassie Brilliant Blue G-250, whereby a shift in the dye occurs from the colloidal form to the molecular dispersed form upon the addition of methanol that enables the dye to disperse into the gel. The proteins are stained with very high sensitivity while background staining is kept to a minimum. A 0.1% w/v Coomassie Brilliant Blue G-250 solution containing 10% w/v ammonium sulphate and 2% v/v phosphoric acid was prepared and subsequently diluted 4:1 with methanol. The diluted solution was used to stain the gel overnight, after which it was briefly washed in 25% v/v methanol and 10% v/v acetic acid. The gel was destained with 25% v/v methanol for approximately 30 minutes.

In order to detect bands of lower concentrations silver staining was performed as it has a lower detection limit than Coomassie staining (50 – 100 ng of protein for Coomassie staining, and 1 – 10 ng of protein for silver staining). The proteins were fixed to the SDS-PAGE gel with a 30% v/v ethanol and 10% v/v acetic acid solution for 30 minutes. The gel was sensitised to the silver stain for 30 minutes with 30% v/v ethanol, 0.5M sodium acetate, 0.5% v/v gluteraldehyde and 0.2% w/v sodium thiosulphate, after which the gel was washed three times for 10 minutes each with distilled water. The sensitised gel was then placed in 0.1% w/v silver nitrate and 0.25% v/v formaldehyde solution for 30 minutes for the silver reaction. The gel was then briefly washed twice with distilled water in order to remove the excess silver nitrate. The gel was developed in 2.5% w/v sodium carbonate, 0.01% formaldehyde until the bands became visible. The developing reaction was stopped by replacing the developing solution with 0.05 M ethylenediaminetetraacetic acid (EDTA). The gel was either stored in the 0.05 M EDTA solution or in distilled water.

2.1.4 Recombinant protein detection and identification

2.1.4.1 Western blot

In order to determine whether *Pf*AdoMetDC/ODC and *Pf*ODC were recombinantly expressed and is present in the isolated protein samples, immunodetection by Western blot was performed. After separating proteins by SDS-PAGE analysis the gel was equilibrated in 10 mM 3-(cyclohexylamino)-1-propanesulfonic acid (CAPS) buffer for 5 minutes. A polyvinyldifluoride (PVDF) membrane was cut to approximately the same size as the SDS-PAGE gel and wet with methanol for 15 seconds, after which it was wet with CAPS buffer. Ten pieces of filter paper were cut and equilibrated in CAPS buffer. Five pieces of the equilibrated filter paper were layered at the bottom of the transfer cell (BioRad) and a wet test tube was rolled over each layer of filter paper to ensure that no bubbles were present. The PVDF membrane was then placed upon the filter paper, followed by the SDS-PAGE gel. The 5 remaining pieces of filter paper was placed upon this as before. The membrane was blotted for 45 minutes at 10 V (Pharmacia 3000/150 power pack). The PVDF membrane was then blocked overnight at 4°C in 20 mL blocking buffer (3% w/v BSA, 0.5% Tween in PBS (137 mM NaCl, 2.7 mM KCl, 8 mM Na_2HPO_4, 1.46 mM KH_2PO_4). The membrane was incubated with a 1:4000 dilution of monoclonal antibody to human *Strep*-Tag-HRP in wash buffer (1% w/v BSA, 0.5% Tween in PBS) for 1 hour at 37°C on a shaking platform. The membrane was washed six times for 10 minutes at 37°C with wash buffer on a shaking platform. For chemiluminescent detection of the *Strep*-tag conjugated proteins present on the membrane, the membrane was incubated with equal volumes of Luminol/Enhancer solution and Stable Peroxidise solution for 5 minutes. The excess reagent was drained from the membrane. Exposure of the chemiluminescent signal to X-ray film (Amersham Hyperfilm ECL) was performed in a dark room in a time range of 1 second to 5 minutes in order to obtain optimum exposure levels. The X-ray film was developed in developing solution (Ilford PQ Universal Paper Developer) for 1 minute, after which it was quickly rinsed in water, and fixed for 3 minutes in fixing solution (Ilford Rapid Fixer). The X-ray film was then left to air dry. Proteins containing a *Strep*-tag were visible on the X-ray film as a dark band.

2.1.4.2 Mass spectrometry sample preparation

In order to determine the identity of the contaminating bands present on SDS-PAGE gels, mass spectrometry (MS) was performed. Proteins were visualised on SDS-PAGE gels by MS compatible silver staining: proteins were fixed to the SDS-PAGE gel with 45% (v/v) methanol and 5% (v/v) acetic acid for 30 minutes. The fixed gel was then rinsed in distilled water for 12 hours. The gel was sensitised for staining with 0.02% (w/v) $Na_2S_2O_3$ for 2 minutes, followed by two brief rinse steps with distilled water. The gel was stained with chilled 0.1% (w/v) $AgNO_3$ for 40 minutes at 4°C, followed with two brief wash steps with distilled water. The gel was developed with 2% (w/v) Na_2CO_3 and 0.004% (v/v) formaldehyde until band

development was observed. Gel development was stopped with 1% (v/v) acetic acid. The gel could then either be stored in distilled water or 1% (v/v) acetic acid at 4°C.

Bands to be identified were cut out of the gel using a surgical blade and gel pieces were cut up into smaller pieces and then placed in 1.5 mL Eppendorf tubes. A small portion of 3 of the bands from the protein marker were cut out to be used as a positive control. A negative control, containing a portion of the gel that did not contain bands, was also prepared. The samples were incubated in 200 µL Water LCMS Chromasolv (Sigma) for 10 minutes, after which the water was removed. This was repeated twice. The samples were incubated in 200 µL 50% (v/v) acetonitrile (ACN) for 10 minutes. The ACN was removed, and the samples were incubated at 10 minutes in 200 µL of 50 mM ammonium bicarbonate (ABC). The ABC was removed, and the samples were incubated in ACN for 10 minutes. The ACN was removed, and the samples were further incubated in ABC for 10 minutes, after which the ABC was removed. One hundred microliters of 100% (v/v) ACN was added to the gel pieces until they turned white (approximately 10 minutes). The ACN was removed, and samples were dried *in vacuo*. Following drying, the samples were incubated in 100 µL 1 mM dithiothreitol (DTT) for 30 minutes at 37°C. The DTT was removed, and the gel pieces were incubated with 200 µL 50 mM ABC for 1 minute. The ABC was removed, and the gel pieces were incubated in 100 µL 50 mM iodoacetamide (IAA) for 60 minutes in the dark. IAA was removed, and 200 µL 50 mM ABC was added to the gel pieces and incubated for 10 minutes. The ABC was removed and the gel pieces were incubated in 200 µL 50% (v/v) ACN for 20 minutes. The ACN was removed and the samples were dried in a Speedyvac for an hour to remove traces of ACN. Trypsin was prepared by adding 180 µL 50 mM ABC to 20 µL trypsin aliquot, and was kept on ice until required. Trypsin was activated before addition to the gel pieces by incubating at 30°C for 15 minutes. 20 µL activated trypsin was added to the dry gel pieces, making sure that the trypsin just covers the gel pieces as excess trypsin would result in autolysis. The trypsin digest was allowed to occur at 37°C for 17 hours. To extract peptides from the gel pieces 15 µL 70% (v/v) ACN, 0.1% (v/v) formic acid (FA) was added and incubated at room temperature for 30 minutes. The supernatant was transferred to a clean Eppendorf tube. Another 15 µL 70% (v/v) ACN, 0.1% (v/v) FA was added to the gel pieces and incubated at room temperature for 15 minutes. The supernatants for each sample were pooled into the same Eppendorf tube. The supernatants were dried in Speedyvac and sent to be analysed at the Central Analytical Facilities at Stellenbosch University for liquid chromatography-mass spectrometry (LC-MS/MS).

Four databases were used for searches of peptide identity using MASCOT as a search engine. For each search a filter was employed that contained the following: Data was limited to only proteins with at least two peptides identified, a high and medium confidence peptide must be identified as well as at least 95% significance for the MASCOT score, these filters improve results that were obtained. Databases used Swissprot for all entries, Swissprot limited to *P. falciparum* entries, Swissprot limited to *E. coli* entries, and PlasmoDB database.

2.1.5 Refolding of inclusion bodies

Refolding of proteins from inclusion bodies after protein expression, extraction and separation of the soluble and insoluble protein fractions was performed by two methods – the KCl and detergent methods.

2.1.5.1 KCl method for protein refolding

The KCl method [138] involves resuspending the pellet in Bugbuster Protein Extraction Reagent (Novagen, EMD Biosciences, Germany) and degrading any remaining bacterial membranes by the addition of 200 µg/mL lysozyme. Six volumes of a 10-fold dilution of "Bugbuster" was then added and vortexed for 5 minutes at 22°C. Samples were then centrifuged at 16 000xg for 15 minutes at 4°C. Supernatants were discarded and the pellets were resuspended in 10-fold dilution of Bugbuster and centrifuged at 16 000xg for 15 minutes at 4°C. The purified inclusion body pellet was resuspended in 10 mL buffer A [50 mL wash buffer (as in 2.1.3.2) supplemented with 0.2 M KCl, 6 M guanidine HCl, 10 mM DTT] and stirred at 4°C for one hour to solubilise the protein. Wash buffer (50 mL), supplemented with 20% glycerol (v/v), 10 mM DTT and 0.2 M KCl was added to the tube drop-wise to achieve a 20-fold dilution in buffer A for the removal of excess denaturant and reducing agent to ensure satisfactory refolding of the protein. Samples were then stirred for 4 hours at 4°C. Samples were spun down at 20 000xg for 30 minutes at 4°C. One millileter *Strep*-tactin was added to each sample, and rotated at 4°C for 30 minutes. The resin-bound protein was spun down for 10 minutes at 4500xg at 4°C, most of the supernatant was removed and the resin transferred to a column and washed with 10 mL wash buffer and eluted with 3 mL elution buffer (as in 2.1.3.2).

2.1.5.2 Detergent method for protein refolding

The detergent method [137] involves resuspending the pellet in a 1% (w/v) n-Octyl-β-D-thioglucopyranosid (Fluka, Sigma-Aldrich, USA), a non-ionic detergent, in wash buffer (as in 2.1.3.2). The sample is then centrifuged at 24 000xg for 30 minutes at 4°C. The supernatant was discarded and the pellet was resuspended in a 1.5% (w/v) N-lauryl sarcosine (Sigma-Aldrich, St Louis, USA), an ionic detergent, solution in wash buffer, and the samples were rotated on a Rotator HAG (Fine PCR, Seoul, South Korea) for 90 minutes at 4°C. Samples were then centrifuged at 24 000xg for one hour at 4°C. Pellets were discarded and wash buffer was added to the supernatant to decrease the sarcosine concentration to 0.3% (w/v) prior to *Strep*-tag affinity chromatography. The samples were then applied to *Strep*-tactin columns and were allowed to flow through the column three times, washed with wash buffer, and eluted from the column in 3 mL of elution buffer.

2.1.6 Enzyme activity assays

2.1.6.1 *Pf*AdoMetDC and *Pf*ODC activity assays

The activities of both domains of recombinantly expressed *Pf*AdoMetDC/ODC and monofunctional *Pf*ODC were determined via a radioactivity assay [84].

The ornithine decarboxylase activity of the recombinantly expressed *Pf*ODC and *Pf*AdoMetDC/ODC were determined by measuring the amount of $^{14}CO_2$ released by the decarboxylation of L-(1-^{14}C)-ornithine (55 mCi/mmol. Amersham Biosciences, England). Reaction mixtures contained 2 µg of recombinant protein mixture, 90 µM ornithine, 125 nCi [1-^{14}C]ornithine, 1 mM DTT, 1 mM EDTA, 40 µM EDTA and 40 mM Tris-HCl (pH 7.5) in a total volume of 250 µL.

The *Pf*AdoMetDC activity of the recombinantly expressed *Pf*AdoMetDC/ODC was determined by measuring the amount of $^{14}CO_2$ released by the decarboxylation of *S*-adenosyl-(carboxy-^{14}C)methionine (56.2 mCi/mmol. Amersham Biosciences, England). Reaction mixtures contained 5 µg of recombinant *Pf*AdoMetDC/ODC, 99 µM AdoMet, 12.5 nCi [^{14}C]AdoMet, 1mM DTT, 1mM EDTA, and 40 mM KH_2PO_4 (pH 7.5) in a total volume of 250 µL.

The reactions were performed in 50 mL glass tubes in duplicate for each protein. The blank reactions contained buffer instead of recombinantly expressed protein solutions. Whatman no. 2 papers were folded lengthwise and inserted into 2 mL open-ended Eppendorf tubes, to which 100 µL hydroxide of hyamine was added to trap the released $^{14}CO_2$ in the form of hyamine carbonate. These were then placed into the glass tubes, which were then sealed with a rubber stopper. The reactions were allowed to take place for 30 minutes at 37°C in a shaking water bath. Reactions were terminated by the injection of 500 µL of 30% (w/v) trichloro-acetic acid which caused the proteins in the reaction mixture to precipitate. The tubes were once again incubated at 37°C in a shaking water bath for 30 minutes. The filter papers were transferred to 4 mL Pony-vial H/I tubes to which 4 mL of Ultima Gold XR scintillation fluid was added. The radioactivity was counted with a Tri-Carb series 2800 TR liquid scintillation counter. The specific activity (SA) of the recombinant protein solutions were calculated with the following formula:

$$SA = \frac{DPM \times nmol\ substrate}{mg\ protein \times \min \times total\ CPM}$$

Statistical analysis was performed using the paired Students t-test.

Part 2.2: Structure-based drug discovery

2.2.1 Virtual screening

The Malaria Box can be requested free-of-charge from the MMV's website (www.mmv.org/malariabox) with the provision that data obtained from research on the Box is published, shared and placed into the public domain to enhance future scientific discovery.

The 400 compounds in the Malaria Box were converted from canonical SMILES to 3D structures and virtually screened against a homology model of *Pf*ODC, in the presence and absence of PLP in the active site, using DiscoveryStudio 3.0 (Accelrys Inc.). The homology model was previously created by G. Wells [91] using the human (PDB id: 1D7K [94]) and *T. brucei* (PDB id: 1F3T [139]) ODC structures as templates. PLP was attached to Cys_{1355} (*Pf*ODC numbering) as a Schiff base.

The homology model was prepared for further analysis in DiscoveryStudio 3.0 using the Prepare Protein protocol. This prepares the protein model for input into other Discovery Studio protocols by performing tasks such as inserting missing atoms in incomplete residues, modelling missing loop regions, deleting alternate conformations, removing waters, standardizing atom names, and protonating titratable residues using predicited pKa's. The homology models were prepared with loops built in, with a maximal loop length of 20 amino acids. Interactions between amino acids in the loops were minimised using CHARMm. The proteins were protonated at a pH of 7.4, ionic strength of 0.145, and energy cut-off of 0.9. Ligands were retained during the protein preparation protocol.

The Malaria Box set of compounds was prepared using the Prepare Ligand protocol. This prepares ligand molecules for docking by standardising charges for common groups, adding hydrogens, changing the ionization state of the compounds to that found between a pH of 6.5 and 8.5. The protocol then determines all possible tautomers and stereoisomers, and discards conformations that are not possible under these conditions, as well as all duplicates.

The active site of the prepared protein structure was identified by selecting the important residues in the active site, as stated in [93]. The prepared ligand files were docked to *Pf*ODC using the LibDock protocol. LibDock is a docking algorithm with a relatively short run time for virtual screening of large compound libraries against identified hot spots (in this case, the selected active site). Docking preferences were set on a high quality. The conformation method for the ligands was set on FAST, with maximum conformations per ligand tested set at 255, and duplicated conformations discarded. As both the ligand library and homology models had been minimised during the preparation protocol, no minimisation protocol was selected during the docking procedure. The results from the virtual screen were then rated using the Jain and Potential of Mean Force (-PMF) docking scores.

The Jain score is an empirical scoring function that evaluates the structures and binding affinities of a series of protein-ligand complexes. The Jain score is a sum of lipophilic interactions, polar attractive and repulsive interactions, solvation of the protein and ligand, and an entropy term for the ligand.

The -PMF scoring function are based on the statistical analysis of the 3D structures of protein-ligand complexes. The scores are calculated by summing pairwise interaction terms over all interatomic pairs of the receptor-ligand complex. The -PMF04 score is an updated version of the -PMF score, where a larger data set was used for parameterization, and metal ions and halogens were included.

2.2.2 Enzyme inhibition assays

Enzyme inhibition assays were performed in the same manner as the activity assays in Section 2.1.3.7. However, the enzyme was incubated with 100 µM of the compound (dissolved in 100% DMSO) to be tested for *Pf*ODC inhibition for 10 minutes on ice. The full-length, wild-type *Pf*AdoMetDC/ODC was used to test for inhibition of *Pf*ODC activity due to the bifunctional protein having ten times more activity than the monofunctional *Pf*ODC domain [85]. The assay was also performed on uninhibited *Pf*AdoMetDC/ODC in order to determine how much the compounds lower the *Pf*ODC activity of the bifunctional protein. DFMO was used as a positive control to determine whether a decrease in observed activity was due to the presence of inhibitor.

The compounds were also screened for inhibition of *Pf*AdoMetDC activity of the bifunctional protein. MDL73811, the specific inhibitor of AdoMetDC, was used as a positive control to determine if decrease in the activity of *Pf*AdoMetDC was due to the presence of an inhibitor. Statistical analysis was performed using the paired Students t-test.

Chapter 3: Results

Part 3.1: High-level recombinant production of *Pf*AdoMetDC/ODC

3.1.1 Codon harmonisation of *Pf*AdoMetDC/ODC

The *P. falciparum adometdc/odc* gene sequence was codon harmonised and the *E. coli* highly expressed codon preference was used as the target codon preference table. Correlation between the *P. falciparum* codon usage frequency and harmonised codon usage frequency were checked graphically, and compared to the codon usage frequency of the recombinant expression host (*E. coli*) (Figure 3.1).

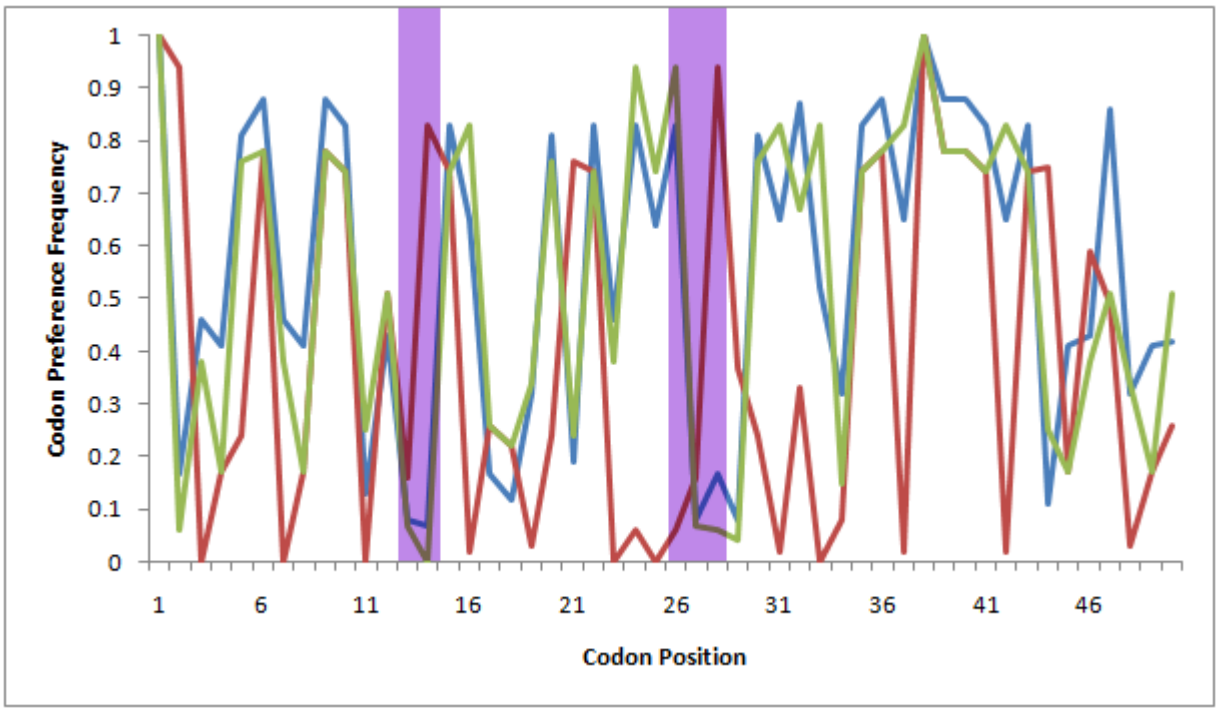

Figure 3.1: Codon harmonisation of *Pf*AdoMetDC/ODC. Representative image for the codon harmonisation of the first 50 codons of the *Pf*AdoMetDC/ODC gene. The blue line indicates the codon fraction for the original native *P. falciparum* AdoMetDC/ODC gene; the red line indicates the codon fraction usage in the *E. coli* target; the green line indicates the codon fraction usage of the codon harmonised gene. There is a good correlation between the native codon preference fraction and the harmonised codon preference fraction when the green and blue lines are in close proximity. Pause sites are indicated by the purple bars. Pause sites are conserved between the native and harmonised versions of the gene.

Codon harmonisation requires the harmonised gene sequence to use codons in *E. coli* that are used at the same frequency as those used by the native *P. falciparum* gene sequence. A good correlation was observed where the codon harmonised gene (Figure 3.1, green line) has a codon preference that is as close as possible to that of the codon preference frequency of the native *P. falciparum* gene (Figure 3.1, blue line). Matching these codon preferences preserves pause sites within the codon harmonised gene. A poor correlation is seen when the codon harmonised gene (Figure 3.1, green line) has a codon preference

frequency that is closer to the codon preference frequency of the *E. coli* genome (Figure 3.1, red line). This would result in a codon optimised gene and a change in the pause sites, which has the potential to affect the folding of the recombinant protein as the newly translated portion will not have enough time to achieve the correct fold. A good correlation to the codon preference for the wild-type gene sequence is observed throughout the harmonised gene sequence.

Four constructs of the *adometdc/odc* genes, containing portions of wild-type and codon harmonised sequences, were constructed (E. Human) (Figure 3.2): i) full-length wild-type *Pf*AdoMetDC/ODC (1 bp – 4260 bp, 1419 aa), ii) full-length harmonised AdoMetDC (1 bp – 4260 bp, 1419 aa), iii) wild-type AdoMetDC (1 bp – 1475 bp, 491 aa) linked to harmonised ODC (1476 bp – 4260 bp, 928 aa), and iv) harmonised AdoMetDC (1 bp – 1475 bp, 491 aa) linked to wild-type ODC (1476 bp – 4260 bp, 928 aa).

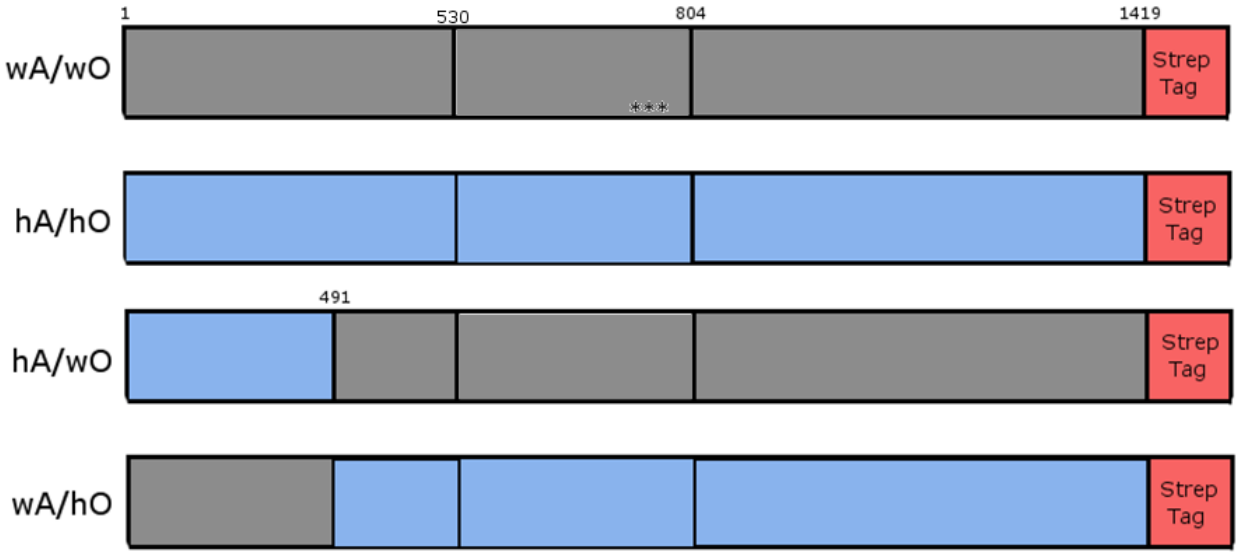

Figure 3.2: The four *Pf*AdoMetDC/ODC chimeric proteins. The *Pf*AdoMetDC/ODC chimeric proteins consist of a combination of wild-type (grey areas) and codon harmonised (blue areas) gene sequences. The hinge region between the *Pf*AdoMetDC and *Pf*ODC domains is located between amino acids 530 and 804. The asterisks indicate Shine-Dalgarno sites that were mutated in the original construct to remove incorrect translational start sites.

Positive clones were identified by E. Human via restriction enzyme digests of isolated plasmid DNA and by sequencing the inserted DNA.

3.1.2 Recombinant expression and isolation of *Pf*AdoMetDC/ODC

All four *Pf*AdoMetDC/ODC constructs in pASK-IBA3 from above were used to transform competent BL21(DE3) star cells. These cells were used to recombinantly express the various *Pf*AdoMetDC/ODC chimeric proteins. The recombinant proteins were subsequently isolated via cell disruption. A total protein sample was removed and the insoluble proteins were pelleted by ultracentrifugation. The concentrations of the total, soluble, and insoluble protein samples were determined by constructing a BSA standard curve (Figure 3.3).

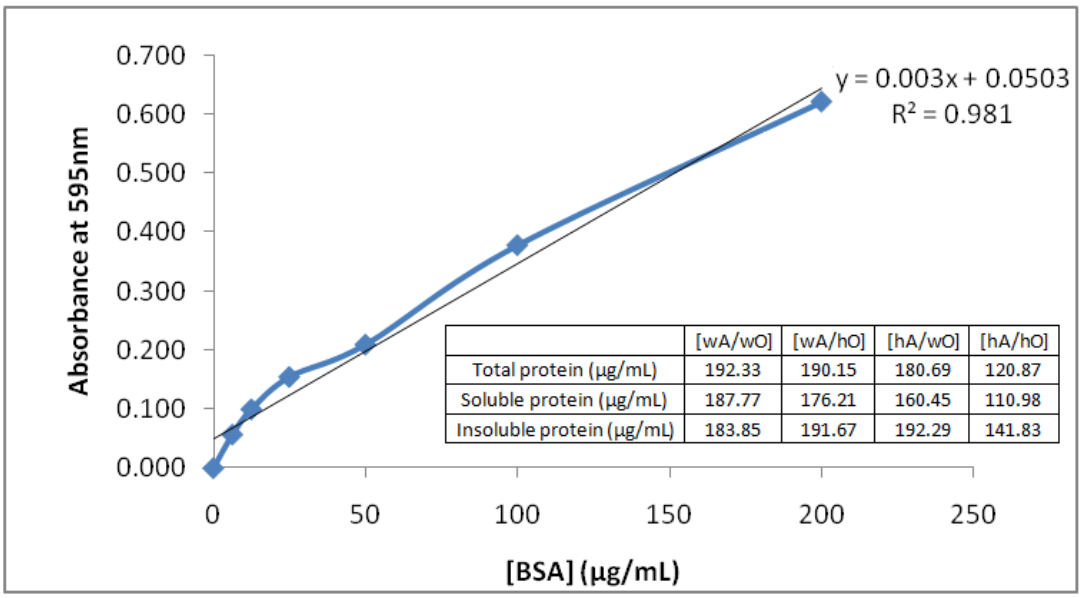

	[wA/wO]	[wA/hO]	[hA/wO]	[hA/hO]
Total protein (µg/mL)	192.33	190.15	180.69	120.87
Soluble protein (µg/mL)	187.77	176.21	160.45	110.98
Insoluble protein (µg/mL)	183.85	191.67	192.29	141.83

Figure 3.3: BSA standard curve for the determination of protein concentration. BSA standards with a concentration ranging from 0 to 200 µg/mL were used to construct a standard curve for the Bradford assay in order to determine the concentration of the protein samples. The table indicates the measured concentrations of the total protein, soluble protein and insoluble protein isolated for the four chimeric *Pf*AdoMetDC/ODC proteins.

Recombinant expression of wA/wO, wA/hO, and hA/wO resulted in similar total levels of protein produced around 180-190 µg/mL. However, recombinant expression of hA/hO resulted in markedly less protein at only 120 µg/mL (Figure 3.3). The total protein, soluble protein and insoluble protein samples for the four *Pf*AdoMetDC/ODC chimeric proteins were loaded quantitatively (2.8 µg each for total and soluble protein samples, and 2.3 µg for insoluble protein samples) on a 7.5% separating SDS-PAGE gel and separated by electrophoresis (Figure 3.4).

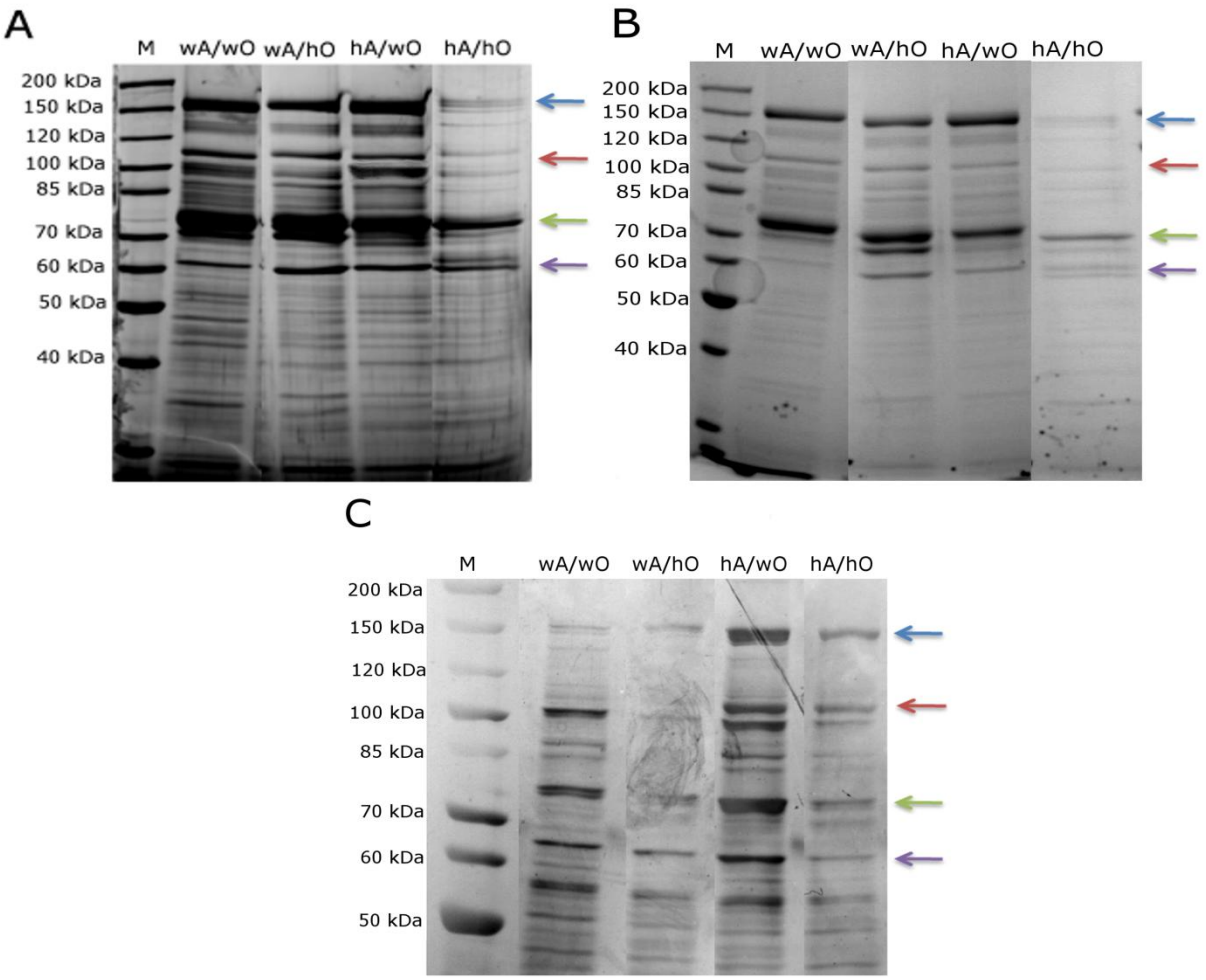

Figure 3.4: SDS-PAGE analysis of the four recombinantly expressed *Pf*AdoMetDC/ODC chimeric proteins. A: Total protein expressed (1.4 µg protein sample loaded in each well), B: soluble protein fraction (2.8 µg protein sample loaded in each well), and C: insoluble protein fraction (2.3 µg protein sample loaded in each well). Major protein bands observed at ~160 kDa (blue arrow), ~112 kDa (red arrow), ~70 kDa (green arrow), and ~60 kDa (purple arrow). Proteins separated using a 7.5% separating gel and visualised by silver staining (protein samples from non-parallel experiments).

Full length *Pf*AdoMetDC/ODC is expected to be seen at approximately 160 kDa. A band at ~160 kDa is present on the gel for the total isolated protein (Figure 3.4A, blue arrow) for all four constructs, with the full length harmonised construct (hA/hO) having a band at ~160 kDa with the least intensity. The gel for soluble proteins (Figure 3.4B, blue arrow) shows that the ~160 kDa is present in the soluble fraction. Major contaminating proteins were present at ~112 kDa (red arrow), ~70 kDa (green arrow) and ~60 kDa (purple arrow). The gel for insoluble proteins (Figure 3.4C) shows that the ~160 kDa protein is present for all four constructs, with the band for hA/wO having the greatest intensity and low levels of wA/wO and wA/hO present, indicating that hA/wO results in a major portion of *Pf*AdoMetDC/ODC being expressed insolubly. This is also true for hA/hO, where higher levels of the protein are present in the insoluble fraction than the soluble fraction. Higher levels of the ~112 kDa contaminating protein are present in the insoluble fraction than the soluble fraction for wA/wO, hA/wO, and hA/hO.

Since a *strep*-tag is present on the C-terminal on the recombinant *Pf*AdoMetDC/ODC proteins, it is possible to purify the protein samples via affinity chromatography to remove contaminating proteins that do not contain a *strep*-tag. The soluble protein samples were purified by s*trep*-tag affinity chromatography. The concentrations of the purified soluble protein samples were determined by constructing a BSA standard curve (Figure 3.5).

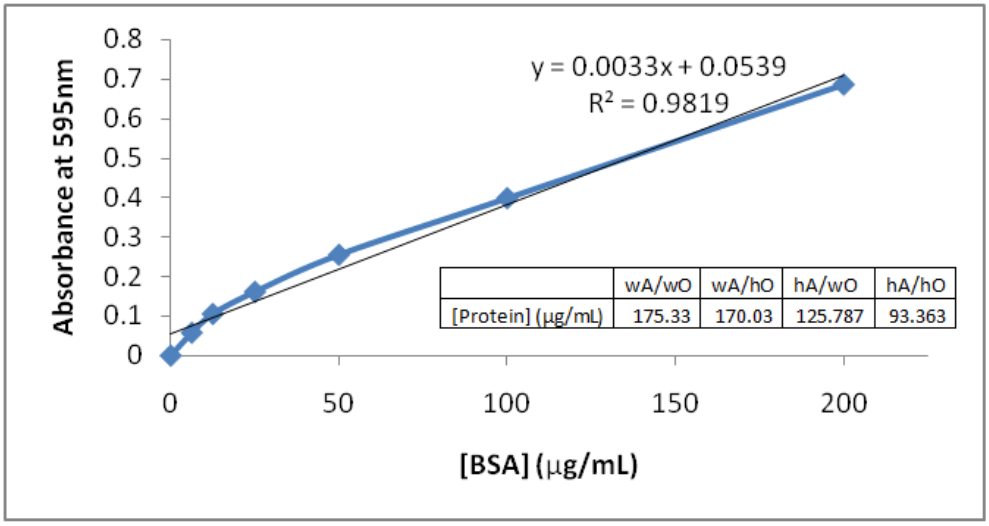

Figure 3.5: BSA standard curve for the determination of protein concentration. BSA standards with a concentration ranging from 0 to 200 µg/mL were used to construct a standard curve for the Bradford assay in order to determine the concentrations of the affinity chromatography purified samples. The table indicates the concentration of the chimeric *Pf*AdoMetDC/ODC proteins after purification.

The wA/wO and wA/hO chimeric proteins exhibited similar protein concentrations after purification (~170 µg/mL). The hA/wO and hA/hO chimeric proteins exhibited lower protein concentration after purification (Figure 3.5, inserted table). The purified protein samples were loaded quantitatively (2.3 µg) on a 7.5% separating SDS-PAGE gel and separated by electrophoresis (Figure 3.6).

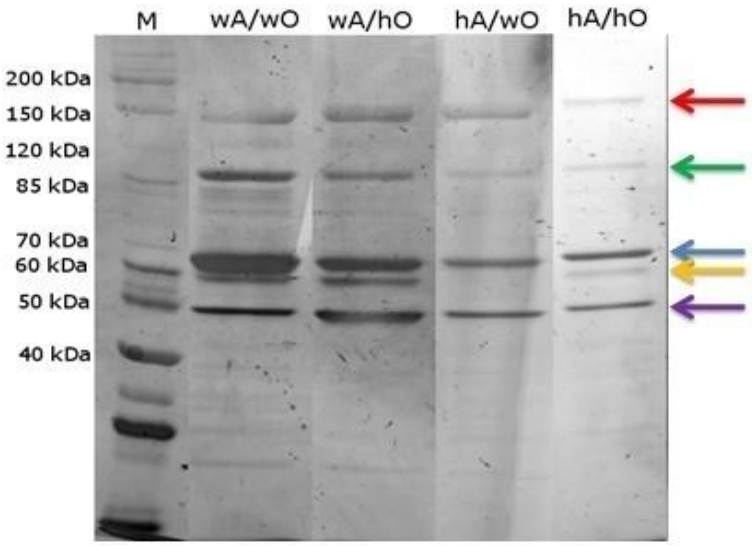

Figure 3.6: SDS-PAGE analysis of the purified soluble fraction of the four recombinantly expressed *Pf*AdoMetDC/ODC chimeric proteins. The four recombinantly expressed *Pf*AdoMetDC/ODC (wA/wO, hA/wO, wA/hO, and hA/hO) samples, after purification by affinity purification, were separated by a 7.5% separating gel. Protein samples were loaded on the same gel but non-uniform lighting during image capturing was observed across the gel. Bands at ~160 kDa (red arrow), ~112 kDa (green arrow), ~70 kDa (blue arrow), ~60 kDa (yellow arrow) and ~50 kDa (purple arrow) were observed. For each sample 2.3 µg of protein was loaded on the gel. Proteins separated using a 7.5% separating gel and visualised by silver staining.

As can be seen in Figure 3.6, the affinity purification of recombinantly expressed protein using *Strep*-Tactin Sepharose does not result in a completely homogenous protein solution. The ~160 kDa band (Figure 3.6, red arrow) representing *Pf*AdoMetDC/ODC is present for all constructs. However, major contaminating proteins are still present after affinity purification at ~112 kDa (Figure 3.6, green arrow), ~70 kDa (Figure 3.6, blue arrow), ~60 kDa (Figure 3.6, yellow arrow) and ~50 kDa (Figure 3.6, purple arrow). This implies either ineffective purification even under rigorously optimised conditions, the contaminating proteins contain a *Strep*-tag or these contaminating proteins interact with the *Strep*-tag containing *Pf*AdoMetDC/ODC chimeric proteins which allow them to co-elute with *Pf*AdoMetDC/ODC. Codon harmonisation did not improve the purity of recombinantly expressed *Pf*AdoMetDC/ODC.

3.1.3 Refolding of *Pf*AdoMetDC/ODC

As harmonisation did not improve the soluble expression of *Pf*AdoMetDC/ODC, protein refolding from inclusion bodies was investigated as a method for obtaining pure soluble protein. Densitometry was performed as a function of the percentage black of the protein bands. The more intense a protein band appears, the higher the percentage black for that protein band will have. Densitometric analysis (Figure 3.7) of the ~160 kDa band of the purified soluble (Figure 3.6) and insoluble (Figure 3.4C) fractions shows that the constructs with a wild-type *Pf*AdoMetDC domain have more *Pf*AdoMetDC/ODC present in the soluble fraction than the insoluble fraction. When the AdoMetDC domain is harmonised there is a

decrease in the amount of *Pf*AdoMetDC/ODC found in the soluble fraction, and an increase in the insoluble fraction. Small variations were observed between the intensity of the bands for the soluble and insoluble wA/wO and wA/hO protein bands. Harmonisation of the *Pf*AdoMetDC domain resulted in a decrease in soluble expression, and an increase in insoluble expression of *Pf*AdoMetDC/ODC.

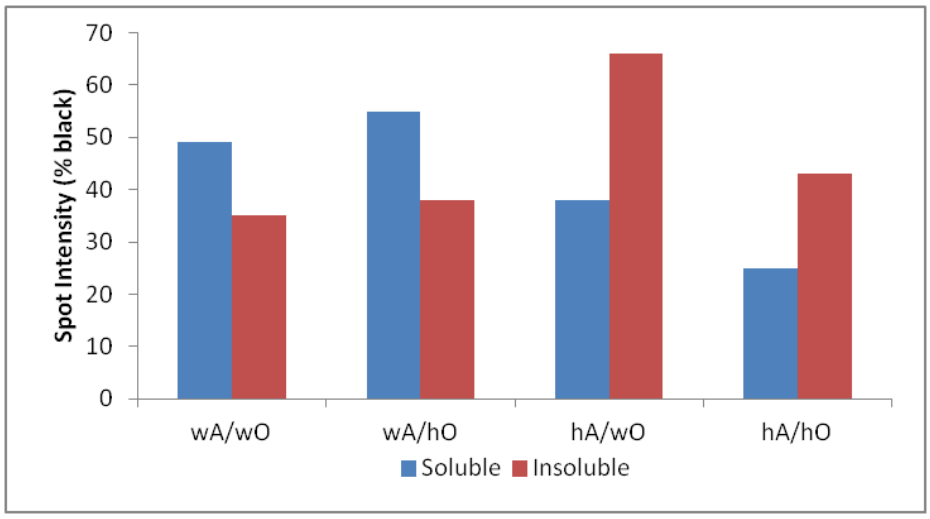

Figure 3.7: Densitometry of soluble and insoluble *Pf*AdoMetDC/ODC for all four chimeric proteins. The intensity of the protein bands for the quantitatively loaded soluble and insoluble *Pf*AdoMetDC/ODC for the four chimeric proteins were measured as a function of the percent black that the bands were.

In order to confirm that the insolubly expressed ~160 kDa protein band in Figure 3.4C (blue arrow) represents *Pf*AdoMetDC/ODC for all the chimeric proteins, Western blot analysis was performed using *Strep* II-HRP conjugated antibody (Figure 3.8). A protein band was present at ~160 kDa for wA/hO, hA/wO and hA/hO, with hA/wO band having the highest intensity. wA/wO was not detected on the Western blot. This may be due to the low concentrations of wA/wO present in the insoluble fraction. The ~112 kDa and ~70 kDa N-terminal deletions of *Pf*AdoMetDC/ODC were also observed on the Western blot.

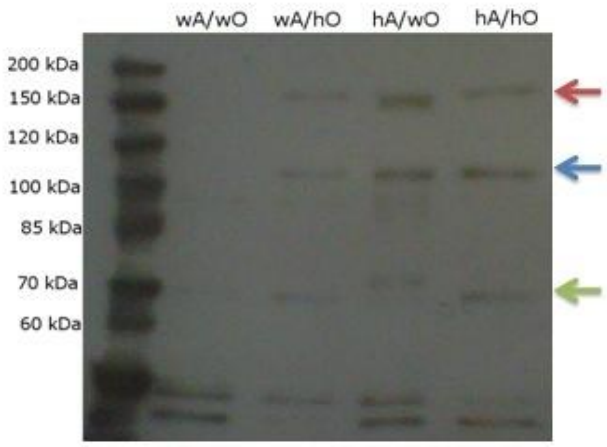

Figure 3.8: Western blot analysis of the insoluble expressed fractions of the *Pf*AdoMetDC/ODC chimeric proteins. Western blot analysis of the insoluble fraction of the recombinantly expressed *Pf*AdoMetDC/ODC chimeric proteins (Figure 3.4C). Protein bands observed at ~160 kDa (red arrow), ~112 kDa (blue arrow), and ~70 kDa (green arrow).

A band at ~160 kDa (Figure 3.8, red arrow) shows that *Pf*AdoMetDC/ODC is expressed as inclusion bodies and is a candidate for refolding, however, wA/wO appears to not be expressed insolubly. The ~112 kDa (Figure 3.8, blue arrow) and ~70 kDa (Figure 3.8, green arrow) N-terminal deletions are also insolubly expressed.

Since the hA/wO construct had the highest insoluble expression when compared to the other constructs, it was used to determine whether refolding by the detergent and KCl methods are able to correctly refold *Pf*AdoMetDC/ODC from inclusion bodies. However, neither method was successful at refolding *Pf*AdoMetDC/ODC from inclusion bodies. SDS-PAGE analysis of the refolded proteins showed no bands, indicating that the proteins did not refold and was thus removed during one of the centrifugation steps.

3.1.4 Identification of recombinantly expressed proteins

Since the recombinant *Pf*AdoMetDC/ODC constructs all contain a *Strep*-tag it is possible to confirm their presence in a protein sample via Western blotting with the use of a *Strep* II-HRP conjugated antibody. If the contaminating proteins are recombinantly expressed from the plasmid and their *Strep*-tag is still present, they will also be detected on the Western blot. Native *E. coli* proteins are not expected to be detected during Western blotting using a anti-*Strep* II-HRP conjugated antibody as a *Strep*-tag is not present. The Unstained PageRuler marker proteins contain an inherent *Strep*-tag and will also be visible on a Western blot using an anti-*Strep* antibody. Protein samples were loaded quantitatively on the blot at 2.3 µg.

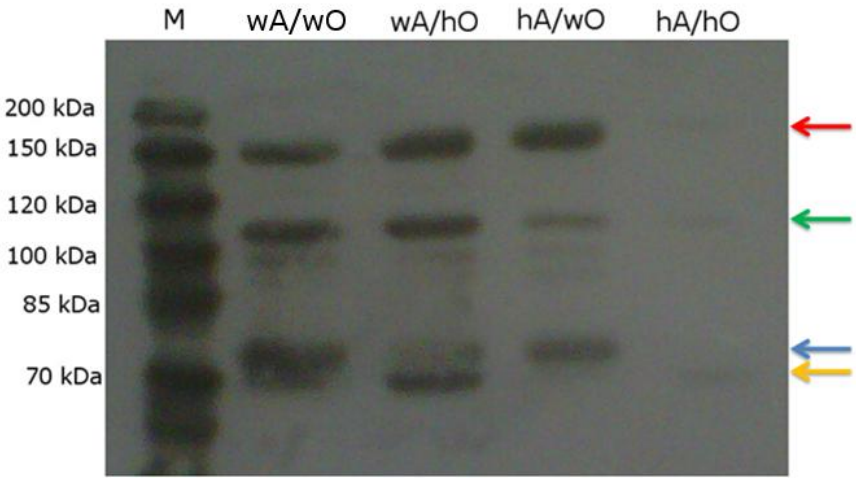

Figure 3.9: Western blot analysis of the purified soluble fraction of the four recombinantly expressed *Pf*AdoMetDC/ODC chimeric proteins. Western blot analysis of the recombinantly expressed *Pf*AdoMetDC/ODC chimeric proteins, using a *Strep*-II-HRP conjugated antibody to visualise proteins that contain a *Strep*-tag. Protein bands presents at ~160 kDa (red arrow), ~112 kDa (green arrow), ~70 kDa (blue arrow), and ~60 kDa (yellow arrow). Protein samples were loaded quantitatively on the blot at 2.3 µg.

Western blot analysis shows bands at ~160 kDa (Figure 3.9, red arrow), bands at ~112 kDa (Figure 3.9, green arrow) and bands at ~70 kDa (Figure 3.9, blue arrow) for the wA/wO, hA/wO and wA/hO samples. Very faint bands are also observable for the hA/hO purified

protein sample. Since the ~160 kDa band is detected on the Western blot it confirms the recombinant expression of *Pf*AdoMetDC/ODC for all four constructs. Since the bands at ~112 kDa, ~70 kDa and ~60 kDa are all identified with the *Strep*-tag, it could indicate that these proteins are truncated or degraded versions of *Pf*AdoMetDC/ODC. The protein bands at ~160 kDa, ~112 kDa, ~70 kDa, ~60 kDa, and ~50 kDa were isolated and sent for identification via LC-MS/MS. The identities of the bands are summarised in Table 3.1.

Table 3.1: LC-MS/MS identification of bands observed on the SDS-PAGE gel.

Band (kDa)	Accession Number	Description	Database	Score[a]	Coverage (%)[b]	#PSMs[c]	#Peptides[d]
160	PF10_0322	AdoMetDC/ODC, *P. falciparum*	PlasmoDB	462	7.47	11	11
112	PF10_0322	AdoMetDC/ODC, *P. falciparum*	PlasmoDB	415	6.62	11	11
70	PF10_0322	AdoMetDC/ODC, *P. falciparum*	PlasmoDB	110	3.61	5	5
70	A1A766	DnaK, *E. coli*	Swissprot, all entries	225	12.51	5	5
60	PF10_0322	AdoMetDC/ODC, *P. falciparum*	PlasmoDB	103	3.42	4	4
50	A1AJ51	GroEL, *E. coli*	Swissprot, all entries	250	14	6	6

a: the protein score is the sum of the highest ions score for each distinct sequence identified by LC-MS/MS.
b: the percentage coverage the peptides had for the identified protein.
c: peptide spectrum match, the number of peptides identified for the sample.
d: the number of unique peptides identified for screening against databases for identification of the protein

A comparison of the MS results indicating peptide coverage over the proteins submitted with the sizes of the bands obtained by SDS-PAGE, provided information on the possible sites of truncation of the proteins. As such, the bands at ~160 kDa represent full-length recombinantly expressed *Pf*AdoMetDC/ODC. However, the bands at ~112 kDa, ~70 kDa and ~60 kDa represent N-terminal truncated versions of *Pf*AdoMetDC/ODC (Figure 3.10). As an example, peptide coverage was only obtained from amino acid 432 onwards for the MS result, confirming a 47 kDa truncation and correlating to the ~112 kDa band seen with SDS-PAGE.

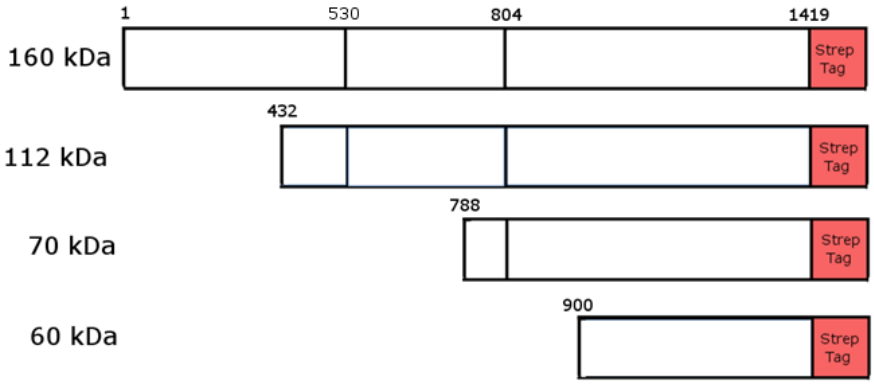

Figure 3.10: Diagrammatic representation of the N-terminal truncated *Pf*AdoMetDC/ODC chimeric proteins. LC-MS/MS determined that the ~112 kDa, ~70 kDa, and ~60 kDa protein bands were N-terminal truncated version of *Pf*AdoMetDC/ODC. Sites of truncations estimated by protein band sizes observed on the SDS-PAGE gel (Figure 3.6) and peptides identified by LC-MS/MS.

Since the *Strep*-tag is on the C-terminal of *Pf*AdoMetDC/ODC the cleavage of amino acids from the N-terminus of the protein will retain the *Strep*-tag on the truncated proteins and will be purified along with the full-length *Pf*AdoMetDC/ODC during affinity chromatography and will be detected on Western blots when using the *Strep*-II-HRP antibody. The band at ~50 kDa was not detected by Western blotting using the *Strep*-II-HRP antibody, indicating that it may be of *E. coli* origin due to lack of a *Strep*-tag. This was confirmed by mass spectrometry, which identified it as the *E. coli* chaperone GroEL. The band at ~70 kDa also contained the *E. coli* chaperone DnaK.

3.1.5 Activity of the *Pf*AdoMetDC/ODC chimeric proteins

Enzyme activity assays for the *Pf*AdoMetDC and *Pf*ODC domain of the four *Pf*AdoMetDC/ODC chimeric proteins were performed in order to determine the effect codon harmonisation had on the activities of each domain (Figure 3.11).

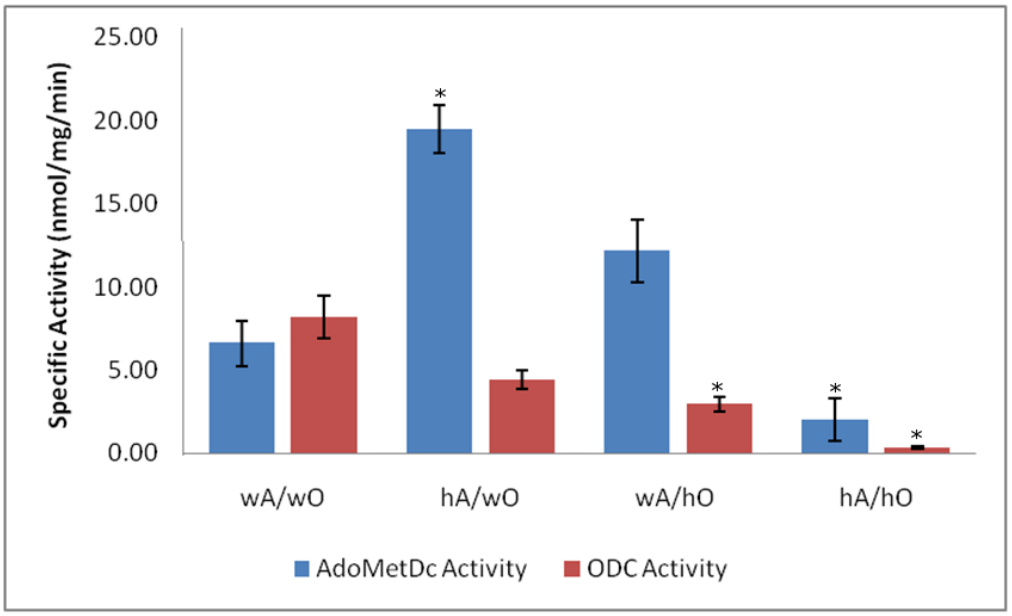

Figure 3.11: Specific activity for *Pf*AdoMetDC and *Pf*ODC for the four *Pf*AdoMetDC/ODC chimeric proteins. The specific activities for the *Pf*AdoMetDC and *Pf*ODC domains for all of the chimeric proteins were tested using a radioactive enzyme assay. Data are represented for three independent biological replicates (n=3) each performed in duplicate, SEM indicated. . (* indicates significance at $P<0.05$).

Harmonisation of only the *Pf*AdoMetDC domain significantly increases the activity of the *Pf*AdoMetDC nearly 3-fold ($P<0.05$, n=3), but insignificantly decreases the activity of the wild-type *Pf*ODC domain by almost half ($P>0.05$, n=3). Harmonisation of only the *Pf*ODC domain significantly decreases the activity of *Pf*ODC by approximately two-thirds ($P<0.05$, n=3), but insignificantly increases the activity of the wild-type *Pf*AdoMetDC domain by nearly 2-fold ($P>0.05$, n=3). Harmonisation of both domains results in a significant decrease of activity for both domains, with *Pf*ODC activity barely detected and *Pf*AdoMetDC activity approximately a third of that of the *Pf*AdoMetDC activity of the full-length wild-type *Pf*AdoMetDC/ODC ($P<0.05$, n=3).

Codon harmonisation did not result in a major improvement on the expression levels or purity of recombinant *Pf*AdoMetDC/ODC. Previous attempts at improving the recombinant expression of the monofunctional *Pf*AdoMetDC domain by codon harmonisation resulted in an improvement in the expression levels as well as the stability of monofunctional *Pf*AdoMetDC. Codon harmonisation of the *Pf*AdoMetDC domain resulted in a 10-fold increase in expression of the α-subunit of *Pf*AdoMetDC. Harmonisation of PfAdoMetDC improved the stability of the enzyme as activity was maintained after storage for two weeks at 4 and−20 ◦C. There was also a reduction of Hsp-70 co-purification in the *Pf*AdoMetDC sample, indicating that there was less pressure placed on *E. coli* during protein translation and folding [129]. Due to the improvement of expression of the monofunctional codon harmonised *Pf*AdoMetDC domain the effects of codon harmonisation of the monofunctional *Pf*ODC domain was subsequently investigated (see section 3.1.6).

3.1.6 Codon harmonisation of *Pf*ODC

As for the *P. falciparum* AdoMetDC/ODC gene sequence, the *Pf*ODC gene sequence was codon harmonised using the algorithm on the SAMI website for *E. coli* highly expressed codon preference as the target codon preference table. Correlation between the *P. falciparum* and harmonised codon preferences were checked graphically (Figure 3.12) and was shown to have a good correlation throughout the gene.

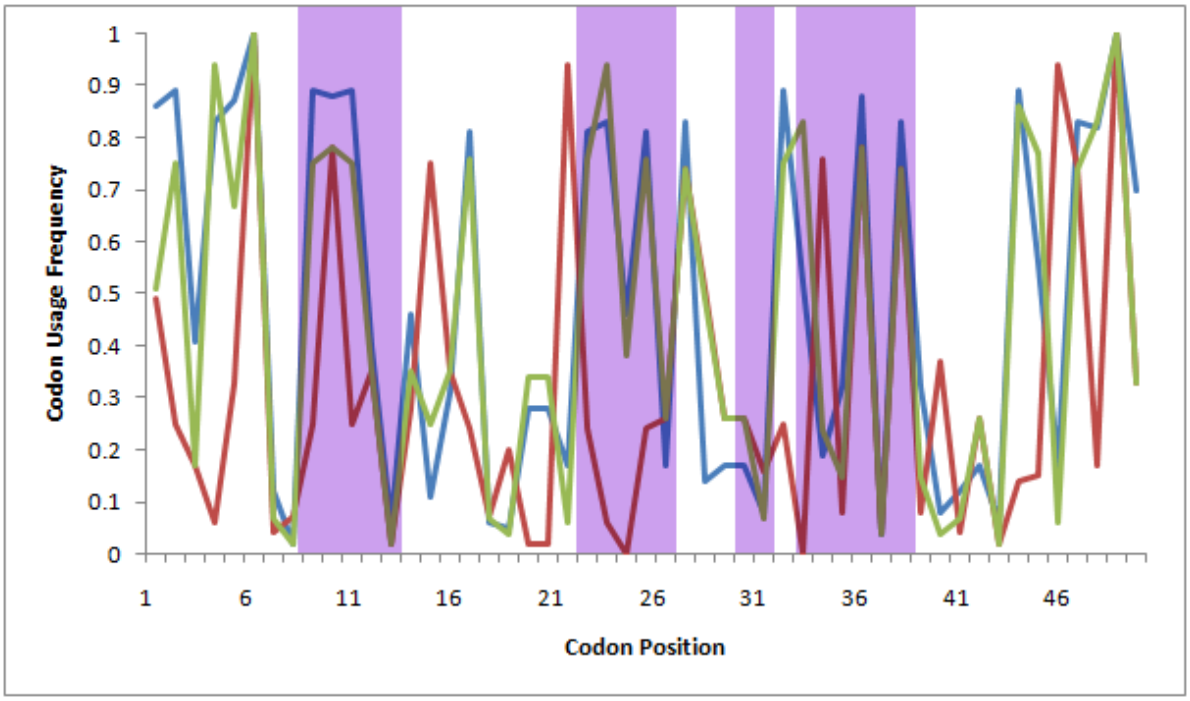

Figure 3.12: Codon harmonisation of *Pf*ODC. Representative image for the codon harmonisation of *Pf*ODC, showing the first 50 codons. The blue line indicates the codon fraction for the original native *P. falciparum odc* gene; the red line indicates the codon fraction usage in the *E. coli* target; the green line indicates the codon harmonised fraction. Purple bars indicate the predicted pause sites.

There is a good correlation between the native codon preference fraction and the harmonised codon preference fraction when the green and blue lines are in close proximity. Pause sites are conserved between the native and harmonised versions of the gene.

Two constructs of the *Pf*ODC domain were created with either wild-type (wODC) or codon harmonised (hODC) gene sequences (Figure 3.13).

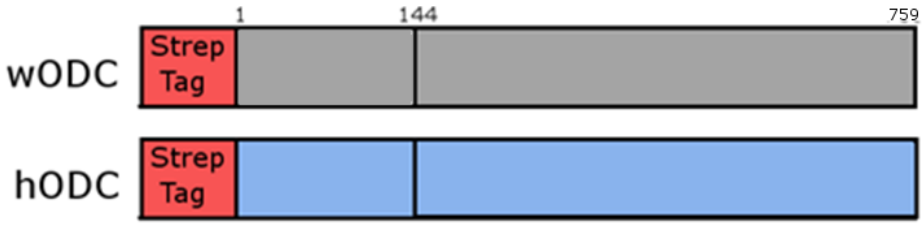

Figure 3.13: Diagrammatic representation of the two *Pf*ODC constructs. Wild-type (wODC) and harmonised (hODC) constructs of the *Pf*ODC gene. Blue areas indicate gene sequences that are codon harmonised, and grey area indicates the wild-type gene sequence.

3.1.7 Recombinant expression and isolation of *Pf*ODC

Expression of the various forms of the monofunctional *Pf*ODC domain was performed as for the full-length *Pf*AdoMetDC/ODC constructs, but with induction for only four hours at 30°C [85]. Total, soluble, and insoluble protein samples were separated by gel electrophoresis to determine in which fraction the *Pf*ODC proteins are expressed (Figure 3.14).

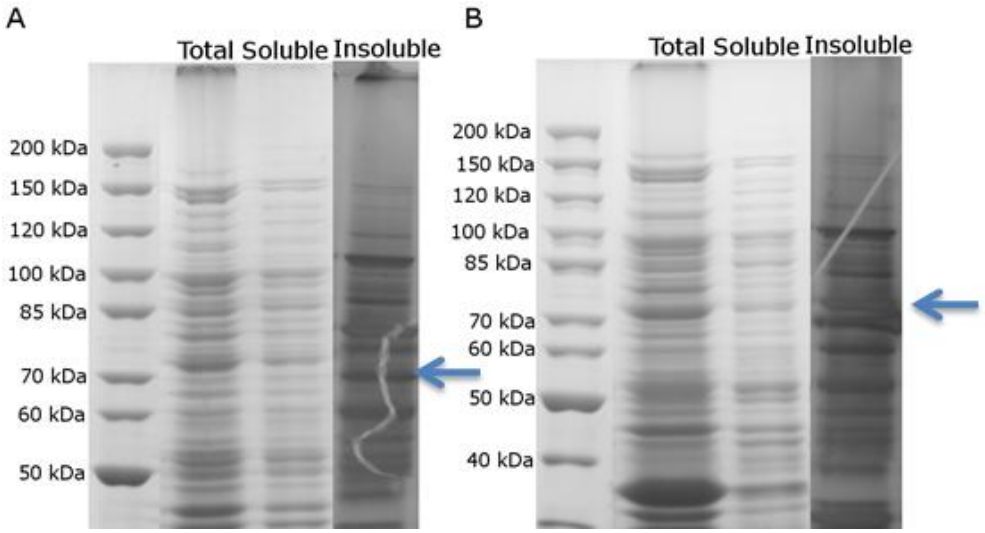

Figure 3.14 SDS-PAGE analyses of the recombinantly expressed *Pf*ODC proteins. A: The total, soluble, and insoluble protein fraction for wODC. B: The total, soluble, and insoluble protein fraction for hODC. Proteins were not quantitatively loaded (non-parallel experiments). Blue arrow indicates the size at which the recombinant monofunctional *Pf*ODC protein is expected to be expressed. Proteins separated using a 7.5% separating gel and visualised by silver staining.

*Pf*ODC is expected to be expressed at approximately 70 kDa. A protein band was present at ~70 kDa for both wODC and hODC for the total, soluble and insoluble fractions (Figure 3.14, blue arrows). After isolating and purifying the recombinantly expressed proteins via *Strep*-Tag affinity chromatography, the concentration of the purified samples was determined via the Bradford method using a BSA standard curve (Figure 3.15).

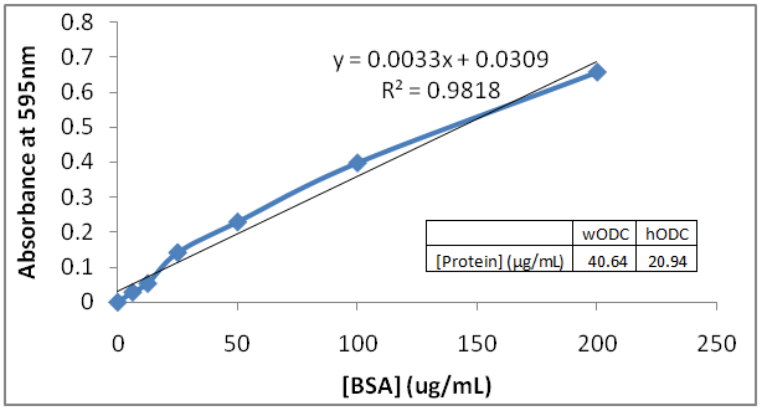

Figure 3.15: BSA standard curve for the determination of protein concentration. BSA standards with a concentration ranging from 0 to 200 µg/mL were used to construct a standard curve for the Bradford assay in order to determine the concentration of the affinity chromatography purified protein samples. Table indicates the concentration for purified wODC and hODC

The purified wODC protein was recombinantly expressed at approximately double the concentration of the purified hODC protein (Figure 3.15). Purified soluble wODC and hODC samples and insoluble wODC and hODC were loaded quantitatively (0.5 µg) on an SDS-PAGE gel with a 7.5% separating gel. SDS-PAGE gel analysis showed that the expression of both constructs yielded low levels of soluble *Pf*ODC with contaminating proteins present even after purification (Figure 3.16A).

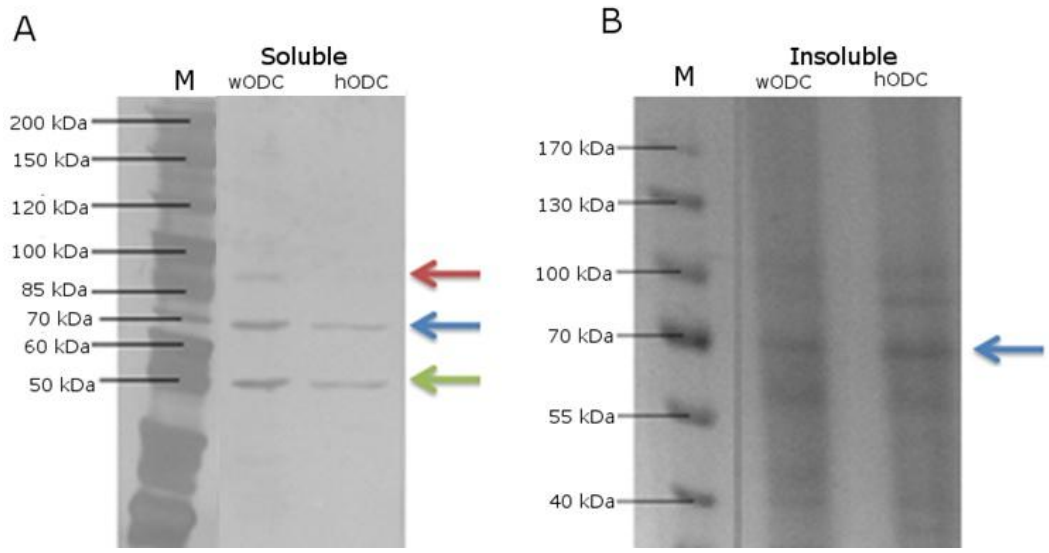

Figure 3.16: SDS-PAGE analysis of the purified soluble fraction and insoluble fraction of the two recombinantly expressed *Pf*ODC proteins. The wODC and hODC proteins were expressed in BL21(DE3) Star cells, isolated and soluble protein fractions were purified by affinity purification. Purified protein samples (A) and insoluble protein samples (B) were separated on a 7.5% separating gel. Soluble proteins were visualised by silver staining and insoluble proteins were visualised by Coomassie Staining. Protein samples loaded quantitatively at 0.5 µg.

The protein band at ~70 kDa is expected to represent recombinantly expressed *Pf*ODC (Figure 3.16A, blue arrow). Contaminating proteins are present at ~85 kDa (Figure 3.16A, red arrow) and ~50 kDa (Figure 3.16A, green arrow) for the wODC sample. The ~85 kDa band was not observed in the soluble hODC sample. The *Pf*ODC constructs are also present as insoluble inclusion bodies (Figure 3.16B, blue arrow).

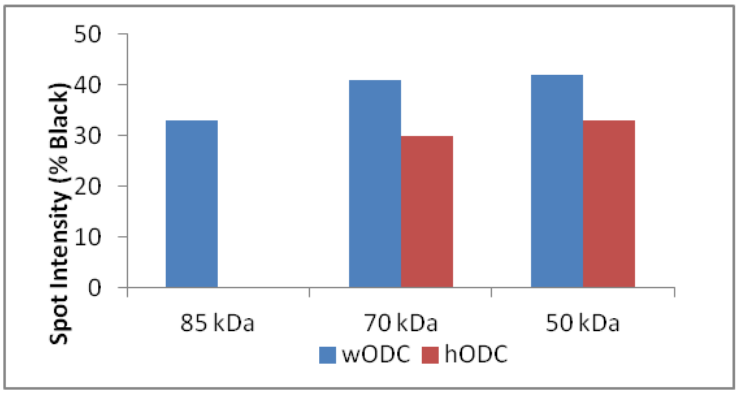

Figure 3.17: Densitometric analysis of the soluble wODC and hODC samples. The intensity of the ~50 kDa, ~70 kDa and ~85 kDa protein bands for the soluble wODC and hODC samples in Figure 3.16A were measured by their percentage black.

Densitometric analysis (Figure 3.17) of the soluble wODC and hODC samples confirmed that the ~70 kDa band and the ~85 kDa and ~50 kDa contaminating bands have a higher intensity for the wODC sample than the hODC sample. This indicates that harmonisation did not improve the expression levels of recombinant monofunctional *Pf*ODC.

3.1.8 Identification of recombinantly expressed proteins

To confirm that ODC was expressed in the soluble fraction, Western blot analysis (Figure 3.18) was performed using a *Strep*-II-HRP conjugated antibody that will visualise the presence of proteins that contain a *Strep*-tag.

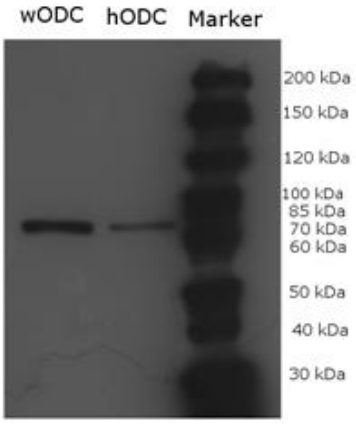

Figure 3.18: Western blot analysis of the soluble fraction of the recombinantly expressed *Pf*ODC constructs. Western blot analysis of the SDS-PAGE gel in Figure 3.16A reveals only the protein band at ~70 kDa.

Only the band at ~70 kDa (Figure 3.16A, blue arrow) was observed on the Western blot (Figure 3.19), indicating that *Pf*ODC was expressed in both wild-type and harmonised forms. The bands at ~85 kDa (Figure 3.16A, red arrow) and ~50 kDa (Figure 3.16A, green arrow) were not observed on the Western blot.

To confirm the identities of the contaminating bands observed on the SDS-PAGE for the soluble fraction (Figure 3.16) mass spectrometry was performed. The bands at ~85 kDa, ~70 kDa, and ~50 kDa were cut out of the gel and prepared for mass spectrometry. The bands were identified by LC-MS/MS (Table 3.2).

Table 3.2: LC-MS/MS identification of bands observed on the SDS-PAGE gel.

Band (kDa)	Accession Number	Description	Database	Score[a]	ΣCoverage[b] (%)	Σ# PSMs[c]	Σ# Peptides[d]
70	PF10_0322	AdoMetDC/ODC, *P. falciparum*	PlasmoDB	104.02	3.49	5	5
	A7ZHA4	DnaK. *E. coli*	Swissprot, all entries	380.33	30.88	31	15
50	PF10_0322	AdoMetDC/ODC, *P. falciparum*	PlasmoDB	107.37	3.56	4	4
	A1AJ51	GroEL, *E. coli*	Swissprot, all entries	265.04	15.15	7	7
85	P85912	Unknown protein 12, *Pseudotsuga menziesii*	Swissprot, all entries	0.00	100	1	1
	Q756G2	Probable E3 ubiquitin-protein ligase, *Ashbya gossypii*	Swissprot, all entries	0.00	0.25	1	1

a: the protein score is the sum of the highest ions score for each distinct sequence identified by LC-MS/MS.
b: the percentage coverage the peptides had for the identified protein.
c: peptide spectrum match, the number of peptides identified for the sample.
d: the number of unique peptides identified for screening against databases for identification of the protein

The ~70 kDa and ~50 kDa protein bands were good hits for *Pf*AdoMetDC/ODC using the PlasmoDB database, indicating that they are *Pf*ODC. The ~85 kDa protein band had no good hits for all databases tested. The possible proteins identified by LC-MS/MS for the ~85 kDa protein band were misannotations for an eight amino acid long protein from *Pseudotsuga menziesii* with unknown function, and a 372.2 kDa probable E3 ubiquitin-protein ligase from *Ashbya gossypii.* Since the ~50 kDa protein band was not detected via Western blotting using a *Strep*-II-HRP conjugated antibody it is probably an N-terminal truncation of the recombinant *Pf*ODC due to the absence of a *Strep*-tag. The four *Pf*ODC peptides identified in the LC-MS/MS sample appeared to cluster around the C-terminal of the protein. However, the coverage was not high enough to be able to conclusively determine this.

3.1.9 Native-PAGE

To determine whether the proteins seen on the SDS-PAGE gel at ~85 kDa (Figure 3.16, blue arrow) and ~50 kDa (Figure 3.16, purple arrow) bind to or have interactions with the recombinantly expressed *Pf*ODC which allows them to elute from the *Strep*-tactin columns with *Pf*ODC a native-PAGE gel was used to analyse the protein sample. Native-PAGE works under the same principles as SDS-PAGE (section 2.1.3.4), but reducing agents such as SDS and mercaptoethanol are not present in the solutions used, and samples are not boiled before loading on the gel. Under native conditions, proteins that form a complex or interact with each other will not separate as they do on an SDS-PAGE gel and will appear as a single protein band. If there are multiple protein bands present then the proteins do not interact with each other.

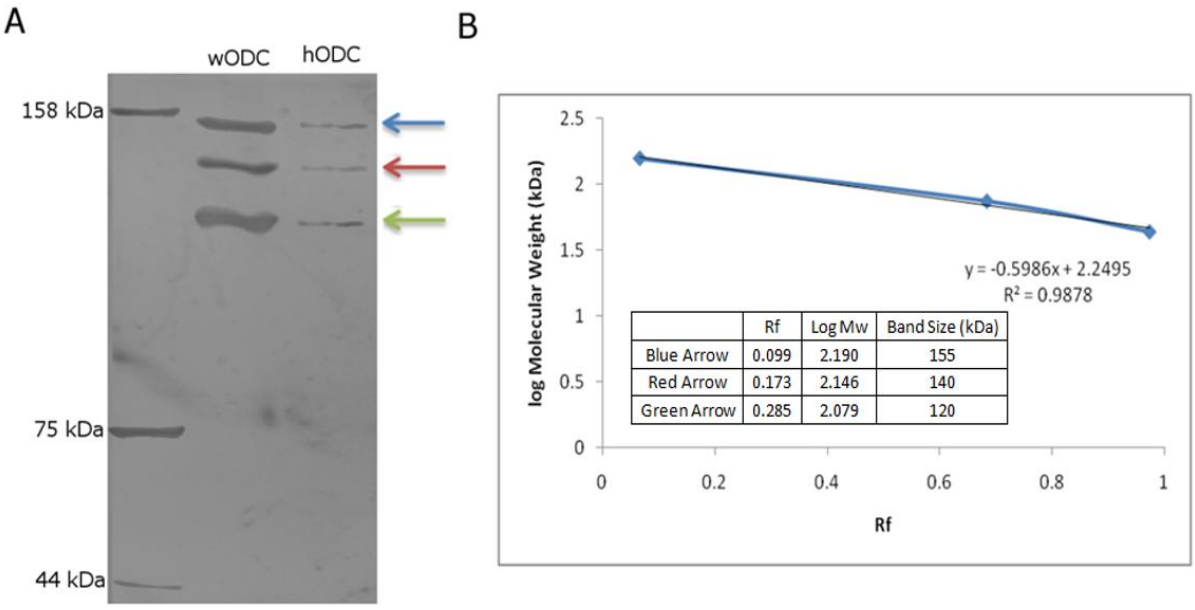

Figure 3.19: Native-PAGE analysis of recombinantly expressed wODC and hODC. **(**A): Recombinantly expressed and purified wODC and hODC samples were separated in native conditions to determine whether contaminating proteins were interacting with them and thus eluting from the *Strep*tactin column during affinity chromatography with the recombinantly expressed samples. Aldolase (158 kDa), Ovalbumin (44 kDa) and Conalbumin (75 kDa) were used as protein standards. For both wODC and hODC, three bands were observed between the 158 kDa and 75 kDa markers. Proteins separated using a 12% separating gel and visualised by silver staining. (B): Rf analysis was performed using the distance travelled by the marker protein bands to determine the sizes of the protein bands in the samples. The blue arrow indicates a protein band of ~155 kDa, the red arrow indicates a protein band of ~140 kDa, and the green arrow indicates a protein band of 120 kDa (in Figure 3.19A).

Native-PAGE (Figure 3.19) indicates three bands between the 158 kDa and 75 kDa marker protein bands. Since active *Pf*ODC is found as a dimer, the band at ~140 kDa (Figure 3.19, red arrow) is expected to represent dimeric *Pf*ODC. The truncated version of *Pf*ODC (~50 kDa protein) may be able to bind to the ~70 kDa protein, resulting in a 120 kDa protein complex. This may be represented by the band above the 75 kDa marker (Figure 3.19, green arrow). The band above the 75 kDa marker may also represent the ~70 kDa *Pf*ODC that associated with the GroEL *E. coli* chaperone protein that was also identified to be present in the ~50 kDa band via LC-MS/MS. If the ~85 kDa is able to bind to the ~70 kDa *Pf*ODC then a complex of approximately 155 kDa will be formed. A band is present for both the wODC and hODC samples just under the 158 kDa marker protein (Figure 3.19, blue arrow) that may represent this interaction. These interactions will explain why the ~85 kDa and ~50 kDa are not removed during affinity purification despite their lack of a *Strep*-tag.

Other interactions that may be possible include the truncated (~50 kDa) *Pf*ODC may also be able to dimerise to form a ~100 kDa dimer. The ~50 kDa and ~85 kDa proteins may be able to interact with each other to result in a 135 kDa protein. However, neither of these scenarios would be able to explain how they co-elute from the *Strep*tactin column with the ~70 kDa *Pf*ODC during affinity chromatography, as they lack a *Step*-tag or interactions with a protein containing a S*trep*-tag.

3.1.10 Refolding of recombinant proteins from inclusion bodies

Since a portion of the recombinant *Pf*ODC is expressed in the insoluble fraction (Figure 3.16B), it may be possible to refold the insoluble protein so that it could be in a soluble and active form. In order to determine whether these constructs are viable candidates for refolding from inclusion bodies, Western blot analysis of the insoluble fraction after ultracentrifugation was performed as above for *Pf*AdoMetDC/ODC (section 3.1.2).

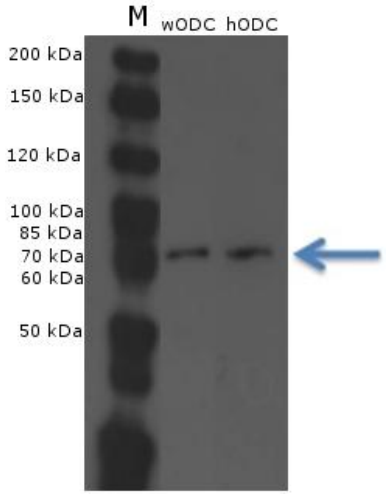

Figure 3.20: Western blot analysis of insolubly expressed proteins detected via *Strep*-II-HRP conjugated antibodies. Western blot analysis of the insoluble fraction (SDS-PAGE gel in Figure 3.16B) reveals only the protein band at ~70 kDa.

The Western blot showed that both the wild-type and harmonised constructs of *Pf*ODC are expressed in the insoluble fraction (Figure 3.20, blue arrow) and may be candidates for protein refolding. Refolding was performed by the detergent and KCl methods. The purified refolded protein samples were loaded and separated on a 7.5% separating SDS-PAGE gel (Figure 3.21).

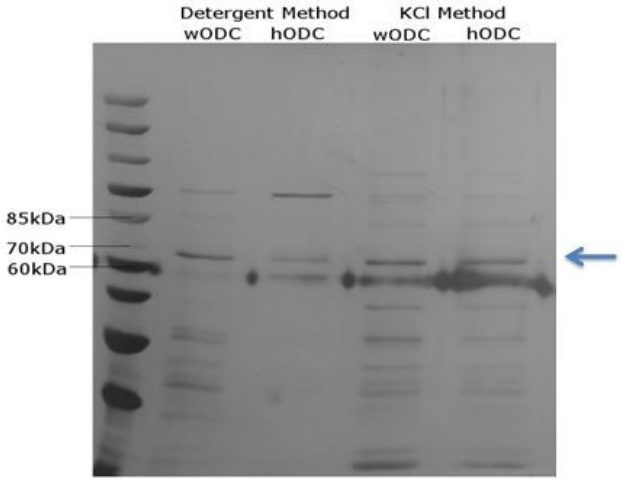

Figure 3.21: SDS-PAGE analysis of wODC and hODC inclusion bodies refolded via the detergent and KCl refolding methods. wODC and hODC inclusion bodies were refolded using the detergent and KCl methods. Both methods resulted in a prominent band at ~70kDa for the wODC and hODC samples (blue arrow). Multiple contaminating protein bands were present. Proteins separated using a 7.5% separating gel and visualised by silver staining.

A band at ~70 kDa was observed for both *Pf*ODC proteins for the refolding methods tested on the SDS-PAGE (Figure 3.21, blue arrow) that could indicate the presence of resolubilised monomeric *Pf*ODC domains. Other protein bands are present on the gel. These may represent native *E. coli* and truncated recombinantly expressed proteins that were insolubly expressed, but were also resolubilised during the refolding procedures. These proteins may not have been efficiently removed during affinity chromatography, or they may have interactions with the *Pf*ODC proteins that allow them to co-elute with *Pf*ODC during affinity chromatography.

Western blot analysis of the resolubilised proteins was also performed but no protein bands were present on the blot for the samples. This may have been due to the *Strep*-tag being made inaccessible to the *Strep*-II-HRP conjugated antibody during the refolding process. PageRuler Unstained Protein Marker bands were observed on the Western blot, additionally serving as a positive control, indicating that there was not an error in the blotting process.

3.1.11 Activity of refolded *Pf*ODC

Since it was not possible to detect whether wODC and hODC were present in the resolubilised protein solutions via Western blotting, another approach to detect whether active *Pf*ODC is present is via an *Pf*ODC activity assay (Figure 3.22). The assay will determine if the suspected resolubilised *Pf*ODC proteins were refolded into an enzymatically active confirmation.

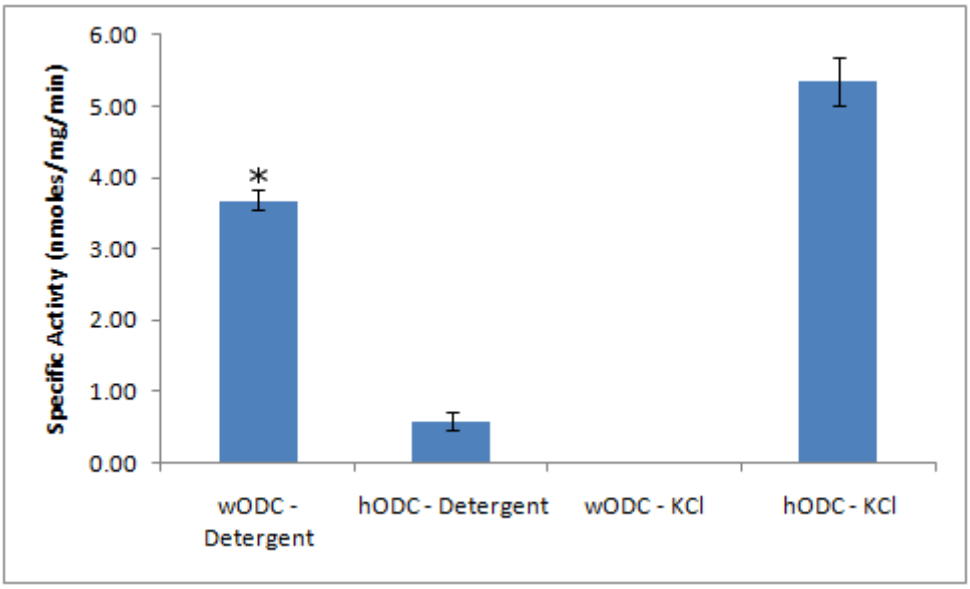

Figure 3.22: Results of the activity assay for wild-type and harmonised *Pf*ODC refolded by the detergent and KCl methods. To determine whether refolded proteins displayed *Pf*ODC activity, a *Pf*ODC activity assay was performed. Data are represented for three independent biological replicates (n=3) each performed in duplicate, SEM indicated (* indicates significance at $P<0.05$).

The refolded proteins had less activity when compared to their soluble counterparts. wODC refolded by the detergent method exhibited an activity of 3.6 nmoles/mg/min, a significant

decrease in activity when compared to wODC from the soluble fraction (15.6 nmoles/mg/min) (P<0.05, n=3). KCl refolded wODC exhibited no activity. Detergent refolded hODC showed an activity of 0.6 nmoles/mg/min, approximately 10.5-fold lower activity than soluble hODC (6.1 nmoles/mg/min). However, this change in activity was not significant (P>0.5, n=3). The hODC fraction refolded by the KCl method showed activity at 5.35 nmoles/mg/min, which showed no significant difference to that of soluble hODC (P>0.5, n=3). Despite the refolded hODC samples showed no significant difference in activity levels to soluble hODC the protein sample had more contaminating proteins when compared to the soluble hODC fraction (see Figures 3.16A and 3.21).

Protein refolding by the KCl and detergent methods does not appear to be a viable method for obtaining high levels of active and pure wODC. Both refolding methods resulted in active hODC that did not differ significantly from soluble hODC, however, the refolded protein sample was not pure even after affinity chromatography purification.

3.1.12 Activity of the *Pf*ODC constructs

To determine the effect codon harmonisation has on the enzymatic activity of *Pf*ODC, radioactivity enzyme assays were performed (Figure 3.23).

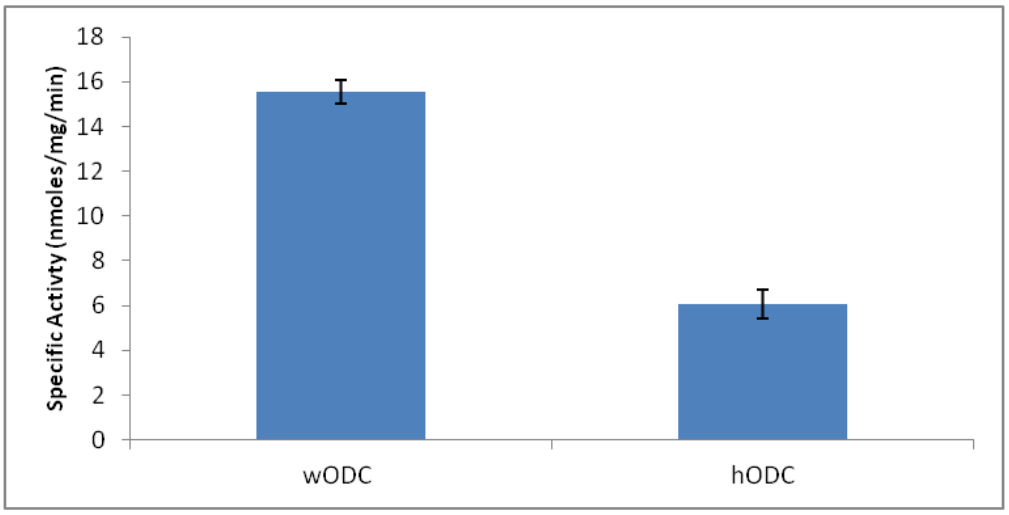

Figure 3.23: Activity assays for wild-type and harmonised *Pf*ODC. The effect harmonisation had on the activity of the monofunctional *Pf*ODC domain was investigated via an activity assay. Data are represented for three independent biological replicates (n=3) each performed in duplicate, SEM indicated.

The wODC construct (15.6 nmoles/mg/min) had 2.5-fold higher activity than the hODC construct (6.1 nmoles/mg/min). Harmonisation of the *Pf*ODC domain did not result in the improvement of the expression or purity levels of recombinantly expressed *Pf*ODC.

Harmonisation on its own did not improve the expression levels of recombinantly expressed monofunctional *Pf*ODC. The effect of expressing wODC and hODC in different expression strains of *E. coli* was then tested, in order to determine whether using another expression

strain of *E. coli* would improve the recombinant expression and activity of monofunctional *Pf*ODC.

3.1.13 Recombinant expression of ODC in multiple *E. coli* cell lines

pASK-IBA3 vector containing either the wild-type or harmonised construct of *Pf*ODC was transformed into chemically competent BL21, BL21(DE3), BL21(DE3) Star, BL21(DE3) pLysS, and Rosetta *E. coli* strains as in section 2.1.2. Protein expression and isolation of recombinantly expressed proteins was followed as in section 2.1.3. Purified protein concentrations were determined by the Bradford BSA protein concentration determination assay with the use of a BSA standard curve (Figure 3.24).

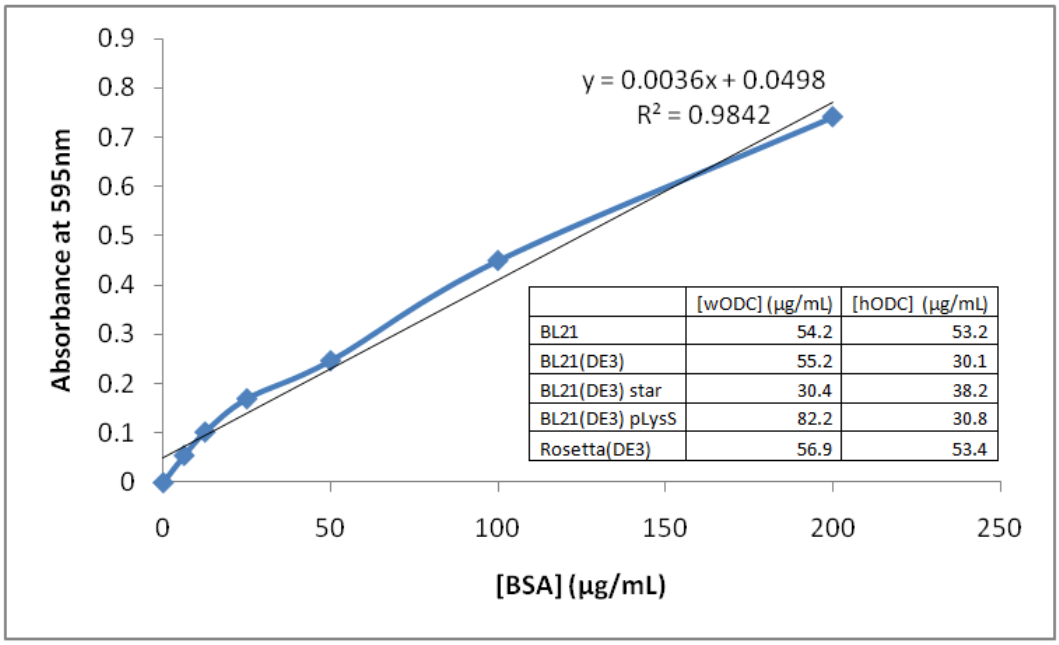

	[wODC] (µg/mL)	[hODC] (µg/mL)
BL21	54.2	53.2
BL21(DE3)	55.2	30.1
BL21(DE3) star	30.4	38.2
BL21(DE3) pLysS	82.2	30.8
Rosetta(DE3)	56.9	53.4

Figure 3.24: BSA standard curve for the determination of protein concentration. BSA standards with a concentration ranging from 0 to 200 µg/mL were used to construct a standard curve for the Bradford assay in order to determine the concentration of the purified protein samples expressed in the various *E. coli* strains. Table shows concentrations for purified wODC and hODC isolated from the various strains.

The wODC protein samples that were recombinantly expressed in the BL21, BL21(DE3), and Rosetta(DE3) strains of *E. coli* had similar concentrations. wODC expressed in the BL21(DE3) pLysS strain had the highest concentration, while wODC expressed in the BL21(DE3) strain had the lowest concentration. hODC expressed in the BL21(DE3) and BL21(DE3) pLysS strains had the lowest concentration, with hODC expressed in the BL21(DE3) star strain at a slightly higher concentration. hODC expressed in the BL21 and Rosetta(DE3) strains had the highest concentration (Figure 3.24, inserted table). Purified protein samples were analysed by quantitatively (0.8 µg) separating the samples on a 7.5% SDS-PAGE gel (Figure 3.25) and Western blot (Figure 3.23) using *Strep*-II-HRP conjugated antibody.

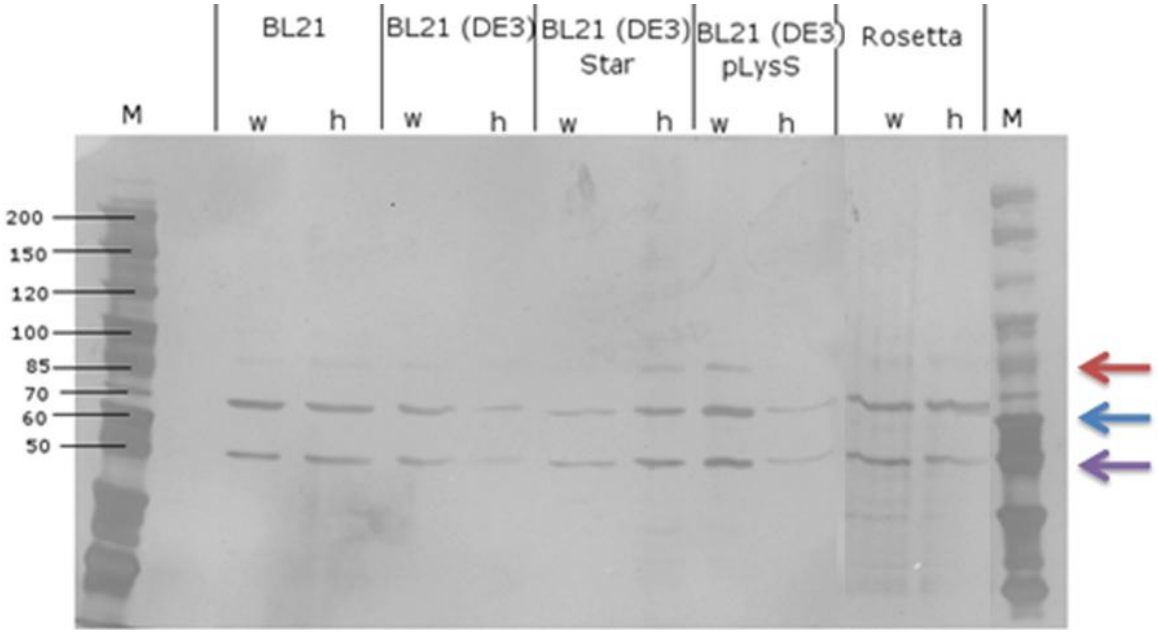

Figure 3.25: SDS-PAGE analysis of wODC and hODC expressed in multiple *E. coli* cell lines. The wODC and hODC constructs were expressed in BL21, BL21(DE3), BL21(DE3) Star, BL21(DE3) pLysS and Rosetta *E. coli* cell lines. Purified protein samples were quantitatively loaded and separated on a 7.5% separating gel and proteins were visualised by silver staining. Protein bands were present at ~85 kDa (red arrow), ~70 kDa (blue arrow), and ~50 kDa (purple arrow). (M: Marker; w: wODC; h: hODC). Protein samples loaded at 0.8 µg of protein per well.

Bands were present on the SDS-PAGE gel at ~85 kDa (Figure 3.22, red arrow), ~70 kDa (Figure 3.25, blue arrow), and ~50 kDa (Figure 3.25, purple arrow). The band at ~70 kDa was also detected on the Western blot (Figure 3.26), and thus represents the recombinantly expressed *Pf*ODC for wODC expressed in BL21(DE3), BL21(DE3) pLysS and Rosetta expression strains and for hODC expressed in BL21, BL21(DE3) Star, and Rosetta expression strains. The bands at ~85 kDa and ~50 kDa were not detected on the Western blot, indicating an absence of a *Strep*-tag on these proteins, as seen in previous Western blots.

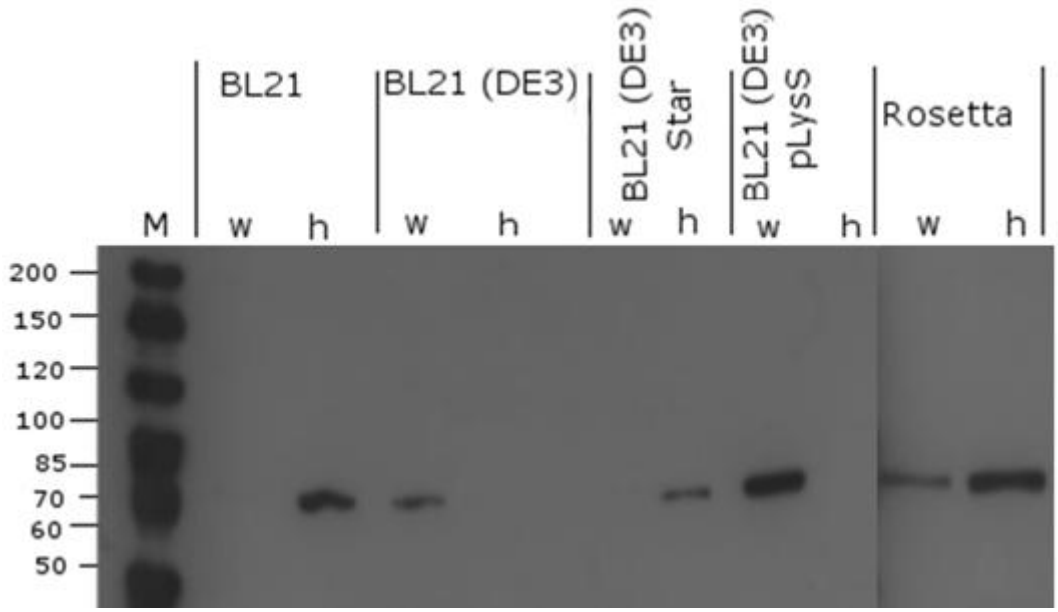

Figure 3.26: Western blot analysis of wODC and hODC expressed in BL21, BL21(DE3), BL21(DE3) Star, BL21(DE3) pLysS, and Rosetta *E. coli* expression hosts. The wODC and hODC constructs were expressed in BL21, BL21(DE3), BL21(DE3) Star, BL21(DE3) pLysS and Rosetta *E. coli* cell lines. Purified protein samples were quantitatively loaded and separated on a 7.5% separating gel. Western blot analysis revealed bands at ~70 kDa for wODC expressed in BL21(DE3), BL21(DE3) pLysS and Rosetta cell lines, and hODC expressed in BL21, BL21(DE3) Star and Rosetta cell lines. (M: Marker (PageRuler Unstained Protein Marker); w: wODC; h: hODC).

The ~70 kDa protein band in Figure 3.25 (blue arrow) was not detected on the corresponding Western blot (Figure 3.26) for wODC expressed in BL21 and BL21(DE3) Star cell lines, and hODC expressed in BL21(DE3) and BL21(DE3) pLysS. This may be due to the possibility of the *Strep*-tag not being exposed to the *Strep*-II-HRP conjugated antibody.

LC-MS/MS was performed on all three bands and the same results as for section 3.1.8 was obtained. The bands at ~70 kDa and ~50 kDa represent forms of *Pf*AdoMetDC/ODC (*Pf*ODC and an N-terminal truncation of *Pf*ODC, respectively), and the ~85 kDa band had no good hits.

Densitometric analysis (Figure 3.27) of the ~70 kDa band (Figure 3.25, blue arrow) showed that the recombinantly expressed *Pf*ODC had the highest density (and thus highest concentration per sample) for wODC expressed in BL21(DE3) pLysS cells and hODC expressed in Rosetta cells.

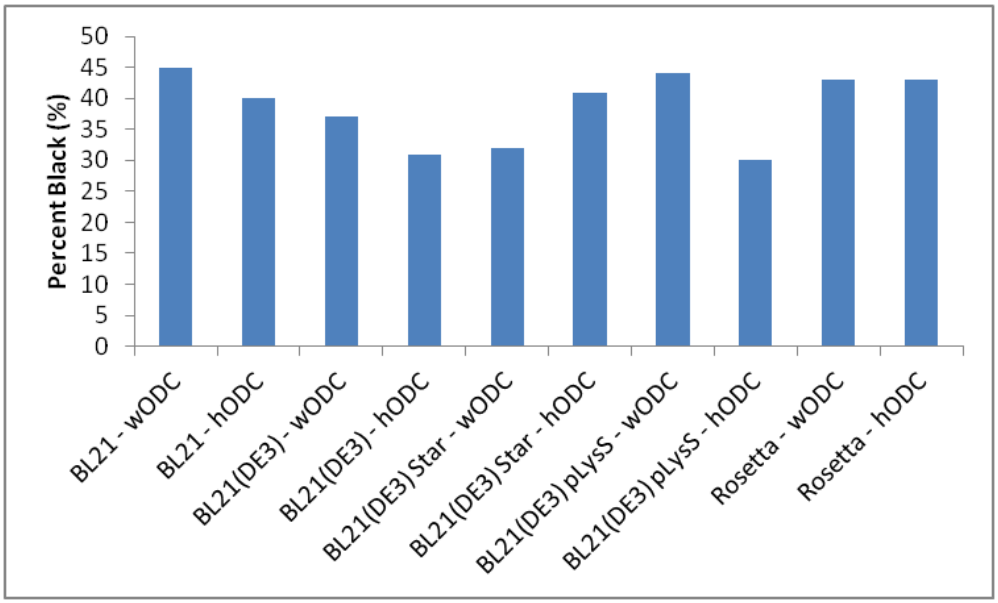

Figure 3.27: Densitometric analysis of the ~70 kDa bands on the SDS-PAGE gel of the *Pf*ODC proteins expressed in multiple cell lines. Densitometric analysis of the ~70 kDa bands on Figure 3.25 was performed to determine which cell line resulted in the highest wODC and hODC expression.

Enzyme activity assays were performed on wODC expressed in Rosetta and BL21(DE3) pLysS cell lines, and hODC expressed in Rosetta and BL21(DE3) Star cell lines as these had the highest densitometry values out of the 11 samples and Western blotting confirmed the presence of recombinant *Pf*ODC in the samples, indicating a higher likelihood of being correctly folded.

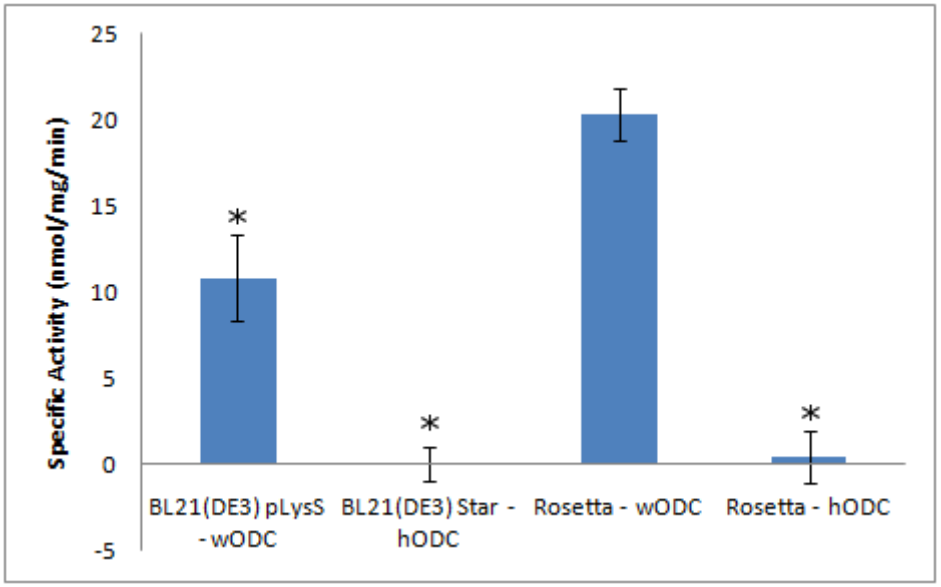

Figure 3.28: Results of the activity assay for wild-type and harmonised *Pf*ODC expressed in different *E. coli* expression hosts. To determine whether the recombinantly expressed proteins displayed *Pf*ODC activity, an *Pf*ODC activity assay was performed. Activity was observed for wODC expressed in BL21(DE3) pLysS cells, and wODC expressed in Rosetta cells. Activity for hODC expressed in BL21(DE3) Star and Rosetta was negligible. Data are represented for three independent biological replicates (n=3) each performed in duplicate, SEM indicated (* indicates significance at $P<0.05$).

*Pf*ODC enzyme activity levels (Figure 3.28) were undetectable for hODC expressed in BL21 and low levels of activity observed for Rosetta. The activity of wODC expressed in BL21(DE3) pLysS was significantly lower ($P<0.05$) than that tested in section 3.1.12 (Figure 3.23). The activity of wODC expressed in the Rosetta strain of *E. coli* did not significiantly differ from that tested in section 3.1.12 (figure 3.3).

Codon harmonisation of *Pf*AdoMetDC/ODC and *Pf*ODC did not improve the expression levels or the purity of the recombinantly expressed proteins. The next part of this study focuses on the vitrual screening of a compound library against the *Pf*ODC homology model to determine which may have inhibitory effects against the *Pf*ODC domain of *Pf*AdoMetDC/ODC.

Part 3.2: Inhibitor-based drug discovery

3.2.1 Virtual screening of the Malaria Box against the *Pf*ODC homology model

The 400 Malaria Box compounds were screened against the *Pf*ODC homology model (Figure 3.29) to determine whether any of the compounds were potential lead compounds for the inhibition of *Pf*ODC. Since *Pf*ODC is inactive when its cofactor, PLP, is not present, the compounds were screened against the homology model of monofunctional *Pf*ODC with and without PLP in the structure.

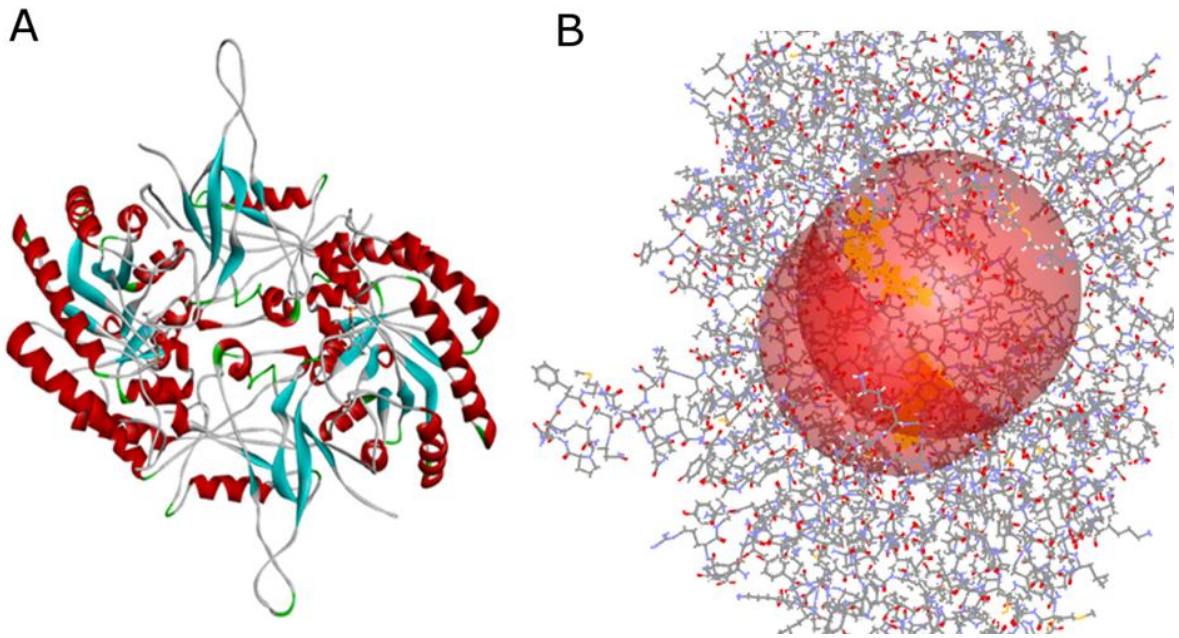

Figure 3.29: *Pf*ODC homology models used for the screening of the Malaria Box compounds. A: homology model of dimeric *Pf*ODC. B: prepared dimeric *Pf*ODC homology model with active site indicated by red spheres.

The top scoring compounds were identified using the Jain and -PMF scoring functions. The top five compounds for each scoring function are listed in Table 3.3. Due to the possibility of a single compound having multiple tautomers and stereoisomers under a specific condition, the total number of tautomers screened against the homology models was 1943. Results for the screening against the homology model with and without PLP were identical for the top screened compounds. This may be due to the active site being relatively large, and the top screened compounds interacting at a part of the active site that is away from the PLP-binding site.

Table 3.3: Scoring results of virtual screening the Malaria Box against the *Pf*ODC homology model. The top five scoring molecules for each scoring function are listed. Compounds that are repeated represent different tautomers of the compound under the conditions screened.

Jain Scoring[a]			-PMF Scoring[b]		
Rank	Name	Jain Score	Rank	Name	-PMF Score
1	TCMDC-124568	13.08	1	TCMDC-125233	-194.23
2	GNF-Pf-2114	11.19	2	SJ000232807	-196.48
3	GNF-Pf-1034	11.07	3	SJ000232807	-197.92
4	GNF-Pf-1034	11.07	4	GNF-Pf-2217	-203.49
5	GNF-Pf-1034	10.6	5	TCMDC-123469	-206.02
530	TCMDC-125281	4.22	1140	TCMDC-125281	-436.95
531	GNF-Pf-4806	4.22	1141	GNF-Pf-5561	-437.32
532	GNF-Pf-4442	4.22	1142	GNF-Pf-3058	-437.34
533	GNF-Pf-4606	4.21	1143	TCMDC-123826	-437.37
534	TCMDC-124422	4.2	1144	GNF-Pf-4543	-437.53
535	TCMDC-124668	4.2	1145	SJ000267766	-437.58

a: a higher score indicates stronger receptor-ligand binding affinity which is more favourable.
b: a lower negative score indicates a stronger receptor-ligand binding affinity.

The top scoring compound for each scoring function (TCMDC-124568 and TCMDC-125233) and two medium scoring compounds (GNF-Pf-4442 and TCMDC-123826) were selected for enzyme inhibition assays. The structures of these compounds are shown in Figure 3.30.

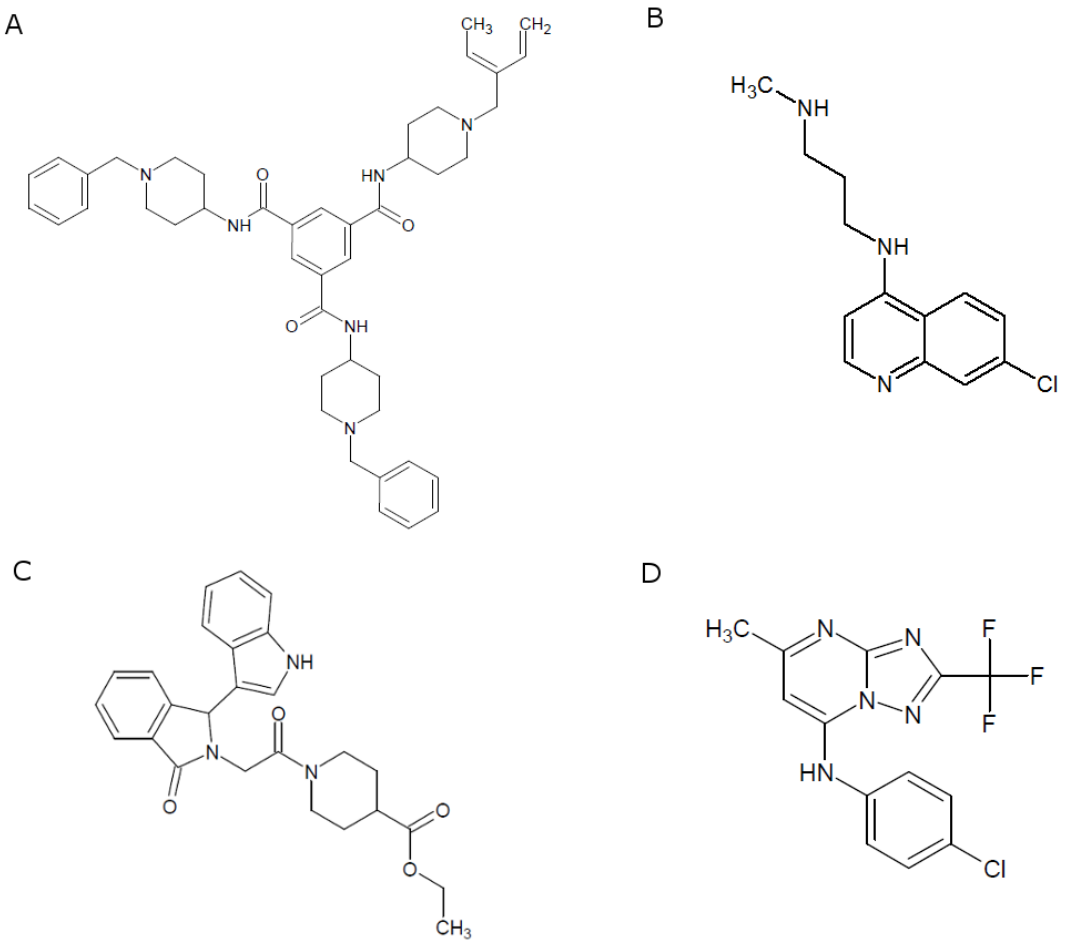

Figure 3.30: Structures of the selected top two scoring and two medium scoring compounds from virtual screening of the Malaria Box against the *Pf*ODC homology model. A: Structure TCMDC-124568; B: structure of TCMDC-125233; C: structure of GNF-Pf-4442; D: structure of TCMDC-123826.

All four compounds have been shown to have activity against parasite cultures at a half maximal effective concentration (EC_{50}) below 1.1 µM (data from MMV, www.mmv.org). The activities of the compounds, their pharmaceutical source and canonical SMILES are summarised in Table 3.4 below.

Table 3.4: The two top scoring and medium scoring compounds selected from the screening of the Malaria Box against the *Pf*ODC homology model for inhibition assays. The ChEMBL ID, pharmaceutical source, activity of the compounds screened against the parasite *in vitro*, and the compounds' canonical SMILES are indicated. Data from MMV (www.mmv.org).

ChEMBL ID	Source	Activity (EC_{50} µM)[c]	Canonical SMILES
TCMDC 124568	GSK[a]	1.039	O=C(NC1CCN(Cc2ccccc2)CC1)c3cc(cc(c3)C(=O)NC4CCN(Cc5ccccc5)CC 4)C(=O)NC6CCN(Cc7ccccc7)CC6
TCMDC 125233	GSK	0.062	CNCCCNc1ccnc2cc(Cl)ccc12
GNF-Pf 4442	GNF[b]	0.519	CCOC(=O)C1CCN(CC1)C(=O)CN2C(c3ccccc3C2=O)c4c[nH]c5ccccc45
TCMDC 123826	GSK	0.117	n1(n2)c(nc(C)cc1Nc(cc3)ccc3Cl)nc2C(F)(F)F

a: GlaxoSmithKline
b: Novartis
c: half maximal effective concentration: the concentration of a drug which induces a response halfway between the baseline and maximum after a specified exposure time. This activity was measured with a whole cell assay against *P. falciparum* infected red blood cells. Data provided by MMV (www.mmv.org).

To obtain an indication of specificity of the interaction between the compounds in the active site of *Pf*ODC, *in silico* analyses identifying specific interactions were performed. Interactions between the four chosen compounds and the active site of *Pf*ODC are displayed as a 2D-diagram in Figure 3.31.

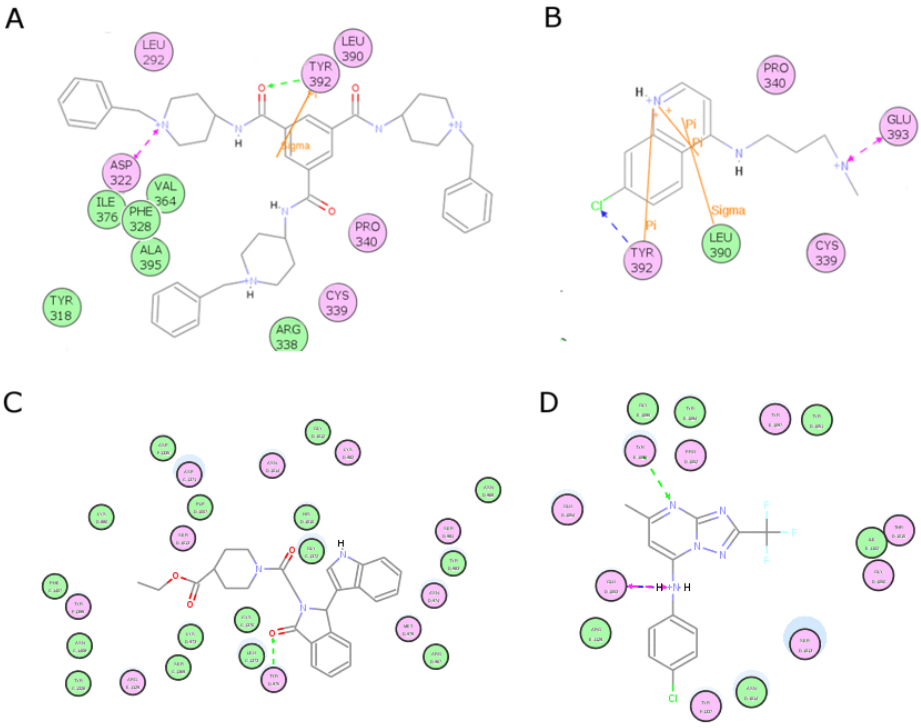

Figure 3.31: Interactions of the four selected compounds with the active site of *Pf*ODC. A: TCMDC-124568. B: TCMDC-125233. C: GNF-Pf-4442. D: TCMDC-123826. Purple and blue arrows indicate ionic interactions, green arrows indicate hydrogen bonding, and orange lines indicate covalent bonding (Sigma-Pi).

TCMDC-124568 is predicted to form a hydrogen bond and Sigma-Pi interactions (covalent bond) with Tyr392, as well as an ionic bond with Asp322 (Figure 3.31A). TCMDC-125233 is predicted to have Sigma-Pi interactions with Tyr392 and Leu390, as well as for an ionic bond with Tyr392 (Figure 3.31B). GNF-PF-4442 is predicted to form a hydrogen bond with Tyr392 (Figure 3.31C). TCMDC-132826 is predicted to have ionic interactions with Glu393 and hydrogen bond with Tyr392 (Figure 3.31D).

3.2.2 ODC enzyme inhibition assay

Enzyme inhibition assays were performed on the full-length wild-type *Pf*AdoMetDC/ODC since the *Pf*ODC activity of the *Pf*ODC domain on its own is only 10% of the bifunctional protein [85]. Enzyme inhibition assays were performed in the same manner as the enzyme activity assay in 2.1.4 except that the enzyme was incubated with 100 µM of the compound on ice for 10 minutes before the activity assays were performed. The effect the four selected compounds had on the activity of the *Pf*ODC domain of PfAdoMetDC/ODC is shown in Figure 3.32.

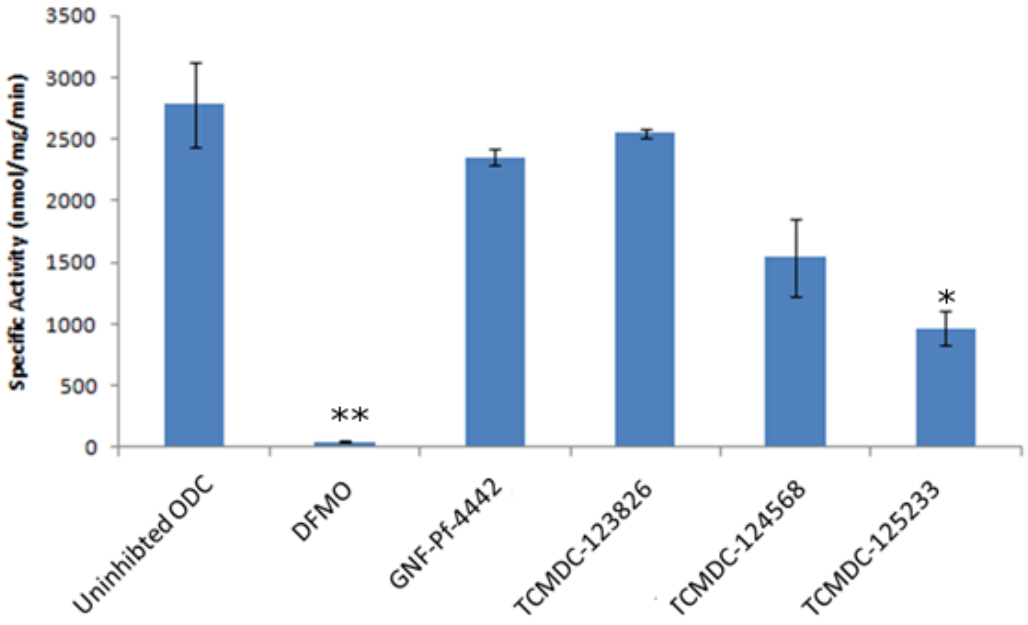

Figure 3.32: *Pf*ODC inhibition assay for the four Malaria Box compounds. The four Malaria Box compounds were assayed for their ability to inhibit the activity of the *Pf*ODC of *Pf*AdoMetDC/ODC. Data are represented for three independent biological replicates (n=3) each performed in duplicate, SEM indicated (* indicates significance at $P<0.05$, ** indicates significance at $P<0.01$).

The DFMO control inhibitor decreased *Pf*ODC activity of the bifunctional *Pf*AdoMetDC/ODC by 98%. GNF-Pf-4442 and TCMDC-123826 showed poor inhibition of *Pf*ODC activity. TCMDC-124568 decreased *Pf*ODC activity by 45%, however this decrease was not significant ($P=0.0831$, n=3). TCMDC-125233 significantly decreased *Pf*ODC activity by 65% ($P<0.05$, n=3) (Figure 3.33).

3.2.3 AdoMetDC enzyme inhibition assay

To determine whether the four selected compounds from the Malaria Box set were affecting other parts of *Pf*AdoMetDC/ODC than just the *Pf*ODC active site, they were also screened for their effect on *Pf*AdoMetDC activity of wild-type *Pf*AdoMetDC/ODC (Figure 3.33). MDL73811 was used as a positive control as it is the specific inhibitor of *Pf*AdoMetDC.

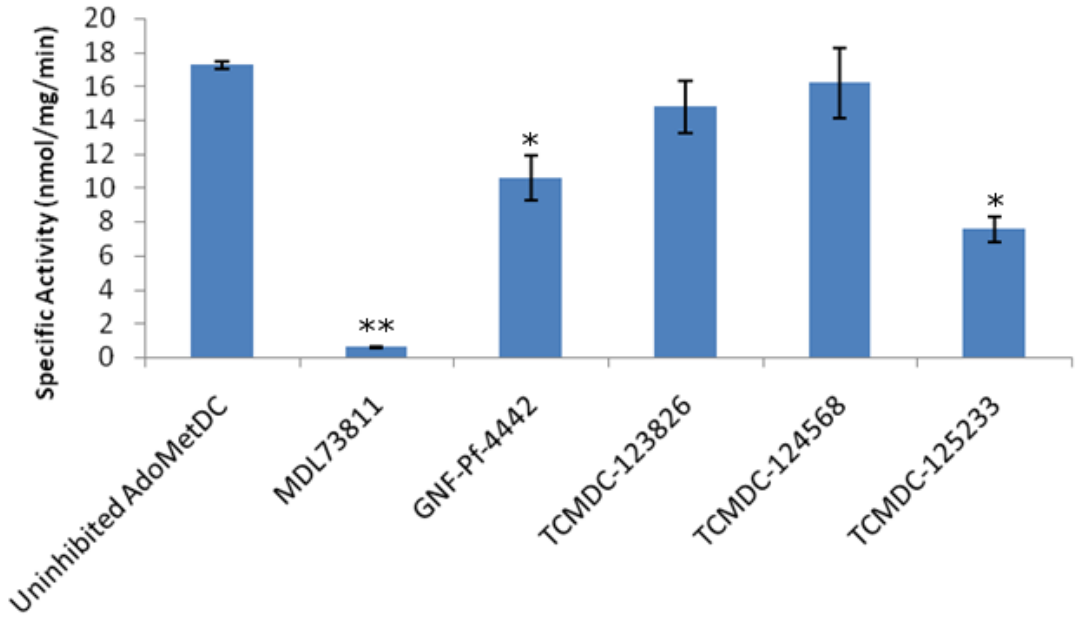

Figure 3.33: *Pf*AdoMetDC inhibition assay for the four Malaria Box compounds. The four Malaria Box compounds were assayed for their ability to inhibit the activity of the *Pf*AdoMetDC of *Pf*AdoMetDC/ODC. Data are represented for three independent biological replicates (n=3) each performed in duplicate, SEM indicated. (* indicates significance at $P<0.05$, * indicates significance at $P<0.01$).

*Pf*AdoMetDC/ODC in the presence of the MDL73811 control inhibitor had its activity decreased by 97%. TCMDC-123826 and TCMDC-124568 had non-significant reductions on *Pf*AdoMetDC activity ($P>0.05$, n=3). GNF-Pf-4442 significantly decreased the activity of the *Pf*AdoMetDC domain by approximately 40% ($P<0.05$, n=3). TCMDC-125233 significantly decreased AdoMetDC activity by 57% ($P<0.05$, n=3).

The percent inhibition the compounds had on the *Pf*AdoMetDC and *Pf*ODC activities of *Pf*AdoMetDC/ODC is summarised in Figure 3.34.

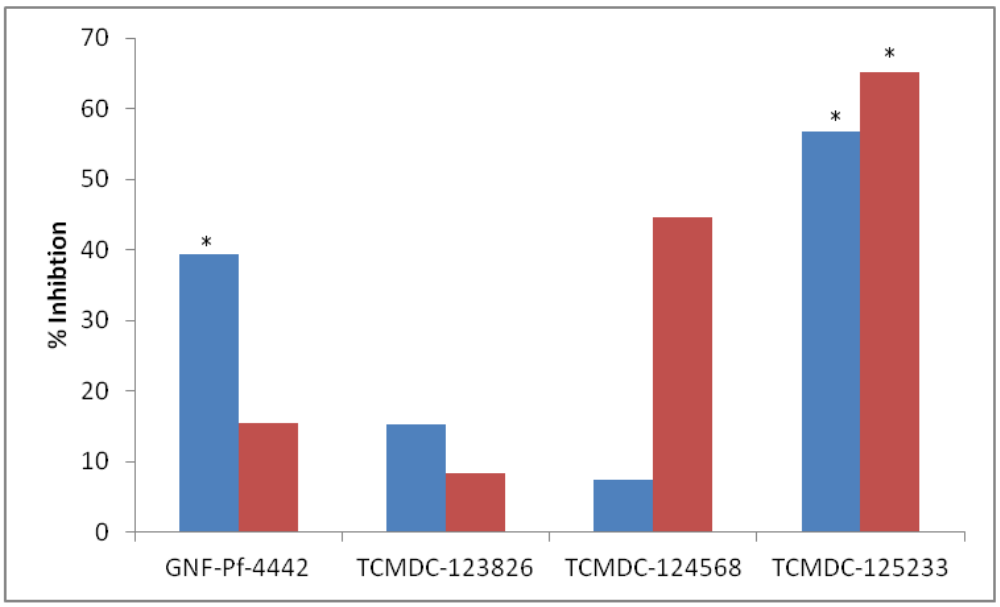

Figure 3.34: Percent inhibition of the four Malaria Box compounds on the activities of *Pf*AdoMetDC and *Pf*ODC. Blue bars represent the percent inhibition (decrease in activity) the compounds had on the activity of the *Pf*AdoMetDC domain. Red bars represent the percent inhibition the compounds had on the activity of the *Pf*ODC domain. (* indicates significance at $P<0.05$).

TCMDC-125233 significantly inhibited the activities of both *Pf*AdoMetDC and *Pf*ODC. GNF-Pf-4442 inhibited both decarboxylase activities but only their inhibitory effect on the activity of the AdoMetDC domain was significant. TCMDC-123826 and TCMDC-124568 did not significantly decrease the activities of either domain of *Pf*AdoMetDC/ODC.

Chapter 4: Discussion

4.1 Recombinant expression of *P. falciparum* proteins

Due to the incomplete understanding of the malaria parasite's biology the discovery of novel drug targets and antimalarials has been curbed [41]. Molecular biology and biochemical studies have been performed on the malaria parasite to identify differences between the biochemistry of the parasite and the host cell. The differences between the metabolic processes between the parasite and the host can be exploited in order to develop parasite-specific drugs. This approach relies on the highly specific and selective inhibition of the parasite's enzymes that are involved in pathways that are vital to parasite growth and survival, without affecting the functioning of the host cell [49]. The polyamine biosynthetic pathway of *P. falciparum* has gained attention as a novel strategy to interfere with parasite viability due to polyamines being essential for growth and differentiation of cells [69]. However, there has been limited success due to the difficulty of working with the enzymes in the parasite's polyamine pathway.

The recombinant expression of plasmodial proteins in a prokaryotic expression host is notoriously difficult, mainly due to the A+T-richness of the *P. falciparum* genome, RNA secondary structures, regions of low complexity and parasite-specific inserts in the gene [93],[123]. As part of a structural genomics initiative, Christopher Mehlin and co-workers recombinantly expressed 1000 *P. falciparum* open reading frames in *E. coli.* Of these, 337 of the targets were observed to express, but the recombinant proteins were mainly insoluble. Only 63 of the expressed targets provided soluble protein in yields ranging from 0.9 to 406.6 mg/L of rich media. The low levels or lack of expression of recombinant plasmodial proteins in *E. coli* was attributed to the high molecular weight, greater protein disorder, a more basic isoelectric point and a lack of homology to *E. coli* proteins. The codon usage and A+T-richness of plasmodial genes was shown not to play a significant role in the recombinant expression. Crystallography requires at least 5 mg of rigorously pure material, however, in most cases the soluble, recombinant expression of *P. falciparum* proteins fail to reach milligram amounts [123]. This study attempted to improve the recombinant expression of *Pf*AdoMetDC/ODC and the monofunctional *Pf*ODC domain. Previous attempts in the recombinant expression of *Pf*AdoMetDC/ODC did not result in high levels of protein being produced, and contaminating proteins were present despite purification by affinity chromatography [84],[128]. The *Pf*ODC domain has been expressed in two different forms, with and without the hinge region that connects the two domains of *Pf*AdoMetDC/ODC. Neither of these were expressed at levels high enough for crystallisation trials, and the presence of truncated proteins were observed during gel electrophoresis [85]. In order to try and improve the recombinant expression levels of *Pf*AdoMetDC/ODC and *Pf*ODC a technique known as codon harmonisation was utilised.

It has recently been discovered that genetic polymorphisms involving a synonymous codon substitution are not neutral as once believed, and that they have been implicated in the development of various disease states mediated through splicing defects [140]. A single synonymous codon substitution within a coding region of a gene can result in a protein with altered substrate specificities [141] or enzymatic activities [142], indicating that this substitution has resulted in a significant change to the protein's structure. Subtle modulation of the nucleotide sequence may serve to regulate protein structure and function. This may result in problems for recombinant protein expression for expression of proteins from organisms with a different codon bias to that of the recombinant expression host. The codon usage frequency patterns for *E. coli* proteins with known structures were analysed and it was found that lower frequency codon preferences tend to cluster within the regions of mRNA that code for link or end segments that separate regions with higher ordered structure [143]. It has been shown that as few as two infrequently used codons can reduce the steady state density of ribosomes on mRNA [144]. This will pause the translation of mRNA and allow the newly synthesised protein to have enough time to correctly fold before the synthesis of the next element.

Codon harmonisation is the process where the synonymous codon changes are made to a gene so that it maintains the same codon frequency usage in the recombinant expression host as it would have in its native host. This will result in the pause sites to be conserved. Evelina Angov and co-workers used a codon harmonised approach to improve the expression of three *P. falciparum* genes in *E. coli*. The expression of the codon harmonised genes exceeded that of the native genes by 4- to 1000-fold. The proteins were soluble and reacted with a variety of functional conformation-specific monoclonal antibodies, suggesting that they were properly folded and in the correct conformation [136].

Four *Pf*AdoMetDC/ODC gene constructs were created by combining portions of wild-type and codon harmonised gene sequences. All four *Pf*AdoMetDC/ODC chimeric proteins contain a *Strep*-tag on their N-terminus which allows the chimeric *Pf*AdoMetDC/ODC to be purified from the protein samples via affinity chromatography. Recombinant expression of the four constructs in *E. coli* and subsequent purification and gel electrophoresis revealed that they are expressed in both the soluble and insoluble protein fraction. The full-length harmonised chimeric protein showed the lowest level of soluble expression. The proteins bands for hA/wO and hA/hO in the insoluble fraction were more prominent than those for wA/wO and wA/hO. Harmonisation of the *Pf*AdoMetDC domain of *Pf*AdoMetDC/ODC resulted in an increase in the amount of *Pf*AdoMetDC/ODC that is insolubly expressed.

Gel electrophoresis revealed four contaminating protein bands at ~112 kDa, ~70 kDa, ~60 kDa and ~50 kDa that co-eluted with the ~160 kDa chimeric *Pf*AdoMetDC/ODC chimeric proteins. The ~70 kDa had been identified as a fragment of *Pf*AdoMetDC/ODC with antiserum raised against the *Pf*ODC domain of the bifunctional protein [85]. The ~112 kDa and ~70 kDa protein bands were also detected via Western blots using a *Strep*-II-HRP

antibody, indicating that they are probably truncated or degraded forms of *Pf*AdoMetDC/ODC due to the presence of the *Strep*-tag. This was confirmed by LC-MS/MS and previous studies [128]. LC-MS/MS also identified the *E. coli* chaperone DnaK in the ~70 kDa protein band. The ~50 kDa was identified as the *E. coli* chaperone GroEL. The presence of chaperone proteins indicates that the recombinant expression of *Pf*AdoMetDC/ODC places strain on the *E. coli* expression host [145].

Previous studies on the recombinant expression of *Pf*AdoMetDC/ODC [128] identified the truncated forms of *Pf*AdoMetDC/ODC being expressed due to Shine-Dalgarno sites upstream in the gene sequence that allowed for an additional start site to be present in the gene. However, in the creation of the genes for chimeric and wild-type *Pf*AdoMetDC/ODC the additional Shine-Dalgarno sites were removed from the gene. N-terminal truncated proteins have been observed for recombinant expression of other *P. falciparum* proteins, such as lactate dehydrogenase, due to internal Shine-Dalgarno sequences [146]. Recombinant expression of *P. falciparum* Liver-Stage Antigen 1 in *E. coli* also resulted in truncated version of the protein being produced due to a start codon present in the gene downstream of the start site being recognised by the ribosome [147]. The presence of a *Strep*-tag on the ~112 kDa and ~70 kDa forms of *Pf*AdoMetDC/ODC indicate that they are likely formed by proteolytic degradation of the full-length protein, as ribosomal slippage during translation may have frame-shift effects and the C-terminal *Strep*-tag would not be correctly translated. LC-MS/MS analysis of the ~112 kDa and ~70 kDa protein bands also indicated that they are fragments of *Pf*AdoMetDC/ODC, which would be unlikely if ribosomal slippage occurred during translation as the incorrect reading frame would be used and the protein would be incorrectly translated. Proteolysis generally occurs from the N-terminus of a protein [148]. Degradation from the N-terminus of the recombinant protein would ensure that the Strep-tag on the C-terminus will be intact, and allow the degraded forms of *Pf*AdoMetDC/ODC to remain in the protein samples after affinity chromatography.

Codon harmonisation of *Pf*AdoMetDC/ODC did not improve the purity or the expression levels of *Pf*AdoMetDC/ODC. Previous studies tried to improve the purity of the recombinant expression of *Pf*AdoMetDC/ODC by placing *Strep*-tag on the C-terminal and a His-tag on the N-terminal of the protein. The isolated protein samples were purified by tandem affinity chromatography, purifying initially with the use of a nickel affinity column to isolate proteins containing a His-tag. This should remove the N-terminally truncated forms of *Pf*AdoMetDC/ODC from the protein isolates as they would lack a His-tag. The purified proteins were then run through a *Strep*tactin column. However, the ~112 kDa and ~70 kDa truncated forms of *Pf*AdoMetDC/ODC, and the chaperone protein GroEL were still present after purification. Western blot analysis for the His and *Strep*-tag only indicated the presence of the *Strep*-tag on the truncated proteins, and both tags for the full length protein. This indicates that these contaminating proteins must interact with the full length *Pf*AdoMetDC/ODC, and prevents them from being removed during affinity chromatography [128].

Previous native-PAGE analysis revealed a complex at ~600 kDa and ~400 kDa. The ~400 kDa protein band could represent the ~330 kDa bifunctional *Pf*AdoMetDC/ODC complex with either the ~70 kDa *Pf*ODC fragment, or the *E. coli* chaperone, DnaK, while the ~600 kDa protein band may consist of the bifunctional *Pf*AdoMetDC/ODC complex in association with the ~112 kDa *Pf*AdoMetDC/ODC fragment, the ~70 kDa *Pf*ODC or DnaK, and the ~60 kDa *E. coli* chaperone GroEL. Alternatively, the ~600 kDa protein band may consist of the bifunctional *Pf*AdoMetDC/ODC complex and two ~70 kDa proteins (either the *Pf*ODC fragment, DnaK, or both) and the ~60 kDa protein, or a single ~70 kDa protein and two ~60 kDa proteins [128].

Codon harmonisation also had an effect on the decarboxylase activities of *Pf*AdoMetDC/ODC (Figure 3.11). Harmonisation of the *Pf*AdoMetDC domain alone increased the activity of the *Pf*AdoMetDC domain by approximately 3-fold, but decreased the activity of the *Pf*ODC domain by nearly half. Harmonisation of the *Pf*ODC domain alone decreased *Pf*ODC activity by nearly a third, and increased the activity of *Pf*AdoMetDC by nearly two-fold. Harmonisation of both domains prevents *Pf*ODC from decreasing *Pf*AdoMetDC activity and *Pf*AdoMetDC from increasing *Pf*ODC activity. Codon harmonisation has the potential to change the way a protein is folded, due to the change in the rate of translation caused by an adapted codon sequence. Since codon harmonisation of *Pf*AdoMetDC/ODC impacted the activity of both domains of the protein, it is possible that it caused a change in the structure of the protein. It is known that certain parts of the *Pf*AdoMetDC/ODC that are away from the active sites play an important role in the functioning of both domains. *Pf*AdoMetDC/ODC contains four parasite specific inserts that have been shown to play a role in protein-protein interactions and activity of the protein. Deletion of the inserts caused a decrease in activity of the corresponding domain. Some deletions also caused a decrease in the activity of the neighbouring, non-mutated domain [87]. If codon harmonisation causes a structural change in regions such as these, it could potentially cause a change in the activity of both domains of *Pf*AdoMetDC/ODC.

The effect of codon harmonisation on the expression and activity of the monofunctional *Pf*ODC domain of *Pf*AdoMetDC/ODC was also investigated. A *Strep*-tag is present on the N-terminus of the recombinant *Pf*ODC proteins which allows the proteins to be isolated via affinity chromatography and to be detected via Western blotting using a *Strep*-II-HRP antibody. Harmonisation decreased the levels of recombinantly expressed *Pf*ODC by approximately a half. Contaminating proteins were observed at ~50 kDa and ~85 kDa after affinity chromatography.

Both the wild-type and harmonised versions of ~70 kDa *Pf*ODC proteins were detected via Western blotting, but the ~50 kDa and ~85 kDa were not observed. The ~50 kDa protein is probably a proteolytically degraded version of the ~70 kDa *Pf*ODC protein, which would result in the absence of a *Strep*-tag being present on the N-terminal of protein. LC-MS/MS confirmed that the ~70 kDa and ~50 kDa protein bands represented a portion of

*Pf*AdoMetDC/ODC, notably the *Pf*ODC protein and a truncated version of *Pf*ODC. The *E. coli* chaperone protein, GroEL, was also identified in the ~50 kDa protein band. The ~85 kDa was not identified by LC-MS/MS, due to low sequence coverage and scoring of the peptides analysed.

Since *Pf*ODC forms a dimer it may be possible that the ~50 kDa truncated protein can interact with the ~70 kDa *Pf*ODC and co-elute with it during affinity chromatography. Native-PAGE analysis of the purified protein samples showed the presence of a protein band at approximately 120 kDa that may represent the association between the ~50 kDa truncated from of *Pf*ODC and the ~70 kDa *Pf*ODC, as well as an association between GroEL and *Pf*ODC. A protein band at approximately 158 kDa was also observed on the native-PAGE. This may represent the unidentified ~85 kDa protein in association with the ~70 kDa *Pf*ODC protein. These two interactions explain why it is possible for the ~50 kDa and ~85kDa to co-elute with *Strep*-tag containing ~70 kDa *Pf*ODC during affinity purification.

Harmonisation also had an effect on the activity of *Pf*ODC, decreasing it by more than half when compared to wild-type *Pf*ODC. As with chimeric *Pf*AdoMetDC/ODC proteins the harmonisation of *Pf*ODC may cause a slight alteration in the structure of the protein that can affect the functioning of the protein. Secondary structure determination would have to be performed in order to validate this.

Other *P. falciparum* proteins, such as dihydrofolate reductase-thymidylate synthase (*Pf*DHFR/TS) [138], glucose-6-phosphate dehydrogenase-6-phosphogluconolactonase [149], and hydroxymethyldihydropterin pyrophosphokinase-dihydropteroate synthase [150], are also expressed as bifunctional complexes. These proteins contain parasite-specific inserts that play a role in the modulation of activities between the two domains of the protein, as decreases in the activities of the domains are observed when the inserts are deleted. This suggests that the inserts could be involved in the interaction of the two catalytic domains of the bifunctional complex.

There are various similarities between *Pf*DHFR/TS and *Pf*AdoMetDC/ODC. *Pf*DHFR/TS is a dimeric enzyme with extensive interdomain interactions that are significantly mediated by the junction region between the two domains, as well as by parasite-specific inserts in the *Pf*DHFR domain. The activity of the *Pf*TS domain is dependent on the integrity of the N-terminal *Pf*DHFR domain and the junction region [151]. Deletion of five residues at the N-terminus of *Pf*DHFR/TS significantly reduced the functioning of *Pf*DHFR, and a further deletion of 15 residues resulted in both domains of *Pf*DHFR/TS being inactive [152]. The N-terminal residues therefore play a role in the activities of both domains of the bifunctional complex, despite the *Pf*TS domain being 320 residues away from the N-terminus.

The expression of monofunctional domains of bifunctional proteins from *P. falciparum* usually results with the domain located on the N-terminus of the protein being more amenable to recombinant expression than the C-terminal domain [87], [153], [154]. This is

particularly true for *Pf*AdoMetDC/ODC, as monofunctional *Pf*AdoMetDC has been expressed at a concentration and purity that have allowed for the initiation of crystallisation trials (personal communication M. Williams, D. le Roux, and J. Sprenger). However, monofunctional *Pf*ODC is at expressed at a level that is lower than that of the full-length bifunctional protein. The *Pf*AdoMetDC domain plays a role in stabilising the *Pf*ODC domain, and interactions between the two domains increase the activity of the *Pf*ODC domain [87], [155].

4.2 Chaperones

Under normal cellular conditions some cytoplasmic proteins are able to correctly fold spontaneously, while aggregation prone proteins require molecular chaperones that interact with the nascent polypeptide chains to prevent aggregation during the folding process [156]. Aggregation of recombinant proteins overexpressed in bacterial cells can occur from either high concentrations of folding intermediates, or from inefficient processing by chaperone proteins [157].

Proteins that are trapped in non-native and aggregation prone conformations are substrates for DnaK and GroEL. DnaK prevents the formation of inclusion bodies by reducing aggregation and promoting proteolysis of misfolded proteins. GroEL operates on the protein transit between soluble and insoluble protein fractions and participates in disaggregation and inclusion body formation [145].

Both GroEL and DnaK were identified as being present in the isolated *Pf*AdoMetDC/ODC and *Pf*ODC protein samples by LC-MS/MS. Since these proteins co-purify with the full-length protein and the *Pf*ODC domain it implies that these chaperones are bound to the protein, probably in an attempt to correct the folding and prevent aggregation of the recombinant proteins. As discussed previously, native-Page analysis indicated the presence of protein bands that may represent *Pf*AdoMetDC/ODC and the monofunctional *Pf*ODC domain with the *E. coli* chaperone proteins. The recombinant expression of proteins in *E. coli* often leads the cells to be under stress, causing the upregulation of heat shock proteins and other molecular chaperones [157].

Co-expression of molecular chaperones has been used for the improved expression of target proteins during recombinant expression. The co-expression of a chaperone and target protein from the same species has seldom been matched, but is becoming more frequently used for the recombinant expression of *P. falciparum* proteins in *E. coli*. Recombinant co-expression of the plasmodial chaperone, *Pf*Hsp70, and *Pf*GTP cyclohydrolase I (*Pf*GCHI), the first enzyme in the plasmodial folate pathway, increased the soluble expression of functional *Pf*GHCI [158]. Co-expression of *Pf*AdoMetDC with *Pf*Hsp70-1 did not improve the solubility of the protein being produced, however, isolated protein samples were purer after affinity chromatography. This could have been due to *Pf*Hsp70-1 shielding nascent *Pf*AdoMetDC, thus preventing its association with the contaminating proteins. Co-

expression of wild-type *Pf*AdoMetDC/ODC with *Pf*Hsp70-1 improved the expression and yield of *Pf*AdoMetDC/ODC. Co-expression of full-length codon harmonised *Pf*AdoMetDC/ODC with *Pf*Hsp70-1 had no improvement on the yield or purity of the *Pf*AdoMetDC/ODC. *Pf*Hsp70-1 may have facilitated the folding and production of the wild-type *Pf*AdoMetDC/ODC protein whose folding could have been impeded due to potential delayed translation due to codon mismatch [159].

4.3 Refolding

One of the main problems experienced with high level protein expression in *E. coli* is the production of insoluble proteins in inclusion bodies [160]. The aggregation of proteins in bacteria is reversible, and many strategies are employed to isolate and refold inclusion bodies. Inclusion body proteins are devoid of biological activity and require elaborate solubilisation, refolding and purification procedures to recover functionally active product [161]. The use of chaotropic reagents during the refolding stages help the protein to reach its native structure by allowing intramolecular interactions and preventing intermolecular interactions [160].

Protein refolding has been successfully exploited for the refolding of *P. falciparum* dihydrofolate reductase and dihydrofolate synthase-folylpolyglutamate synthase from inclusion bodies that yielded active protein in sufficient amounts for enzyme function determinations [138], [137]. *P. falciparum* cysteine protease falcipain-1 has also been refolded in an enzymatically active monomeric form that also exhibited high immunogenic activity [162]. *P. falciparum* cysteine protease falcipain-2 was refolded at high enough levels for the crystallisation of this protein [163].

All four *Pf*AdoMetDC/ODC chimeric proteins, wODC and hODC were expressed in the insoluble protein fraction. Their presence in the insoluble fraction was confirmed by Western blot analysis. Since hA/wO had the highest concentration in the inclusion bodies of the four chimeric proteins, and still exhibited *Pf*AdoMetDC and *Pf*ODC activity in the soluble fraction it was chosen as a candidate for protein refolding along with wODC and hODC. Refolding of the inclusion bodies was attempted by the KCl [137] and detergent methods [138].

The KCl method for protein refolding involves using guanidine as a denaturant and DTT as a reducing agent to solubilise inclusion bodies. The denaturant and reducing agent is slowly removed by dilution. Protein solubilisation from the inclusion body using high concentrations of chaotropic reagents result in the loss of secondary structure leading to the random coil formation of the protein structure and exposure of the hydrophobic surface. The presence of glycerol and KCl in the buffer solution helps to protect the hydrophobic surfaces and allow the protein to correctly refold. This method did not refold hA/wO, probably due to its large size requiring it to be in the presence of denaturants and reducing agents for a longer period to allow for effective solubilisation and refolding from

inclusion bodies [161]. A band at ~70 kDa was observed for both the refolded wODC and hODC samples, however, this band was not detected during Western blot analysis. This could be due to the refolding procedures refolding the protein in such a way that the *Strep*-tag is no longer available to the *Strep*-II-HRP antibody. The refolded protein samples were not pure, despite an affinity purification step included after refolding. Activity assays showed that the ODC activity for the refolded hODC sample did not significantly differ from that of soluble hODC. The refolded wODC sample did not show observable activity for this refolding method.

The detergent method for protein refolding involves using the non-ionic detergent n-Octyl-β-D-thioglucopyranosid for solubilisation of inclusion bodies, and the ionic detergent N-lauryl sarcosine to aid in protein refolding. The sarcosine concentration has to be decreased after refolding to prevent any downstream effects, such as effecting protein function. This method did not refold hA/wO, probably for the same reasons mentioned for the KCl method. A protein band was observed at ~70 kDa for both wODC and hODC refolded by this method; however, they were not detected by Western blotting using a *Strep*-II-HRP antibody, as for the KCl method. Contaminating proteins were present for both samples despite the affinity purification step. *Pf*ODC activity assays showed that both refolded samples exhibited *Pf*ODC activity, with refolded hODC activity not significantly differing from soluble hODC. The refolded wODC sample had an activity that was significantly lower than the activity of soluble wODC.

Protein refolding methods tend to be protein specific and extensive optimisation is required to produce functional refolded proteins [164]. The two tested methods did not result in refolded hA/wO. Optimisations are probably required to effectively resolubilise and refold the 160 kDa protein from inclusion bodies. The KCl and detergent method did result in refolded and active *Pf*ODC, however, many contaminating proteins were still present even after affinity purification. Optimisation will be required in removing these contaminating proteins.

4.4 Recombinant expression of *Pf*ODC in different expression strains

The effect of wODC and hODC expression in different *E. coli* cell lines was also tested. BL21(DE3), BL21(DE3) Star, BL21(DE3) Star pLysS, and Rosetta strains were used to determine which variations in the recombinant expression hosts could improve the expression of ODC. The BL21 strains are derived from *E. coli B* but all contain a mutation in the *lon* and *OmpT* protease genes, making them deficient in the two major proteases and allowing them to be hosts for optimal recombinant protein expression. The DE3 designation means the strains contain the λ DE3 lysogen which carries the gene for T7 RNA polymerase under control of the *lac*UV5 promoter. IPTG is required to induce expression of the T7 RNA polymerase. The Star strains carry a mutated *rne* gene (*rne131*) which encodes a truncated RNase E enzyme that lacks the ability to degrade mRNA, resulting in an increase in mRNA

stability. The pLysS strain carries the pLysS plasmid which produces T7 lysozyme which reduces basal transcription of genes under the control of a T7 promoter. The Rosetta cell line is a BL21(DE3) derivative that is designed to enhance the expression of eukaryotic proteins that contain codons rarely used in *E. coli*. These strains supply tRNAs for the codons AUA, AGG, AGA, CUA, CCC, and GGA on a compatible chloramphenicol resistant plasmid. The tRNA genes are driven by their native promoters.

Recombinant expression of wild-type *Pf*ODC was highest in the BL21(DE3) pLysS and Rosetta strains of *E. coli*. The wODC expressed in the Rosetta strain had almost twice as much activity than that expressed in the BL21(DE3) pLysS strain. It is possible that the tRNAs for rare codons supplied by the Rosetta strain allow wODC to fold in such a way that it would have enhanced activity than wODC expressed in a strain that is deficient of the extra tRNAs encoded by the Rosetta strain. Recombinant expression of the harmonised *Pf*ODC was highest in BL21(DE3) Star and Rosetta strains of E. *coli.* The *Pf*ODC activity of hODC expressed in the BL21(DE3) Star cell line was negligible. hODC expressed in Rosetta had an *Pf*ODC activity that was barely detectable. The harmonisation of the *Pf*ODC domain does not result in improved expression levels or purity in *E. coli*, and the expressed protein has low activity levels. The use of different expression strains for the recombinant expression of wild-type *Pf*ODC appears to have a more promising result than codon harmonisation. Based on protein yields and activity using a strain that provides additional tRNA's and using the wild-type *Pf*ODC gene results in higher expression and activity of *Pf*ODC, rather than harmonising the gene sequence, which has a detrimental effect on the expression levels and activity of *Pf*ODC, despite having success with other plasmodial proteins [136].

Attempts at improving the recombinant expression of *Pf*AdoMetDC/ODC and the *Pf*ODC domain, using a codon harmonisation approach and multiple *E. coli* cell lines, did not improve the purity and yield of the proteins to a level that is required for crystallisation. Although this approach has worked for other plasmodial proteins [136] it did not improve the yield or purity of recombinant *Pf*AdoMetDC/ODC probably due to the large size of the protein and interactions between the two domains that are not yet completely understood.

The future of recombinant expression of *P. falciparum* proteins in *E. coli* might rely on protein engineering. Excision of disordered regions of *P. falciparum* proteins will reduce the mass and pI of the protein, both of which have been shown to enhance the chances of soluble expression [87]. However, this will be problematic for proteins with unknown structure, as the removal of plasmodial inserts may affect the functioning of the protein [87].

4.5 Virtual screening

VS has recently been applied to tackle plasmodial drug targets such as falcipains [165], dihydrofolate reductase [166], spermidine synthase [167], enoyl-acyl carrier protein

reductase [168], myosin tail interacting protein-myosin A complex [169] and others, with encouraging results as novel leads for optimisation were discovered.

In the absence of an experimentally derived 3D structure of a protein it is possible to create a model of a protein based on its homology to proteins from other organisms. However, this may be a problem for plasmodial proteins for various reasons. An important factor for successful homology modelling is the alignment of the target sequence to that of template structures. There is a biased amino acid composition of plasmodial proteins (due to the A+T-richness of the plasmodial genome) there is a low sequence similarity to homologues which makes alignment to template structures and identification of core-conserved regions problematic [170]. Plasmodial proteins tend to have large parasite-specific inserts, and these tend to confuse multiple and structural alignment programs [87].

There are a number of techniques that have been developed in order to overcome these problems. After an initial alignment of the target sequence to the template sequences the approximate insert positions can be determined [87]. The target sequence can then be split according to the long inserts and realigned to the template sequences. The inserts will then be left out of the modelling process. Improvements to the model can be achieved by using hydrophobic cluster analysis to identify hydrophobic sites that may have been protected by the insert regions [171]. Since there is a high level of uncertainty associated with the alignment of plasmodial proteins, it is usually not possible to rectify all structural anomalies. However, it is possible to identify the parts of the alignment causing the anomalies by performing standard quality checks on a large sample of models. These problem areas can then be altered or removed in order to improve the resulting models [172].

An important factor in achieving reproduction of experimental binding is the ability to differentiate the difference between accurately docked ligand poses from incorrect binding modes. Scoring functions are either forcefield-based (sum of the protein-ligand and ligand strain energies), empirically derived (based on reproducing experimental data *in silico*) or knowledge based methods (by determining correct poses rather than calculating the binding energies between ligand and protein). Most docking programs use scoring functions that are forcefield-based and empirically derived [173]. The scores for compounds docked against the model with and without PLP present in the active site were identical. This is due to the active site of *Pf*ODC being quite large, and the top scoring compounds interacting in a part of the active site that is away from the PLP-binding site [93]. The top scoring compound for each the Jain and -PMF scoring functions were selected to screen for inhibition against the *Pf*ODC domain. Inhibition assays were also performed on the *Pf*AdoMetDC domain to determine the effects the compounds had on the activities of both domains of *Pf*AdoMetDC/ODC.

The two compounds that scored in the medium-range for inhibition of *Pf*ODC assayed for inhibition against *Pf*ODC activity (GNF-Pf-4442 and TCMDC-123826) showed insignificant levels in reduction of *Pf*ODC activity (below 15%) as expected as they were not predicted to

inhibit *Pf*ODC as much as the other two compounds tested. However, GNF-Pf-4442 significantly inhibited *Pf*AdoMetDC activity by 40%. The two high scoring compounds (TCMDC-124568 and TCMDC-125233) screened were also tested for inhibition of *Pf*ODC. TCMDC-124568 decreased *Pf*ODC activity by 45%, however this result did not show significance. TCMDC-125233 significantly decreased *Pf*ODC activity by 65%. TCMDC-124568 insignificantly decreased *Pf*AdoMetDC activity by less than 10%, meanwhile TCMDC-125233 significantly decreased *Pf*AdoMetDC activity by 56%. Since TCMDC-125233 inhibits the activity of both domains it may have non-specific effects by targeting parts of the protein other than the active sites that play an important role in the functioning of both domains of *Pf*AdoMetDC/ODC such as parasite-specific inserts [155].

4.6 TCMDC-125233

TCMDC-125233 (N-(7-chloroquinolin-4-yl)-N'-methylpropane-1,3-diamine) is structurally related to the antimalarial chloroquine, with changes in the carbon tail that resembles the diamine putrescine. As TCMDC-125233 is able to inhibit the activity of both domains of *Pf*AdoMetDC/ODC it can either interact with the active site of both domains of the protein, or with a regulatory component of the protein that is important for the functioning of both domains of the protein. Docking scores for the virtual screening of TCMDC-125233 against the active site of the homology model of *Pf*AdoMetDC were lower than that for *Pf*ODC (ranging from 2- to 4-fold lower) but indicated that interactions were possible (personal communication , P. Burger).

The putrescine tail of TCMDC-125233 may be specific for the *Pf*ODC domain, as the *Pf*ODC domain of *Pf*AdoMetDC/ODC is strongly feedback-inhibited by putrescine, unlike single-enzyme orthologues in other organisms [86]. However, the effects of inhibition of *Pf*ODC can be reversed by exogenous putrescine, allowing the subsequent reactions in polyamine biosynthesis to continue [174]. The parasite has polyamine uptake mechanisms that will allow the parasite to overcome polyamine enzyme inhibition through the uptake of exogenous polyamines [175]. Additional activities of the polyamine pathway and uptake mechanisms may need to be targeted in order to effectively inhibit the action of the polyamine pathway. The use of a drug that is possible to inhibit the activities of both domains of *Pf*AdoMetDC/ODC would be beneficial as inhibition of both domains of *Pf*AdoMetDC/ODC results in an additive growth-inhibitory effect, with a total block in the polyamine biosynthesis [176]. The active sites for *Pf*AdoMetDC and *Pf*ODC are structurally conserved when compared to their mammalian orthologues, however, the bifunctional arrangement and parasite-specific inserts that play a role in the activity of both domains, make it an attractive drug target as it would be possible to design drugs that are specific to *Pf*AdoMetDC/ODC [87].

Polyamine analogues are a group of drugs that contain a polyamine moiety, which allows them to interfere at multiple sites of the polyamine pathway. This minimises the

compensatory changes that are seen with single enzyme inhibitors. Polyamine analogues have been designed to regulate polyamine metabolism through mechanisms that the natural polyamines use, without substituting the polyamines in terms of function. Polyamine analogues should decrease intracellular polyamine pools, resulting in growth inhibition and death [177]. The presence of a putrescine tail on TCMDC-125233 may allow it to utilise the parasite's putrescine transport mechanisms to enter the parasite, and affect the functioning of the enzymes in the polyamine pathway. This may explain why TCMDC-125233 has a low EC_{50} of 0.06 µM, as utilising polyamine transporters will allow it to more easily reach its target within the parasite, however, further testing will be required to determine whether this is part of the mechanism utilised by TCMDC-125233.

Chapter 5: Conclusion

In this study we investigated a novel approach to improving the recombinant expression of *Pf*AdoMetDC/ODC, as well as the monofunctional *Pf*ODC domain, through altering the gene sequence of *Pf*AdoMetDC/ODC so that it is more *E. coli* like but still retaining *P. falciparum* qualities, in a process known as codon harmonisation. Codon harmonisation ensures that a gene will be translated at the same rate in the recombinant expression host (*E. coli*) as it would in the native host (*P. falciparum*). This will allow the newly translated recombinant protein to fold in a manner that more closely resembles folding in *P. falciparum*. Four versions of the *Pf*AdoMetDC/ODC gene were constructed, with various parts of the gene containing either the wild-type or codon harmonised gene sequence. However, codon harmonisation did not increase the amount of *Pf*AdoMetDC/ODC produced or the purity levels. Codon harmonisation of the entire gene resulted in a decrease in the expression of the *Pf*AdoMetDC/ODC. The *Pf*ODC domain appears to be refractory to codon harmonisation, with there being lower amounts of recombinant protein produced and both domains of *Pf*AdoMetDC/ODC having lower activity levels when the *Pf*ODC domain is codon harmonised. Harmonisation of the *Pf*AdoMetDC domain alone, however, increased the amount of PfAdoMetDC/ODC expressed and the activity of the *Pf*AdoMetDC domain.

Codon harmonisation of the portion of the *Pf*AdoMetDC/ODC gene that encodes for *Pf*ODC resulted in decreased levels of monofunctional *Pf*ODC being recombinantly expressed. The codon harmonised protein also exhibited lower levels of activity than the wild-type protein. In the absence of the *Pf*AdoMetDC domain the expression and activity levels of the *Pf*ODC domain are poor, indicating that the C-terminal *Pf*ODC domain requires interaction with the N-terminal *Pf*AdoMetDC domain in order to be stably expressed. Harmonisation was not able to improve the expression levels of monofunctional, as the absence of an N-terminal expression partner (*Pf*AdoMetDC) was more detrimental than the expected improvement of expression using codons frequently used by the *E. coli* expression host.

Possible inhibitors of *Pf*ODC were identified using VS. One of the drugs significantly inhibited the activity of both domains of *Pf*AdoMetDC/ODC. Another drug significantly inhibited the activity of the *Pf*AdoMetDC domain, but not the *Pf*ODC domain. Inhibition of both domains of *Pf*AdoMetDC/ODC will totally block the biosynthesis of polyamines and a single drug that is able to inhibit both activities will be greatly beneficial.

Future studies should focus on further trying to improve the recombinant expression of the bifunctional *Pf*AdoMetDC/ODC complex as well as the monofunctional *Pf*ODC domain. The use of protein tags on the N-terminal of *Pf*ODC may increase its stability and improve the expression levels. The use of mammalian and *Baculovirus*/insect expression systems may be exploited in order to improve recombinant expression. Further structural characterisation of the bifunctional complex, as well as validation of interdomain interactions are required in order to understand the functioning of *Pf*AdoMetDC/ODC. Virtual screening of the “Malaria

Box" compounds against the homology model of *Pf*AdoMetDC and the crystal structure of *Pf*SpdS should be undertaken in order to identify possible compounds that may inhibit their activities, as well as confirmation by enzyme inhibition assays.

References

1 Heddini, A. (2002) Malaria pathogenesis: a jigsaw with an increasing number of pieces. International Journal for Parasitology. **32**, 1587 - 1598

2 Bronner, U., Divis, P., Farnert, A. and Singh, B. (2009) Swedish traveller with *Plasmodium knowlesi* malaria after visiting Malaysian Borneo. Malaria Journal. **8**, 15

3 WHO. (2010) World Malaria Report 2010. WHO Press, Geneva, Switzerland

4 Craft, J. C. (2008) Challenges facing drug development for malaria. Current Opinion in Microbiology. **11**, 428 - 433

5 Bannister, L. and Mitchell, G. (2003) The ins, outs and roundabouts of malaria. TRENDS in Parasitology. **19**, 209-214

6 el Shoura, S. M. (1994) *Falciparum* malaria in naturally infected human patients: VIII. Fine structure of intraerythrocytic asexual forms before and during chloroquine treatment. Applied Parasitology. **35**, 207-218

7 Spielmann, T. and Beck, H. P. (2000) Analysis of stage-specific transcription in *Plasmodium falciparum* reveals a set of genes exclusively transcribed in ring stage parasites. Molecular and Biochemical Parasitology. **111**, 453-458

8 Pouvelle, B., Buffet, P. A., Lépolard, C., Scherf, A. and Gysin, J. (2000) Cytoadhesion of *Plasmodium falciparum* ring-stage-infected erythrocytes. Nature Medicine. **6**, 1264-1268

9 Adams, S. (2002) Breaking down the blood-brain barrier: Signaling a path to cerebral malaria? TRENDS in Parasitology. **18**, 360-366

10 Scherf, A., Pouvelle, B., Buffet, P. A. and Gysin, J. (2001) Molecular mechanisms of *Plasmodium falciparum* placental adhesion. Cellular Microbiology. **3**, 125-131

11 Salmon, B. L., Oksman, A. and Goldberg, D. E. (2001) Malaria parasite exit from the host erythrocyte: A two-step process requiring extraerythrocytic proteolysis. Proceedings of the National Academy of Sciences. **98**, 271-276

12 Alano, P. (2007) *Plasmodium falciparum* gametocytes: still many secrets of a hidden life. MicroReview. **66**, 291-302

13 Nicastria, E., Pagliaa, M. G., Severinib, C., Ghirgaa, P., Bevilacquaa, N. and Narcisoa, P. (2008) *Plasmodium falciparum* multiple infections disease severity and host characteristics in malaria affected travellers returning from Africa. Travel Medicine and Infectious Disease. **6**, 205-209

14 Winzeler, E. A. (2008) Malaria research in the post-genomic era. Nature. **455**, 751-756

15 Talman, A., Domarle, O., McKenzie, F., Ariey, F. and Robert, V. (2004) Gametocytogenesis : the puberty of *Plasmodium falciparum*. Malaria Journal. **3**, 24

16 Impoinvil, D., Ahmad, S., Troyo, A., Keating, J., Githeko, A., Mbogof, C., Kibe, L., Githure, J., Gadh, A., Hassan, A., Orshan, L., Warburg, A., Calderon-Arguedas, O., Sanchez-Loria, V., Velit-Suarezm, R., Chadee, D., Novak, R. and Beier, J. (2007) Comparison of mosquito control programs in seven urban sites in Africa, the Middle East, and the Americas. Health Policy. **83**, 196-212

17 Jacups, S., Kurucz, N., Whitters, R. and Whelan, P. (2011) Habitat Modification for Mosquito Control in the Ilparpa Swamp, Northern Territory, Australia. Journal of Vector Ecology. **36**, 292-299

18 Shaalan, E. A. and Canyon, D. V. (2009) Aquatic insect predators and mosquito control. Tropical Biomedicine. **26**, 223-261

19 LePrince, J. A. A. (1915) Control of Malaria: Oiling as an Antimosquito Measure. Public Health Reports (1896-1970). **30**, 599-608

20 Walker, K. and Lynch, M. (2007) Contributions of *Anopheles* larval control to malaria suppression in tropical Africa: review of achievements and potential. Medical and Veterinary Entomology. **21**, 2-21

21 Curtis, C. F. and Mnzava, A. E. (2000) Comparison of house spraying and insecticide-treated nets for malaria control. Bulletin of the World Health Oganization. **78**, 1389-1400

22 Mabaso, M. L., Sharp, B. and Lengeler, C. (2004) Historical review of malarial control in southern African with emphasis on the use of indoor residual house-spraying. Tropical Medicine and International Health. **9**, 846-856

23 Curtis, C. F., Jana-Kara, B. and Maxwell, C. A. (2003) Insecticide treated nets: impact on vector populations and relevance of initial intensity of transmission and pyrethroid resistance. Journal of Vector Borne Diseases. **40**, 1-8

24 Roberts, D. R. and Andre, R. G. (1994) Insecticide resistance issues in vectorborne disease control. American Journal of Tropical Medicine and Hygiene. **50**, 21-34

25 Curtis, C. F. (1996) An overview of mosquito biology, behaviour and Importance. Ciba Foundation Symposium. **200**, 3-7

26 Patz, J. A., Graczyk, T. K., Geller, N. and Vittor, A. Y. (2000) Effects of environmental change on emerging parasitic diseases. International Journal for Parasitology. **30**, 1395-1405

27 Knudsen, A. B. and Slooff, R. (1992) Vector-borne disease problems in rapid urbanization: new approaches to vector control. Bulletin of the World Health Oganization. **70**, 1-6

28 Barat, L. M. (2006) Four malaria success stories: how malaria burden was successfully reduced in Brazil, Eritrea, India, and Vietnam. American Journal of Tropical Medicine and Hygiene. **74**, 12-16

29 Rafikov, M., Bevilacqua, L. and Wyse, A. P. P. (2009) Optimal control strategy of malaria vector using genetically modified mosquitoes. Journal of Theoretical Biology. **258**, 418-425

30 Blanford, S., Chan, B. H., Jenkins, N., Sim, D., Turner, R. J., Read, A. F. and Thomas, M. B. (2005) Fungal pathogen reduces potential for malaria transmission. Science. **308**, 1638-1641

31 Scholte, E. J., Ng'habi, K., Kihonda, J., Takken, W., Paaijmans, K., Abdulla, S., Killeen, G. F. and Knols, B. G. (2005) An entomopathogenic fungus for control of adult African malaria mosquitoes. Science. **308**, 1641-1642

32 Kanzok, S. M. and Jacobs-Lorena, M. (2006) Entomopathogenic fungi as biological insecticides to control malaria. TRENDS in Parasitology. **22**, 49-51

33 Dondorp, A. M., Nosten, F., Yi, P., Das, D., Phyo, A. P., Tarning, J., Khin Maung Lwin, Ariey, F., Hanpithakpong, W., Lee, S. J., Ringwald, P., Silamut, K., Imwong, M., Chotivanich, K., Lim, P., Herdman, T., An, S. S., Yeung, S., Singhasivanon, P., Day, N. P. J., Lindegardh, N., Socheat, D. and White, N. J. (2009) Artemisinin Resistance in *Plasmodium falciparum* Malaria. The New England Journal of Medicine. **361**, 455-467

34 Genton, B. (2008) Malaria vaccines: a toy for travellers or a tool for eradication? Expert Review of Vaccines. **7**, 597-611

35 Aponte, J. J., Aide, P., Renom, M., Mandomando, I., Bassat, Q., Sacarlal, J., Manaca, M. N., Lafuente, S., Barbosa, A., Leach, A., Lievens, M., Vekemans, J., Sigauque, B., Dubois, M., Demoitié, M., Sillman, M., Savarese, B., McNeil, J. G., Macete, E., Ballou, W. R., Cohen, J. and Alonso, P. L. (2007) Safety of the RTS,S/AS02D candidate malaria vaccine in infants living in a highly endemic area of Mozambique: A double blind randomised controlled phase I/IIb trial. Lancet. **370**, 1543-1551

36 Tsuboia, T., Takeoa, S., Arumugama, T. U., Otsukic, H. and Torii, M. (2009) The wheat germ cell-free protein synthesis system: A key tool for novel malaria vaccine candidate discovery. Acta Tropica. **114**, 171-176

37 Duffy, P. E. (2007) *Plasmodium* in the placenta: parasites, parity, protection, prevention and possibly preeclampsia. Parasitology. **134**, 1877-1881

38 Carter, R. (2001) Transmission blocking malaria vaccines. Vaccine. **19**, 2309-2314

39 Greenwood, B. (2009) Can malaria be eliminated? Transactions of the Royal Society of Tropical Medicine and Hygiene. **103S**, S2-S5

40 Arrow, K., Panosian, C. and Gelband, H. (2004) Saving Lives, Buying Time: Economics of Malaria Drugs in an Age of Resistance.

41 Olliaro, P. (2001) Mode of action and mechanisms of resistance for antimalarial drugs. Pharmacology & Therapeutics. **89**, 207-219

42 Olliaro, P. and Wells, T.N.C. (2009) The global portfolio of new antimalarial medicines under development. Clinical Pharmacology and Therapeutics. **85**, 584-595

43 Surolia, N. and Padmanaban, G. (1991) Chloroquine inhibits heme-dependent protein synthesis in *Plasmodium falciparum*. Proceedings of the National Academy of Sciences. **88**, 4786-4790

44 Ginsburg, H. and Geary, T. G. (1987) Current concepts and new ideas on the mechanism of action of quinoline-containing antimalarials. Biochemical Pharmacology. **36**, 1567-1576

45 van der Jagt, D. L., Hunsaker, L. A. and Campos, N. M. (1986) Characterization of a hemoglobin-degrading, low molecular weight protease from *Plasmodium falciparum*. Molecular and Biochemical Parasitology. **18**, 389-400

46 Meshnick, S. R. (1990) Chloroquine as an intercalator: a hypothesis revived. Parasitology Today. **6**, 77-79

47 Schlitzer, M. (2007) Malaria chemotherapeutics part I: History of antimalarial drug development, currently used therapeutics, and drugs in clinical development. ChemMedChem. **44**, 944-986

48 Plowe, C. V., Kublin, J. G. and Doumbo, O. K. (1998) *P. falciparum* dihydrofolate reductase and dihydropteroate synthase mutations: epidemiology and role in clinical resistance to antifolates. Drug Resistance Updates. **1**, 389-396

49 Burrows, J. N., Chibale, K. and Wells, T. N. C. (2011) The State of the Art in Anti-Malarial Drug Discovery and Development. Current Topics in Medicinal Chemistry. **11**, 1226-1254

50 Brki, T. (2009) Artemisinin resistance could endanger fight against malaria. The Lancet Infection. **9**, 213

51 Sowunmi, A., Gbotosho, G., Happi, C., Adedeji, A., Fehintola, F., Tambo, E. and Fateye, B. (2007) Therapeutic efficacy and effects of artemether-lumefantrine and amodiaquinesulfalene-pyrimethamine on gametocyte carriage in children with uncomplicated *Plasmodium falciparum* malaria in Southwestern Nigeria. The American Journal of Tropical Medicine and Hygiene. **2**, 235-241

52 Hasuian, A., Purba, L., Kenangalem, E., Wuwung, R., Ebsworth, E., Maristela, R., Penttinen, P., Laihad, F. and Anstey, N. (2007) Dihydroartemisinin-piperaquine versus artesunated amodiaquine: Superior efficacy and posttreatment prophylaxis against multidrug-resistant *Plasmodium falciparum* and *Plasmodium vivax* malaria. Clinical Infectious Diseases. **44**, 1067-1074

53 Srivastava, I. K. and Vaidya, A. B. (1999) A mechanism for the synergistic antimalarial action of atovaquone and proguanil. Antimicrobial Agents and Chemotherapy. **43**, 1334-1339

54 Hasting, I., Korenromp, E. and Boland, P. (2007) The anatomy of a malaria disaster: drug policy choice and mortality in African children. The Lancet Infection. **7**, 748-749

55 Stepniewska, K. and White, N. (2008) Pharmacokinetics determinants of the window of selection for antimalarial drug resistance. Antimicrobial Agents and Chemotherapy. **5**, 1589-1596

56 Jana, S. and Paliwal, J. (2007) Novel molecular targets for antimalarial chemotherapy. International Journal of Antimicrobial Agents. **30**, 4-10

57 Ancelin, M., Calas, M., Vidal-Sailhan, V., Herbute, S., Ringwald, P. and Vial, H. (2003) Potential inhibitors of *Plasmodium* phospholipid metabolism with a broad spectrum of *in vitro* antimalarial activities. Antimicrobial Agents and Chemotherapy. **47**, 2590-2597

58 Vial, H. (1996) Recent developments and rationale towards new strategies for malaria chemotherapy. Parasite. **3**, 3-23

59 Roggero, R., Zufferey, R. and Minca, M. (2004) Unraveling the mode of action of the antimalarial choline analog G25 in *Plasmodium falciparum* and *Saccharomyces cerevisiae*. Antimicrobial Agents and Chemotherapy. **48**, 2816-2824

60 Palmer, A. J., Ghani, R. A., Kaur, N., Phanstiel, O. and Wallace, H. M. (2009) A putrescine-anthracene conjugate: a paradigm for selective drug delivery. Biochemistry Journal. **424**, 431-438

61 Kirk, K., Martin, R. E., Broer, S., Howitt, S. M. and Saliba, K. J. (2005) *Plasmodium* permeomics: membrane transport proteins in the malaria parasite. Current Topics in Microbiology and Immunology. **295**, 325-356

62 Joet, T., Eckstein-Ludwig, U., Morin, C. and Krishna, S. (2003) Validation of the hexose transporter of *Plasmodium falciparum* as a novel drug target. Proceedings of the National Academy of Science. **100**

63 Blackman, M. (2000) Proteases involved in erythrocyte invasion by the malaria parasite: function and potential as chemotherapeutic targets. Current Drug Targets. **1**, 59-83

64 Salmon, B. L., Oksman, A. and Goldberg, D. E. (2000) Malaria parasite exit from the host erythrocyte: a two-step process requiring extraerythrocytic proteolysis. Proceedings of the National Academy of Science. **98**, 271-276

65 Bailly, E., Jambou, R., Savel, J. and Jaureguiberry, G. (1992) *Plasmodium falciparum*: differential sensitivity in vitro to E-64 (cysteine protease inhibitor) and Pepstatin A (aspartyl protease inhibitor). Journal of Protozoology. **39**, 593-599

66 McFadden, G. I. and Roos, D. S. (1999) Apicomplexan plastids as drug targets. Trends in Microbiology. **7**, 328-333

67 Seiler, N. (2003) Thirty years of polyamine-related approaches to cancer therapy. Retrospect and prospect. Part 1. Selective enzyme inhibitors. Current Drug Targets. **4**, 537-564

68 Hamana, K. and Matsuzaki, S. (1999) Polyamines as a chemotaxonomic marker in bacterial systematics. Critical Reviews in Microbiology. **18**, 261-283

69 Müller, I. B., Gupta, R. D., Luersen, K., Wrenger, C. and Walter, R.D. (2008) Assessing the polyamine metabolism of *Plasmodium falciparum* as chemotherapeutic target. Molecular & Biochemical Parasitology. **160**, 1-7

70 Kerppola, T. K. (1998) Transcriptional cooperativity: Bending over backwards and doing the flip. Structure. **6**, 549-554

71 Hobbs, C. A., Paul, B. A. and Gilmour, S. K. (2002) Deregulation of polyamine biosynthesis alters intrinsic histone acetyltransferase and deacetylase activities in murine skin and tumors. Cancer Research. **62**, 67-74

72 Heby, O. (1981) Role of polyamines in the control of cell proliferation and differentiation. Differentiation. **19**, 1-20

73 Russell, D. H. (1985) Ornithine decarboxylase: A key regulatory enzyme in normal and neoplastic growth. Drug Metabolism Reviews. **16**, 1-88

74 Poulin, R., Pelletier, G. and Pegg, A. E. (1995) Induction of apoptosis by excessive polyamine accumulation in ornithine decarboxylase-overproducing L1210 cells. Biochemical Journal. **311**, 723-727

75 Tome, M. E., Fiser, S. M., Payne, C. M. and Gerner, E. W. (1997) Excess putrescine accumulation inhibits the formation of modified eukaryotic initiation factor 5A (eIF-5A) and induces apoptosis. Biochemical Journal. **328**, 847-854

76 Birkholtz, L.-M., Williams, M., Niemand, J., Louw, A. I., Persson, L. and Heby, O. (2011) Polyamine homoeostasis as a drug target in pathogenic protozoa: peculiarities and possibilities. Biochemical Journal. **438**, 229-244

77 Tabor, C. W. and Tabor, H. (1984) Polyamines. Annual Review of Biochemistry. **53**, 749-790

78 Müller, S., Coombs, G. H. and D.Walter, R. (2001) Targeting polyamines of parasitic protozoa in chemotherapy. TRENDS in Parasitology **17**, 242-249

79 Heby, O. and Persson, L. (1990) Molecular genetics of polyamine synthesid in eukaryotic cells. Trends in Biochemical Science. **15**, 153-158

80 Ramya, T. N. C., Surolia, N. and Surolia, A. (2006) Polyamine synthesis and salvage pathways in the malaria parasite *Plasmodium falciparum*. Biochemical and Biophysical Research Communications. **348**, 579-584

81 Teng, R., Junankar, P. R., Bubb, W. A., Rae, C., Mercier, P. and Kirk, K. (2009) Metabolite profiling of the intraerythrocytic malaria parasite *Plasmodium falciparum* by (1)H NMR spectroscopy. NMR in Biomedicine. **22**, 292-302

82 Das Gupta, R., Krause, T., Bergmann, B., Muller, I., Khomutov, A., Müller, S., Walter, R. and Luersen, K. (2005) 3-Aminooxy-1-aminopropane and derivatives have an antiproliferative effect on cultured *Plasmodium falciparum* by decreasing intracellular polyamine concentrations. Antimicrobial Agents and Chemotherapy. **49**, 2857-2864

83 Haider, N., Eschbach, M. L., Dias Sde, S., Gilberger, T. W., Walter, R. D. and Luersen, K. (2005) The spermidine synthase of the malaria parasite *Plasmodium falciparum*: molecular and biochemical characterisation of the polyamine synthesis enzyme. Molecular and Biochemical Parasitology. **142**, 224-236

84 Müller, S., Da'dara, A., Luersen, K., Wrenger, C., Das Gupta, R., Madhubalai, R. and Walter, R. D. (2000) In the human malaria parasite *Plasmodium falciparum*, polyamines are synthesized by a bifunctional ornithine decarboxylase, *S*-adenosylmethionine decarboxylase. The Journal of Biological Chemistry. **275**, 8097-8102

85 Krause, T., Lüersen, K., Wrenger, C., Gilberger, T., Müller, S. and Walter, R. D. (2000) The ornithine decarboxylase domain of the bifunctional ornithine decarboxylase/S-adenosylmethionine decarboxylase of *Plasmodium falciparum*: Recombinant expression and catalytic properties of two different constructs. Biochemistry Journal. **352,** 287-292.

86 Wrenger, C., Lüersen, K., Krause, T., Müller, S. and Walter, R. (2001) The *Plasmodium falciparum* bifunctional ornithine decarboxylase, *S*-adenosyl-L-methionine decarboxylase, enables a well balanced polyamine synthesis without domain–domain interaction. Journal of Biological Chemistry. **276**, 29651-29656

87 Birkholtz, L., Wrenger, C., Joubert, F., Wells, G., Walter, R. and Louw, A. (2004) Parasite-specific inserts in the bifunctional *S*-adenosylmethionine decarboxylase/ornithine decarboxylase of *Plasmodium falciparum* modulate catalytic activities and domain interactions. Biochemistry Journal. **377**, 439-448

88 Jackson, L. K., Baldwin, J., Akella, R., Goldsmith, E. J. and MA., M. A. P. (2004) Multiple active site conformations revealed by distant site mutation in ornithine decarboxylase. Biochemistry. **43**, 12990-12999

89 Allen, R. R. and Klinman, J. P. (1981) Stereochemistry and kinetic isotope effects in the decarboxylation of *S*-adenosylmethionine as catalyzed by the pyruvoyl enzyme, *S*-adenosylmethionine decarboxylase. Journal of Biological Chemistry. **256**, 3233-3239

90 Ekstrom, J. L., Tolbert, W. D., Xiong, H., Pegg, A. E. and Ealick, S. E. (2001) Structure of a human *S*-adenosylmethionine decarboxylase self-processing ester intermediate and mechanism of putrescine stimulation of processing as revealed by the H243A mutant. Biochemistry Journal. **40**, 9495-9504

91 Wells, G.A. (2010). Molecular modeling elucidates parasite-specific features of polyamine pathway enzymes of *Plasmodium falciparum.* In Department of Biochemistry. University of Pretoria, Pretoria. *Doctor Philosophiae.* p.125

92 Wells, G., Birkholtz, L.M., Joubert, F., Walter, R. and Louw, A. (2006) Novel properties of malarial *S*-adenosylmethionine decarboxylase as revealed by structural modelling. Journal of Molecular Graphics and Modelling. **24**, 307-318

93 Birkholtz, L., Joubert, F., Neitz, A. W. H. and Louw, A. I. (2003) Comparative properties of a three-dimensional model of *Plasmodium falciparum* ornithine decarboxylase. Proteins: Structure, Function, and Bioinformatics. **50**, 464-473

94 Almrud, J. J., Oliveira, M. A., Kern, A. D., Grishin, N. V., Phillips, M. A. and Hackert, M. L. (2000) Crystal structure of human ornithine decarboxylase at 2.1 A resolution: structural insights to antizyme binding. Journal of Molecular Biology. **295**, 7-16

95 Grishin, N. V., Osterman, A. L., Brooks, H. B., Phillips, M. A. and Goldsmith, E. J. (1999) X-ray structure of ornithine decarboxylase from *Trypanosoma brucei*: the native structure and the structure in complex with alpha-difluoromethylornithine. Biochemistry. **38**, 15174-15184

96 Dufe, V. T., Qui, W., Müller, I., Hui, R., Walter, R. D. and Al-Karadaghi, S. (2007) Crystal structure of *Plasmodium falciparum* spermidine synthase in complex with the substrate decarboxylated *S*-adenosylmethionine and the potent inhibitors 4MCHA and AdoDATO. Journal of Molecular Biology. **373**, 167-177

97 Wu, H., Min, J., Ikeguchi, Y., Zeng, H., Dong, A., Loppnau, P., Pegg, A. E. and Plotnikov, A. N. (2007) Structure and mechanism of spermidine synthases. Biochemistry. **46**, 8331-8339

98 Dufe, V. T., Qui, W., Müller, I. B., Hui, R., Walter, R. D. and Al-Karadaghi, S. (2007) Crystal structure of *Plasmodium falciparum* spermidine synthase in complex with the substrate decarboxylated *S*-adenosylmethionine and the potent inhibitors 4MCHA and AdoDATO. Journal of Molecular Biology. **373**, 167-177

99 Casero, R. A. and Pegg, A. E. (2009) Polyamine catabolism and disease. Biochemistry Journal. **412**, 323-338

100 Jennings, F. W., Atouguia, J. M. and Murray, M. (1996) The importance of 2,3-dimercaptopropinol (British anti-lewisite, BAL) in the trypanocidal activity of topical melarsoprol. Acta Tropica. **62**, 83-89

101 Clark, K., Niemand, J., Reeksting, S., Smit, S., van Brummelen, A., Williams, M., Louw, A. and Birkholtz, L. (2009) Functional consequences of perturbing polyamine metabolism in the malaria parasite, *Plasmodium falciparum*. Amino Acids. **38**, 633-644

102 Assaraf, Y. G., Golenser, J., Spira, D. T. and Bachrach, U. (1984) Polyamine levels and the activity of their biosynthetic enzymes in human erythrocytes infected with the malarial parasite, *Plasmodium falciparum*. Biochemistry Journal. **222**, 815-819

103 Wright, P. S., Byers, T. L., Cross-Doersen, D. E., McCann, P. P. and Bitonti, A. J. (1991) Irreversible inhibition of *S*-adenosylmethionine decarboxylase in *Plasmodium falciparum*-infected erythrocytes: Growth inhibition *in vitro*. Biochemical Pharmacology. **41**, 1713-1718

104 Bitonti, A. J., Dumont, J. A., Bush, T. L., Edwards, M. L., Stemerick, D. M., McCann, P. P. and Sjoerdsma, A. (1989) Bis(benzyl)polyamine analogues inhibit the growth of chloroquine-resistant human malaria parasites *(Plasmodium falciparum)* in vitro and in combination with α-difluoromethylornithine cure murine malaria. Proceedings of the National Academy of Science. **86**, 651-655

105 Kaiser, A. E., Gottwald, A. M., Wiersch, C. S., Lindenthal, B., Maier, W. A. and Seitz, H. M. (2001) Effect of drugs inhibiting spermidine biosynthesis and metabolism on the in vitro development of *Plasmodium falciparum*. Parasitology Research. **87**, 963-972

106 Gelb, M. H. (2007) Drug discovery for malaria: a very challenging and timely endeavor. Current Opinion in Chemical Biology. **11**, 440-445

www.mmv.org

107 Hughes, J., Rees, S., Kalindjian, S. and Philpott, K. (2011) Principles of early drug discovery. British Journal of Pharmacology. **162**, 1239-1249

108 Yang, Y., Adelstein, S. J. and Kassis, A. I. (2009) Target discovery from data mining approaches. Drug Discovery Today. **14**, 147-154

109 Wang, S., Sim, T. B., Kim, Y.-S. and Chang, Y.-T. (2004) Tools for target identification and validation. Current Opinion in Chemical Biology. **8**, 317-377

110 Renslo, A. R. and McKerrow, J. H. (2006) Drug discovery and development for neglected parasitic diseases. Nature Chemical Biology. **2**, 701-710

111 Howbrook, D. N., van der Valk, A. M., O'Shaughnessy, M. C., Sarker, D. K., Baker, S. C. and Lloyd, A. W. (2003) Developments in microarray technologies. Drug Discovery Today. **8**, 642-651

112 Khersonsky, S. M., Jung, D. W., Kang, T. W., Walsh, D. P., Moon, S., Jo, H., Jacobson, E. M., Shetty, V., Neubert, T. A. and Chang, Y. T. (2003) Facilitated forward chemical genomics using tagged triazine library and zebrafish embryo screening. Journal of the American Chemical Society. **125**, 11804-11805

113 Sem, D. S., Yu, L., Coutts, S. M. and Jack, R. (2001) Object-oriented approach to drug design enabled by NMR SOLVE: first real-time structural tool for characterizing protein-ligand interactions. Journal of Cellular Biochemistryl. **37**, 99-105

114 Fox, S., Farr-Jones, S., Sopchak, L., Boggs, A., Nicely, A. W. and Khoury, R. (2006) High-throughput screening; Update on practices and success. Journal of Biological Screening. **11**, 864-869

115 Boppana, K., Dubey, P. K., Jagarlapudi, S. A. R. P., Vadivelan, S. and Rambabu, G. (2009) Knowledge based identification of MAO-B selective inhibitors using pharmacophore and structure based virtual screening models. European Journal of Medicinal Chemistry. **44**, 3584-3590

116 Law, R., Barker, O., Barker, J. J., Hesterkamp, T., Godemann, R. and Andersen, O. (2009) The multiple roles of computational chemistry in fragment-based drug design. Journal of Computational Aided Molecular Design. **23**, 459-473

117 Birkholtz, L., Blatch, G., Coetzee, T., Hoppe, H., Human, E., Morris, E., Ngcete, Z., Oldfield, L., Roth, R. and Shonhai, A. (2008) Heterologous expression of plasmodial proteins for structural studies and functional annotation. Malaria Journal. **7**, 197

118 Wermuth, C. G., Ganellin, C. R., Lindberg, P. and Mitscher, L. A. (1998) Glossary of terms used in medicinal chemistry (IUPAC Recommendations 1998). Pure and Applied Chemistry. **70**, 1129-1143

119 Lipinski, C. A., Lombardo, F., Dominy, B. W. and Feeney, P. J. (2001) Experimental and computational approaches to estimate solubility and permeability in drug discovery and development settings. Advanced Drug Delivery Review. **46**, 3-26

120 Nwaka, S., Riopel, L., Ubben, D. and Craft, J. C. (2004) Medicines for Malaria Venture new developments in antimalarials. Travel Medicine and Infectious Disease. **2**, 161-170

121 Guiguemde, W. A., Shelat, A. A., Bouck, D., Duffy, S., Crowther, G. J., Davis, P. H., Smithson, D. C., Connelly, M., Clark, J., Zhu, F., Jimenez-Diaz, M. B., Martinez, M. S., Wilson, E. B., Tripathi, A. K., Gut, J., Sharlow, E. R., Bathurst, I., ElMazouni, F., Fowble, J. W., Forquer, I., McGinley, P. L., Castro, S., Angulo-Barturen, I., Ferrer, S., Rosenthal, P. J., DeRisi, J. L., Sullivan, D. J., Lazo, J. S., Roos, D. S., Riscoe, M. K., Phillips, M. A., Rathod, P. K., VanVoorhis, W. C., Avery, V. M. and Kiplin Guy, R. (2010) Chemical genetics of *Plasmodium falciparum*. Nature. **465**, 311-315

122 Gamo, F.-J., Sanz, L. M., Vidal, J., deCozar, C., Alvarez, E., Lavandera, J.-L., Vanderwall, D. E., Green, D. V. S., Kumar, V., Hasan, S., Brown, J. R., Peishoff, C. E., Cardon, L. R. and Garcia-Bustos, J. F. (2010) Thousands of chemical starting points for antimalarial lead identification. Nature. **465**, 305-310

123 Mehlin, C., Boni, E., Buckner, F. S., Engel, L., Feist, T., Gelb, M. H., Haji, L., Kima, D., Liu, C., Mueller, N., Myler, P. J., Reddya, J. T., Sampsonh, J. N., Subramanian, E., Voorhis, W. C. V., Worthey, E., Zucker, F. and Hol, W. G. J. (2006) Heterologous expression of proteins from *Plasmodium falciparum*: Results from 1000 genes. Molecular & Biochemical Parasitology. **148**, 144-160

124 Gowda, D. C. and Davidson, E. A. (1999) Protein glycosylation in the malaria parasite. Parasitology Today. **15**, 147-152

125 Aravind, L., Iyer, L. M., Wellems, T. E. and Miller, L. H. (2003) *Plasmodium* biology: genomic gleanings. Cell. **115**, 771-785

126 Pizzi, E. and Frontali, C. (2001) Low-complexity regions in *Plasmodium falciparum* proteins. Genome Research. **11**, 218-229

127 Hafner, E., Tabor, C. and Tabor, H. (1979) Mutants of *Escherichia coli* that do not contain 1,4-diaminobutane (putrescine) or spermidine. Journal of Biological Chemistry. **24**, 12419-12426

128 Niemand, J. (2007) A phage display study of interacting peptide binding partners of malarial *S*-adenosylmethione decarboxylase/ornithine decarboxylase. In Department of Biochemistry, University of Pretoria, Pretoria. *Magister Scientiae,* p.62

129 Williams, M. (2011) Biochemical and structural characterization of novel drug targets regulating polyamine biosynthesis in the human malaria parasite, *Plasmodium falciparum*. In Department of Biochemistry, University of Pretoria, Pretoria. D*octor Philosophiae,* p.96

130 Gustafsson, C., Govindarajan, S. and Minshull, J. (2004) Codon bias and heterologous protein expression. TRENDS in Biotechnology. **22**, 346-353

131 Andersson, G. E. and Kurland, C. G. (1991) An extreme codon preference strategy: codon reassignment. Molecular Biology Evolution. **8**, 530-544

132 Kink, J. A. (1991) Efficient expression of the *Paramecium* calmodulin gene in *Escherichia coli* after four TAA-to-CAA changes through a series of polymerase chain reactions. Journal of Protozoology. **38**, 441-447

133 Nambiar, K. P. (1984) Total synthesis and cloning of a gene coding for the ribonuclease S protein. Science. **223**, 1299-1301

134 Thanaraj, T. A. and Argos, P. (1996) Protein secondary structural types are differentially coded on messenger RNA. Protein Science. **5**, 1973-1983

135 Phoenix, D. A. and Korotkov, E. (1997) Evidence of rare codon clusters within *Escherichia coli* coding regions. FEMS Microbiology Letters. **155**, 63-66

136 Angov, E., Hillier, C. J., Kincaid, R. L. and Lyon, J. A. (2008) Heterologous protein expression is enhanced by harmonizing the codon usage frequencies of the target gene with those of the expression host. PLoS ONE. **3**, 1-10

137 Human, E. (2007) Kinetic analysis of a recombinantly expressed *Plasmodium falciparum* dihydrofolate synthase-folylpolyglutamate synthase. In Department of Biochemistry, University of Pretoria, Pretoria. *Magister Scientiae,* p.74

138 Sirawaraporn, W., Prapunwattana, P., Sirawaraporn, R., Yuthavong, Y. and Santi, D. V. (1993) The dihydrofolate reductase domain of *Plasmodium falciparum* thymidylate synthase-dihydrofolate reductase. Gene synthesis, expression, and anti-folate-resistant mutants. The Journal of Biological Chemistry. **268**, 21637-21644

139 Jackson, L. K., Goldsmith, E. J. and Phillips, M. A. (2003) X-ray structure determination of *Trypanosoma brucei* ornithine decarboxylase bound to D-ornithine and to G418: insights into substrate binding and ODC conformational flexibility. Journal of Biological Chemistry. **278**, 22037-22043

140 Sauna, Z. E., Kimchi-Sarfaty, C., Ambudkar, S. V. and Gottesman, M. M. (2007) The sounds of silence: synonymous mutations affect function. Pharmacogenomics. **8**, 527-532

141 Kimchi-Sarfaty, C., Oh, J. M., Kim, I. W., Sauna, Z. E. and Calcagno, A. M. (2007) A ''silent'' polymorphism in the MDR1 gene changes substrate specificity. Science. **315**, 525-528

142 Komar, A. A., Lesnik, T. and Reiss, C. (1999) Synonymous codon substitutions affect ribosome traffic and protein folding during *in vitro* translation. FEBS Letters. **462**, 387-391

143 Thanaraj, T. A. and Argos, P. (1996) Protein secondary structural types are differentially coded on messenger RNA. Protein Science. **5**, 1973-1983

144 Zhang, S., Goldman, E. and Zubay, G. (1994) Clustering of low usage codons and ribosome movement. Journal of Theoretical Biology. **170**, 339-354

145 Mogk, A., Mayer, M. P. and Deuerling, E. (2002) Mechanisms of protein folding: molecular chaperones and their application in biotechnology. ChemBioChem. **3**, 807-814

146 Turgut-Balik, D., Shoemark, D. K., Moreton, K. M., Sessions, R. B. and Holbrook, J. J. (2001) Over-production of lactate dehydrogenase from *Plasmodium falciparum* opens a route to new antimalarials. Biotechnology Letters. **23**, 917-921

147 Hillier, C. J., Ware, L. A., Barbosa, A., Angov, E., Lyon, J. A., Heppner, D. G. and Lanar, D. E. (2005) Process Development and Analysis of Liver-Stage Antigen 1, a Preerythrocyte-Stage Protein-Based Vaccine for *Plasmodium falciparum*. Infection and Immunity. **73**, 2109-2115

148 Makrides, S. C. (1996) Strategies for achieving high-level expression of genes in *Escherichia coli.* Microbioligical Reviews. **60**, 512-538

149 Crooke, A., Radfar, A., Diez, A. and Bautista, J. M. (2006) Protein processing in *Plasmodium falciparum*? Anales de la Real Academia de Farmacia. **72**, 629-642

150 Kasekarn, W., Sirawaraporn, R., Chahomchuen, T., Cowman, A. F. and Sirawaraporn, W. (2004) Molecular characterization of bifunctional hydroxymethyldihydropterin pyrophosphokinase-dihydropteroate synthase from *Plasmodium falciparum*. Molecular & Biochemical Parasitology. **137**, 43-53

151 Shallom, S., Zhang, K., Jiang, L. and Rathod, P. K. (1999) Essential protein-protein interactions between *Plasmodium falciparum* thymidylate synthase and dihydrofolate reductase domains. Journal of Biological Chemistry. **274**, 37781-37786

152 Wattanarangsan, J., Chusacultanachai, S., Yuvaniyama, J., Kamchonwongpaisan, S. and Yuthavong, Y. (2003) Effect of N-terminal truncation of *Plasmodium falciparum* dihydrofolate reductase on dihydrofolate reductase and thymidylate synthase activity. Molecular and Biochemical Parasitology. **126**, 97-102

153 Brobey, R. K. B., Sano, G., Itoh, F., Aso, K., Kimura, M., Mitamura, T. and Horii, T. (1996) Recombinant *Plasmodium falciparum* dihydrofolate reductase-based in vitro screen for antifolate antimalarials. Molecular and Biochemical Parasitology. **81**, 225-237

154 Rattanachuen, W., Jönsson, M., Swedberg, G. and Sirawaraporn, W. (2009) Probing the roles of non-homologous insertions in the N-terminal domain of *Plasmodium falciparum* hydroxymethylpterin pyrophosphokinase-dihydropteroate synthase. Molecular and Biochemical Parasitology. **168**, 135-142

155 Williams, M., Sprenger, J., Human, E., Al-Karadaghi, S., Persson, L., Louw, A. I. and Birkholtz, L. M. (2011) Biochemical characterisation and novel classification of monofunctional *S*-adenosylmethionine decarboxylase of *Plasmodium falciparum*. Molecular and Biochemical Parasitology. **180**, 17-26

156 Hartl, F. U. and Hayer-Hartl, M. (2002) Molecular chaperones in the cytosol: From nascent chain to folded protein. Science. **295**, 1852-1858

157 Sorensen, H. and Mortensen, K. (2005) Soluble expression of recombinant proteins in the cytoplasm of Escherichia coli. Microbial Cell Factories. **4**, 1

158 Stephens, L. L., Shonhai, A. and Blatch, G. L. Co-expression of the *Plasmodium falciparum* molecular chaperone, PfHsp70, improves the heterologous production of the antimalarial drug target GTP cyclohydrolase I, PfGCHI. Protein Expression and Purification. **77**, 159-165

159 Makhoba, X. H. (2011) The development of a molecular chaperone-based system to improve the heterologous production of *Plasmodium falciparum* AdoMetDC protein in *E. coli*. In Biochemistry and Microbiology, University of Zululand, Richards Bay. *Magister Scientiae,* p.49

160 Carrio, M. M. and Villaverde, A. (2002) Construction and deconstruction of bacterial inclusion bodies. Journal of Biotechnology. **96**, 3-12

161 Vallejo, L. F. and Rinas, U. (2004) Strategy for recovery of active protein through refolding of bacterial inclusion body proteins. Microbial Cell Factories. **3**, 2-12

162 Kumar, A., Kumar, K., Korde, R., Puri, S. K., Malhotra, P. and Cauhan, V. S. (2007) Falcipain-1, a *Plasmodium falciparum* Cysteine protease with vaccine potential. Infection and Immunity. **75**, 2026-2034

163 Sijwali, P. S., Brinen, L. S. and Rosenthal, P. J. (2001) Systematic optimization of expression and refolding of the *Plasmodium falciparum* cysteine protease Falcipain-2. Protein Expression and Purification. **22**, 128-134

164 Singh, S. M. and Panda, A. K. (2005) Solubilization and refolding of bacterial inclusion body. Journal of Bioscience and Bioengineering. **99**, 303-310

165 Desai, P. V., Patny, A., Sabnis, Y., Tekwani, B., Gut, J., Rosenthal, P., Srivastava, A. and Avery, M. (2004) Identification of novel parasitic cysteine protease inhibitors using virtual screening. 1: The ChemBridge database. Journal of Medicinal Chemistry. **47**, 6609-6615

166 Adane, L., Patel, D. S. and Bharatam, P. V. (2010) Shape- and chemical feature-based 3D-pharmacophore model generation and virtual screening: Identification of potential leads for *P. falciparum* DHFR enzyme inhibition. Chemical Biology and Drug Design. **75**, 115-126

167 Jacobsson, M., Garedal, M., Schultz, J. and Karlen, A. (2008) Identification of *Plasmodium falciparum* spermidine synthase active site binders through structure-based virtual screening. Journal of Medicinal Chemistry. **51**, 2777-2786

168 Nicola, G., Smith, C. A., Lucumi, E., Kuo, M. R., Karagyozov, L., Fidock, D. A., Sacchettini, J. C. and Abagyan, R. (2007) Discovery of novel inhibitors targeting enoyl-acyl carrier protein reductase in *Plasmodium falciparum* by structure-based virtual screening. Biochemical and Biophysical Research Communications. **358**, 686-691

169 Kortagere, S., Welsh, W. J., Morrisey, J. M., Daly, T., Ejigiri, I., Sinnis, P., Vaidya, A. B. and Bergman, L. W. (2010) Structure-based design of novel small-molecule inhibitors of *Plasmodium falciparum*. Journal of Chemical Information and Modeling. **50**, 840-849

170 Bastien, O., Lespinats, S., Roy, S., Métayer, K., Fertil, B., Codani, J. J. and Maréchal, E. (2004) Analysis of the compositional biases in *Plasmodium falciparum* genome and proteome using *Arabidopsis thaliana* as a reference. Gene. **336**, 163-173

171 Callebaut, I., Prat, K., Meurice, E., Mornon, J.P. and Tomavo, S. (2005) Prediction of the general transcription factors associated with RNA polymerase II in *Plasmodium falciparum*: conserved features and differences relative to other eukaryotes. BMC Genomics. **6**, 100

172 de Beer, T., Wells, G., Burger, P., Joubert, F., Marechal, E., Birkholtz, L. and Louw, A. (2009) Antimalarial Drug Discovery: *In Silico* Structural Biology And Rational Design. Infectious Disorders - Drug Targets. **9**, 403-318

173 Baxter, C. A. (2000) New approach to molecular docking and its application to virtual screening of chemical databases. Journal od Chemical Information and Modeling. **40**, 254-262

174 Das Gupta, R., Krause, T., Bergmann, B., Muller, I. B., Khomutov, A., Müller, S., Walter, R. D. and Luersen, K. (2005) 3-Aminooxy-1-aminopropane and derivatives have an antiproliferative effect on cultured *Plasmodium falciparum* by decreasing intracellular polyamine concentrations. Antimicrobial Agents and Chemotherapy. **49**, 2857–2864

175 Niemand, J., Louw, A., Birkholtz, L. and Kirk, K. (2012) Polyamine uptake by the intraerythrocytic malaria parasite, *Plasmodium falciparum*. International Journal for Parasitology. **42**, 921-929

176 van Brummelen, A. C., Olszewski, K., Wilinski, D., Llinas, M., Louw, A. and Birkholtz, L. (2009) Co-inhibition of the *Plasmodium falciparum S*-adenosylmethionine decarboxylase/ornithine decarboxylase reveals perturbation-specific compensatory mechanisms by transcriptome, proteome and metabolome analyses. Journal of Biological Chemistry. **284**, 4635-4646

177 Wallace, H. M. and Fraser, A. F. (2003) Polyamine analogues as anticancer drugs. Biochemical Society Transactions. **31**, 393-396